Essays on Sovereign Default

A THESIS
SUBMITTED TO THE DEPARTMENT OF ECONOMICS
OF THE UNIVERSITY OF BIRMINGHAM
BY

Liang Shi

IN PARTIAL FULFILLMENT OF THE REQUIREMENTS
FOR THE DEGREE OF
Doctor of Philosophy

Pei Kuang, Supervisor
Anindya Banerjee, Co-Supervisor

August, 2022

Acknowledgements

I am grateful to my supervisors Pei Kuang and Anindya Banerjee for their guidance, encouragement and support during the past four years. Their dedication to students is admirable and any positive qualities my work may have are evidence of that. I also thank Kaushik Mitra for all the time and comments he have given to me and my work. I am grateful to David Dickinson, Ceri Davis, Yi Liu and all my colleagues of the Department of Economics at the University of Birmingham for their help in completing my PhD, their support and friendship. The easy-to-use and high performance computing support from the BlueBEAR also contributes to my PhD thesis. The CIMS Summer Schools on DSGE Modelling at the University of Surrey are highly appreciated as they guided me to relevant quantitative methods in Macroeconomics.

Dedication

To my parents who support me in the pursuit of my academic goals, and to my girlfriend who has been with me throughout this long journey.

Abstract

This thesis consists of three chapters on sovereign default. The first chapter investigates the influences of fiscal austerity on sovereign debt yield spreads, which has caused heated debates since the Eurozone debt crisis in 2010s. The analysis in this chapter is based on an endogenous sovereign default model with private capital accumulation and fiscal rule. The model provides several contributions: First, it rationalizes the empirical evidence of state-dependent relationships between fiscal austerity and debt spreads: When the economy is under high financial stress characterised by high levels of outstanding debt and low productivity, government spending cuts increase spreads. By contrast, under low financial stress, fiscal austerity reduces spreads. Second, as in Greek data, the model predicts that the pre-default spread surge will be accompanied by fiscal consolidation. Third, it reveals a non-negligible role played by the wealth effect: if expected to be long-lived, austerity harms investment, damages production and eventually raises spreads. In conclusion, even though fiscal austerity could reduce sovereign spreads and debt-to-GDP ratios in the long term, its short-term self-defeating probabilities could be non-trivial.

The second chapter discusses efficiently deriving numerical solutions to macroeconomic models on Matlab with the GPU (Graphic Processing Unit) Parallel Computing toolkit. For many non-linear models such as the endogenous sovereign default model in chapter one, we resort to the discretized value function iteration (DVFI) approach to obtain robust solutions. Unfortunately, this method is typically slow and the speed problem worsens when a high number of grid points for state variables is needed. This paper shows that the GPU toolkit on the commonly used Matlab platform provides an up to tenfold speed boost compared with using the conventional CPU method. Using the appropriate algorithm is important to achieve this and Matlab favours a combination of vectorization and serial execution, i.e. the Looping Over Exogenous Shocks (LOES) approach. With LOES, records show the solving time spent on Matlab CPU and GPU is significantly shorter than its Julia counterparts. Moreover, implementing GPU computation is easy on Matlab.

The third chapter studies the impacts of shifting long-run growth expectation on sovereign default risk. We show the new evidence of negative non-linear relationships

between potential GDP growth forecasts and government debt spreads during the recent Eurozone sovereign debt crisis (2009-2016). Existing equilibrium default models assuming full information rational expectation (FIRE) on trend growth struggle to explain the new evidence because correlation between trend growth and simulated spreads is not statistically significant. In this paper, we build a new sovereign default model where the knowledge of trend growth is assumed to be imperfect and hence agents have to learn about it to make optimal decisions. The simulation results show that embedding such a learning mechanism in sovereign default model provides an easy solution to rationalize our new evidence.

Contents

List of Figures **vi**

List of Tables **viii**

1 Fiscal Austerity, Investment and Sovereign Default **1**

1.1 Introduction 1

1.2 The Model 6

1.2.1 Household 6

1.2.2 Production environment 6

1.2.3 The government 7

1.2.4 Recursive representation 9

1.3 Quantitative Results 11

1.3.1 Calibration and business cycle statistics 11

1.3.2 Typical default episodes 14

1.4 The state-dependent effects of fiscal austerity 16

1.4.1 The role of capital 20

1.4.2 The role of wealth effect 23

1.4.3 Explaining state dependence 26

1.5 Sensitivity Analysis 29

1.5.1 Persistence of fiscal shock 29

1.6 Discussions 31

1.7 Conclusion 34

2 Matlab-Based GPU Computation of Sovereign Default Models **35**

2.1 Introduction 35

2.2 Endogenous Sovereign Default Models 39

2.2.1 The Model with One-Period Debt . . . 40
2.2.2 The Model with Long-Term Debt . . . 52
2.3 Neoclassical Growth Model for Comparison . . . 56
2.4 Conclusion . . . 60

3 Sovereign Debt Pricing with Shifting Long-run Growth Expectations 61
3.1 Introduction . . . 61
3.2 New evidence . . . 65
3.3 The model . . . 70
3.3.1 The FIRE model . . . 70
3.3.2 Learning about Trend . . . 74
3.4 Calibration and Computation . . . 78
3.5 Results . . . 81
3.5.1 Quantitative results . . . 81
3.5.2 Impulse Response Analysis . . . 86
3.5.3 Typical Default Episodes . . . 89
3.5.4 Output loss . . . 91
3.6 Sensitivity analysis . . . 93
3.6.1 Size of Errors about Trend Belief . . . 93
3.6.2 Long-Maturity Debt . . . 95
3.7 Conclusion . . . 96

Bibliography 98

A Appendix to Chapter 1 104
A.1 Deriving Optimal Consumption and Labour . . . 104
A.2 Solving Long-Maturity Debt with Taste Shock . . . 105

B Appendix to Chapter 2 109
B.1 Solving Long-Maturity Debt with Taste Shock . . . 109
B.2 Debt Price Schedules . . . 111

C Appendix to Chapter 3 114
C.1 First Order Conditions . . . 114
C.2 Algorithm . . . 116
C.3 Relevant Figures for Long-Maturity Debt . . . 117

List of Figures

1.1 Default Episodes Greece 15

1.2 Bond price with fixed productivity and capital 17

1.3 Bond price with fixed debt and capital 18

1.4 Default set with fixed productivity and debt/capital 19

1.5 Value functions with fixed productivity and debt 21

1.6 Contour slopes of spreads 22

1.7 IRFs to austerity shock 24

1.8 Illustration of model mechanism 26

1.9 Conditional IRFs to austerity shock 28

1.10 Debt price with $\rho_g = 0.95$ 30

1.11 Debt price with $\rho_g = 0.93$ 32

1.12 Conditional IRF to austerity shock, $\rho_g = 0.95$ and $\rho_g = 0.93$ 33

3.1 Spreads and trend forecasts data 68

3.2 Spreads and trend forecasts, Greek default 69

3.3 Debt Price with fixed growth beliefs 83

3.4 Spreads and trend beliefs, simulation 86

3.5 IRF to -1% transitory shock 88

3.6 Typical default episodes comparison, FIRE and Learning 90

3.7 Output Loss Illustration 92

A.1 Debt price with median productivity 108

A.2 Debt price with median productivity and fiscal shock 108

B.1 One-period debt price 112

B.2 Long-maturity debt price 113

C.1 Debt prices with different trend beliefs, long-maturity 118

C.2 IRF to -1% transitory shock, long-maturity 119

C.3 Typical default episodes comparison, FIRE and Learning, long-maturity 120

List of Tables

1.1 Parameters calibrated independently 12

1.2 Parameters calibrated to match business cycle statistics 13

1.3 Other business cycle statistics from data and simulation 14

2.1 Speed Comparison, 3 Algorithms for CPU, One-period Debt Model . . 47

2.2 Speed Comparison, LOES Algorithm, One-Period Debt Model 49

2.3 Speed Comparison, FV Algorithm, One-Period Debt Model 50

2.4 Speed Comparison, Matlab v.s. Julia, One-Period Debt Model 51

2.5 Speed Comparison, Long-Term Debt Model 55

2.6 Speed Comparison, neoclassical growth model via FV 58

2.7 Speed Comparison, neoclassical growth model via LOES 59

3.1 Correlation between spreads and potential GDP growth forecasts . . . 66

3.2 Data-Based Estimation of linear and non-linear relationships 69

3.3 Calibration, the Learning Model 80

3.4 Statistics from Data and Simulation 82

3.5 Simulation-Based Estimation of linear and non-linear relationships . . 85

3.6 Sensitivity analysis of trend uncertainty. 94

Chapter 1

Fiscal Austerity, Investment and Sovereign Default

1.1 Introduction

In late 2009 the Eurozone sovereign debt crisis surfaced. Sizable fiscal consolidation measures that feature sharp government spending cut is implemented for crisis-striken members, especially for the southern European countries. For instance, between 2010 and 2013, the Greek total government expenditure is cut by 27.8 billion euros, which is equivalent to 11.6% of the 2009 GDP[1]. These austerity measures were aimed at slowing down the rapid rise in governmental debt to GDP ratios, improving fiscal position and hence alleviating the accumulating doubts about solvency. On the contrary, sovereign default premium, measured as the spreads in government bond yields vis-à-vis default-free reference bond, kept rising as austerity packages were implemented[2]. For Greece, sovereign debt spreads grew continuously and eventually peaked at 22% before the 2012 default. This raises the question that, in terms of financial market response, whether austerity helps to mitigate or exacerbates the debt crisis.

[1]See the estimation in Gechert and Rannenberg (2015).

[2]See the figure A.2 in the online appendix of Born et al. (2020). Credit default swap (CDS) spreads, another measurement of default risk, also witnessed sharp increment in the meantime.

Although it is widely acknowledged that austerity slows down economic growth and hence undermines market confidence, whether this adverse effect outweighs the benefit of improved fiscal position is in heated debates. As it turns out, we should take the specific situations of the economy into account. For example, Cottarelli (2012) highlights a nonlinear relationship: the more fiscal tightening hurts growth, the more it will rise up spreads. When growth is less sensitive, austerity could lower spreads. Corsetti et al. (2012) also emphasizes that the question depends on financial circumstances: countries already facing a high and volatile risk premium is different from those enjoying negligible default risk. Recent empirical work in Born et al. (2020) verifies that the relationship between default premium and fiscal austerity is state-dependent: if the premium is initially high (low), government spending cuts will push the spread even higher (lower).

This paper seeks to answer the question of under what circumstances fiscal austerity increases or decreases sovereign debt spreads when the market takes the risk of default into pricing. To do so, I construct a stochastic dynamic model with three features. First, the model incorporates unsecured debt and strategic default. Following Chatterjee and Eyigungor (2012), the government issues unsecured long-term bonds and whether to default on this external debt is its endogenous choice. Foreign lenders charge a premium that accounts for this default risk. Second, motivated by the total investment decline in periphery Eurozone countries[3], the model includes capital accumulation as in Gordon and Guerron-Quintana (2018) and Arellano et al. (2018). Third, government expenditure follows a realistic fiscal rule as in Leeper et al. (2010) that consists of both an endogenous cyclical component and a discretionary spending shock. Fiscal austerity is modelled as a negative discretionary shock. The interplay of above characteristics generates intriguing dynamics: The combination of fiscal shock and King–Plosser–Rebelo utility (King et al., 1988) gives rise to wealth effect, while the co-existence of defaultable debt, wealth effect and investment contributes to a state-dependent relationship between discretionary fiscal policy and default premium.

Quantitative analysis shows that the above mentioned state-dependent relationship rationalizes the main empirical findings in Born et al. (2020). Specifically, in states

[3]Namely, Greece, Italy, Portugal and Spain, all severely affected by debt crisis and fiscal austerity in the 2010s.

of high total factor productivity (TFP) and/or low indebtedness, i.e. when spreads are initially low, fiscal austerity tends to reduce sovereign debt spreads. By contrast, when the economy has low TFP and/or high debt outstanding, i.e. spreads are initially high, fiscal austerity enhances the incentives of default and hence increases spreads to further higher levels. In other words, fiscal austerity helps to strengthen financial market confidence when the economy enjoys low spreads but could be self-defeating when foreign lenders already charge a high risk premium. Other fundamentals of the model drive the spread in a linear way: given government spending shock, spreads decrease (increase) as TFP and investment rises (drops), and ascend (descend) with more (less) debt. Policies functions have linear relationship with fiscal shock: austerity (expansion) leads to depresses (stimulates) investment and borrowing.

This paper also investigates the sources of state-dependent relationship between spreads to austerity. Default risk plays an essential role. When spending cut is implemented at small default risk, the market confidence boost from lower debt outstanding outweighs the adverse effect of lower production. Therefore, the spread slopes down. Conversely, when default risk is looming, the losses from economic slowdown outweigh the gains from better fiscal position and hence spreads rise up. Austerity shock reduces investment, which in turn exacerbates this state-dependent relationship: Reduction in capital stock reduces default risk when the risk is already small, but expands the risk when the economy is already on the brink of default[4]. As shown in the robust test, comparing with the default risk channel, the motion of capital only reinforces the state-dependent relationship.

What would happen if a debt crisis haunted economy implements unexpected spending-based consolidation? This question is answered with a case study of Greece where our model well matches Greek business cycle statistics and default episodes. It turns out the probability of encountering self-defeating austerity is non negligible: Debt spreads, as well as debt-to-GDP ratio and net repayment obligation, rise up following an austerity shock. The previously mentioned state-dependence plays an important role here. If the impulse response is conditional on the economy already

[4]Reader are referred to the discussion of "autarky channel" and "smoothing channel" in Gordon and Guerron-Quintana (2018) that supports the above mentioned exacerbation effects from incorporating investment.

having high risk premium, the spread surge becomes more than threefold higher than the unconditional case. By contrast, conditional on being in the states of enjoying low default premium, spreads immediately fall down. Eventually, in all three scenarios, spreads returns to the pre-shock level and fall even lower. The high persistence of austerity[5], the investment and production contractions all contribute to this result.

Literature review. This article is related to two strands of research. The first strand is on the recent sovereign debt crisis and fiscal austerity in southern European countries. Lane (2012) regards the pre-crisis periods as a missed opportunity to tighten fiscal policy, especially when individual member countries are restricted to use monetary tools to unwind the high stress in bond market. Gechert and Rannenberg (2015) argue that the 2010-2014 period is a wrong timing for fiscal austerity for Greece and the governmental expenditure cuts should have been gradually implemented after recovery. Mendoza et al. (2014) reveal that to implementing tax-based consolidation the Europe should evaluate the negative spillovers that work through international markets. House et al. (2020) estimate that austerity accounts for large cross-country GDP variations in advance economies. They show the highly contractionary austerity even worsened some countries' fiscal position. Kuang and Mitra (2021) exhibit a mutual reinforcement mechanism of austerity and pessimism, and the resulting prolonged recession in the European Union. The above three DSGE-based studies do not take sovereign default risk into consideration. Bi (2012) and Corsetti et al. (2013) find that government spending cut reduces risk premium when default risk is taken in account, Jointly incorporating default and investment, Galli (2021) advocates third-party liquidity support to correct the externalities associated with under-investment to realize good equilibrium in a debt crisis. However, default is not a strategic choice in above models. As will be shown in our paper, endogenous default is key to rationalizing the negative impact of fiscal retrenchment on sovereign debt spreads. Recent empirical finding in Born et al. (2020) of the state-dependent relationship between risk premium and unexpected fiscal spending cut[6] is a direct motivation to my paper.

[5]As mentioned in Kanellopoulos and Kousis (2018), Greek austerity has long duration: the first package was passed in 2010 and the recent package continues until at least 2020. In 2017, the fourteenth austerity package, Medium-term Fiscal Strategy Framework 2018-2021, was approved by the Hellenic Parliament.

[6]In stark contrast, David et al. (2022) show that news of the approval of austerity is related to spreads falls. However, their sample excludes developed economies, such as crisis-striken countries in recent Eurozone debt crisis.

The second strand of literature relates to models with sovereign default and fiscal policy. The endogenous/strategic default framework in this paper follows Eaton and Gersovitz (1981) and Arellano (2008), and the structure of long-term unsecured debt is borrowed from Chatterjee and Eyigungor (2012). I solve the convergence problem involved in long-term debt with the taste shock method in Gordon (2019). Our paper also relates to the papers incorporating capital within the endogenous default framework, such as Park (2017), Arellano et al. (2018) and Gordon and Guerron-Quintana (2018). Research on the impact of fiscal austerity within endogenous default models emerges in recent years. Arellano and Bai (2017) show that distortionary tax based austerity deepens recession. However, in their model, government spending is static and does not influence production. Bianchi et al. (2019) show that optimal fiscal policy could be procyclical: at higher debt levels, the government should cut spending to reduce the possibility of a default crisis. Anzoategui (2021) incorporates nominal wage rigidity and, as in our paper, calibrated government spending rule. He shows the likelihood of encountering self-defeating austerity is very small in the case of Spain, and it is related to the persistence of austerity and fiscal multiplier. Overall, these studies do not provide a rationale for the state-dependent relationship between spreads and austerity. Our paper fills this gap and provides detailed explanation of the mechanism behind the rationale.

The rest of this paper is organized as follows. Section 1.2 presents the model in detail. Section 1.3 shows that the model calibration provides a good match to Greek business cycle statistics and default episodes. Section 1.4 answers how fiscal austerity affects sovereign debt spreads. First I illustrate that government spending shocks impose state-dependent impacts on spreads. In later subsections, the mechanism for such state-dependence is comprehensively investigated and explained. We find that the likelihood of self-defeating austerity is non negligible. Section 1.5 presents the sensitivity analysis and highlights that the expected persistence of austerity matters. In the end, section 1.7 draws the conclusions.

1.2 The Model

The model is in discrete time and infinite horizon. It describes an economy populated with two agents: the representative household and a benevolent government.

1.2.1 Household

The representative household chooses optimal amount of consumption and labour supply to maximize expected discounted utility in infinite horizon:

$$\max_{C_t, H_t} \mathbb{E}_0 \sum_{t}^{\infty} \beta^t u(C_t, H_t) \tag{1.1}$$

where $u(\cdot)$ follows the widely used King–Plosser–Rebelo (KPR) form preference (King et al., 1988):

$$u(C_t, H_t) = \ln(C_t) - \theta \frac{H_t^{1+\chi}}{1+\chi} \tag{1.2}$$

where θ governs the magnitude of disutility of supplying labour, and χ denotes the inverse of Frisch elasticity. Consumption must satisfy a flow budget constraint:

$$C_t = Y_t - \tilde{I}_t - T_t \tag{1.3}$$

where Y_t is the domestic production, $\tilde{I}_t$ is the investment after capital adjustment cost and T_t stands for a lump sum tax imposed on the household.

1.2.2 Production environment

The production is determined by capital stock K_t, labour input H_t and exogenous productivity shock z_t. Production technology follows the standard Cobb-Douglass form:

$$Y_t = e^{z_t} K_t^{\alpha} H_t^{1-\alpha} \tag{1.4}$$

Productivity follows a standard AR(1) process:

$$z_t = \rho_z z_{t-1} + \varepsilon_t^z \tag{1.5}$$

with $|\rho_z| < 1$ and ε_t^z being independently, identically, and normally distributed, i.e., $\varepsilon_t^z \sim i.i.N(0, \sigma_z^2)$. The motion of capital is described by a standard law:

$$I_t = K_{t+1} - (1-\delta)K_t \tag{1.6}$$

where δ is a constant rate of capital depreciation. Following literature, a capital adjustment cost is included, because otherwise it is generally difficult to match the ratio of investment volatility over production volatility. We denote $\tilde{I}_t$ as the investment with capital adjustment cost, which is borrowed from Arellano et al. (2018):

$$\tilde{I}_t = I_t + \frac{\phi}{2}\left(\frac{K_{t+1} - K_t}{K_t}\right)^2 K_t \tag{1.7}$$

where parameter ϕ governs the magnitude of adjustment cost.

1.2.3 The government

The government is benevolent in the sense that it aims at maximizing the household's expected discounted utility. Long-maturity sovereign bonds B_t are issued by the government. Following Chatterjee and Eyigungor (2012), the issuer is obligated to pay coupon $\eta > 0$ for each unit of debt outstanding. In each period, a λ share of debt outstanding matures while the remaining $1-\lambda$ share does not. The principal and coupon repayment of maturing bonds equals $[\lambda + (1-\lambda)\eta]B_t$. New debts are issued at price q_t, and hence the net income from issuing sovereign debts is $q_t B_{t+1} - [\lambda + (1-\lambda)(\eta + q_t)B_t]$. The net cash flow from international lenders is transferred to the household to finance their consumption.

The government could either choose to honour or default its sovereign debt obligation. If debts are repaid, the country is defined to be in good financial status, indicated as the default indicator $\mathcal{D}_t$ taking the value of 0. Otherwise, the economy is in bad

financial status that is denoted as $\mathcal{D}_t = 1$ and the government cannot issue sovereign bonds in the international financial market. This "financial autarky" assumption is commonly used in endogenous sovereign default literature à la Eaton and Gersovitz (1981). Moreover, as commonly assumed in sovereign default models, the economy also suffers from an ad hoc productivity loss if it falls into bad financial status[7]. The loss function $L(z_t)$ takes a quadratic form as in Chatterjee and Eyigungor (2012):

$$L(z_t) = \max\left\{0, \kappa_1 \exp(z_t) + \kappa_2 \exp(z_t)^2\right\} \tag{1.8}$$

where κ_1 and κ_2 are parameters. See Uribe and Schmitt-Grohé (2017) for a discussion on different styles of default loss functions. The productivity after penalty is $e^{z_t} - L(z_t)$. In each period of the bad financial status, there is a constant probability μ that the country regains the good financial status, i.e. the access to external financing. Upon entering that status, financial autarky and productivity penalty are immediately lifted.

Government expenditure is determined by a fiscal rule as in Leeper et al. (2010):

$$G_t = \psi_1 Y_t + \psi_2(1 - \mathcal{D}_t)B_t + u_t^G, \qquad u_t^G = \rho_G u_{t-1}^G + \varepsilon_t^G \tag{1.9}$$

with $\psi_1 > 0$, $\psi_2 < 0$. u_t^G denotes an exogenous discretionary part of government spending, with $|\rho_G| < 1$ and $\varepsilon_t^G \sim i.i.N(0, \sigma_G^2)$. The spending is financed by net foreign debt borrowing $(1 - \mathcal{D}_t)\Big\{q_t B_{t+1} - \Big[\lambda + (1-\lambda)(\eta + q_t)\Big]B_t\Big\}$ and lump-sum tax revenue T_t. In other words, the government's budget constraint is:

$$T_t + q_t(B_{t+1} - (1-\lambda)B_t) = G_t + [\lambda + (1-\lambda)\eta]B_t \tag{1.10}$$

As in Bianchi et al. (2019) and Anzoategui (2021), I abstract from distortionary tax rates. According to House et al. (2020), other austerity measures such as cutting off transfers or raising taxes do not explain the cross country variation in GDP for European countries between 2010 and 2014. In fact, government expenditure cut remains significant during the recent Eurozone sovereign debt crisis even if the effects of business cycles are controlled. As shown in the Table 2 of Kuang and Mitra (2021) the structural balance of Greece rose up by 10 percent in 2012 comparing with 2009.

[7]Mendoza and Yue (2012) and Park (2017) offer examples of endogenous default loss.

1.2.4 Recursive representation

I denote $\mathcal{S} = (S, B, K, \mathcal{D})$ as the set of state variables of the model, where $S = (z, u^G)$ is the set of exogenous shocks. The government solves the following problem to determine whether or not outstanding sovereign debts will be repaid.

$$V(S, B, K) = \max_{\mathcal{D}=0,1} (1 - \mathcal{D}) V^g(S, B, K) + \mathcal{D} V^b(S, K) \tag{1.11}$$

where V^g is the value of being in good financial status, V^b refers to the value of being in bad status. Following the common assumption of no confiscation after default, capital K remains a state variable in V^b. Given productivity and government spending shock, the problem of repaying debt and maintaining a good financial status is characterized by:

$$V^g(S, B, K) = \max_{C,H,B',K'} u(C, H) + \beta \mathbb{E}_{S'|S} V(S', B', K') \tag{1.12}$$

subject to evolution law of capital (1.7) and resource constraint:

$$C = (1 - \psi_1)Y + qB' - \Big[\psi_2 + \lambda + (1 - \lambda)(\eta + q)\Big]B - \tilde{I} - u^G \tag{1.13}$$

The problem of falling into bad financial status is

$$V^b(S, K) = \max_{C,H,K'} u(C, H) + \beta \mathbb{E}_{S'|S} \Big[(1 - \mu)V^b(S', K') + \mu V(S', 0, K')\Big] \tag{1.14}$$

which is subject to (1.7) and resource constraint:

$$C = (1 - \psi_1)\Big(e^z - L(z)\Big)K^\alpha H^{(1-\alpha)} - \tilde{I} - u^G \tag{1.15}$$

$V(S, 0, K)$ indicates that in the re-entry period, all debt obligations are exempted. Given a debt and capital states, default ($\mathcal{D}(S, B, K) = 1$) is desirable when the value of repaying is smaller than the value of reneging:

$$\mathcal{D}(S, B, K) = \begin{cases} 0, & \text{if } V^g(S, B, K) > V^b(S, K). \\ 1, & \text{if } V^g(S, B, K) \leq V^b(S, K). \end{cases} \tag{1.16}$$

Sovereign debts are purchased by risk-neutral international lenders and they equate debt price to the expected discounted repayment:

$$q(S, B', K') = \frac{\mathbb{E}_{S'|S}(1 - \mathcal{D}')\Big[\lambda + (1 - \lambda)\Big(\eta + q(S', B'', K'')\Big)\Big]}{1 + r^*} \tag{1.17}$$

where $B'' = B(S', B', K')$ and $K'' = K(S', B', K')$ are debt and capital policies based on respective policy functions. Notice that there is no assurance of a solution for (1.17) when exogenous shocks and endogenous states are discrete (see Chatterjee and Eyigungor (2012) for a detailed discussion). The inclusion of capital in discrete term makes the convergence of value function iteration even more difficult, as discussed in Gordon and Guerron-Quintana (2018). Following the method proposed in Gordon (2019), I introduce taste shocks on the joint policies for debt issuance B' and investment K', which is denoted as A', as well as default choices $\mathcal{D}$ to facilitate the convergence of solving via discretized value function iteration approach. The method of introducing taste shocks has been used in recent sovereign default models with long-term debts, for example Arellano et al. (2020). Please see the appendix for any further detail.

Definition 1 (Model equilibrium)**.** Given exogenous state S, endogenous state of debt holding B and capital stock K, a recursive equilibrium of the model consists of policy functions of default choice $\mathcal{D}$, output Y private consumption C, working hours H, investment $\tilde{I}$, debt issuance B', capital policy K', value functions $V(S, B, K)$, $V^g(S, B, K)$, $V^b(S, K)$ and bond price schedule q, such that:

1. Given bond price schedule q, the value functions (1.11), (1.12) and (1.14) solve the economy's problem.
2. Given a default decision, sovereign debt price q satisfies risk-neutral rule (1.17).
3. Y, C, H and $\tilde{I}$ depend on equilibrium conditions and default loss function.

1.3 Quantitative Results

1.3.1 Calibration and business cycle statistics

The first group of parameters are calibrated following endogenous default literature, as shown in Table 1.1. The maturity structure of long-maturity bond is the same as in Chatterjee and Eyigungor (2012): debt matures with probability 5% ($\lambda = 0.05$, average maturity is 20 quarters) and coupon rate is 3% ($\eta = 0.03$). Following Na et al. (2018) the re-entry probability in each quarter μ is 0.0385, implying an average of 6.5 years of staying in autarky after default. The serial correlation of productivity shock takes 0.90, in line with Aguiar and Gopinath (2006) and other literature. For the discretionary part of fiscal rule, the persistence is calibrated to match a half-life of 6.5 years (i.e. $\rho_G = 0.975$) to be in line with the Greek governmental budget cuts from early 2010 to at least 2020 (see Kanellopoulos and Kousis (2018)) [8]. The standard deviation of ε_t^G is set to be 0.65 percent to match the insignificant correlation between Greek sovereign debt spreads and the government expenditure in the whole sample period[9]. Depreciation rate of capital stock takes the commonly used 2.5% per quarter in macroeconomics literature. Disutility of labour θ is chosen such that the steady state of labour is normalized to 1. Frisch elasticity of labour supply takes 3 ($\chi = 1/3$) to be within the range of the macro Frisch elasticities summarised in Peterman (2016).

The second group of parameters are summarized in Table 1.2. They are calibrated to match the business cycle statistics and the default episodes of Greece between 2000 and 2017. The default event is scheduled at March 2012 (Chambers and Gurwitz, 2014), when Greece and its external creditors completed a debt restructuring agreement. The parameters for the cyclical part of fiscal rule are similar to Kuang and Mitra (2021) and it matches the average government expenditure to GDP ratio. Productivity loss parameters ψ_1 and ψ_2, subjective discount factor β as well as the standard

[8]High persistence of government spending shock is common in the literature. For example, Leeper et al. (2010) estimates this parameter to be 0.97. Anzoategui (2021) estimates the persistence to be 0.95 in a case study of Spain. House et al. (2020) set the persistence to be 0.93 to match a half-life of 2.5 years. The impulse response analysis in a later section explores the cases with different ρ_G.

[9]The correlation is low because the sample includes both booming and crisis periods. As will be shown in the later part of this paper, this correlation is state-dependent.

Table 1.1: Parameters calibrated independently

Description	Parameters	Value
Share of capital	α	1/3
Relative risk aversion	σ	2
Probability of reentry	μ	0.0385
Coupon rate	η	0.03
Reciprocal of average maturity	λ	0.05
Depreciation rate	δ	0.025
Quarterly risk-free rate	r^*	0.01
Reciprocal of Frisch Elasticity	χ	1/3
Persistence of TFP shock	ρ_z	0.90
Persistence of government shock	ρ_G	0.975
Disutility of labour	θ	2.18

deviations of ε_t^z and ε_t^G are jointly calibrated to match the average sovereign spreads, the volatility of outputs and the average governmental debt-to-GDP ratio. As in other sovereign default models that incorporate capital accumulation, such as Park (2017), Gordon and Guerron-Quintana (2018) and Arellano et al. (2018), a high capital adjustment cost parameter ϕ is important to match the excess volatility of investment over output.

As shown in Table 1.3, the calibrated model is capable to match Greek business cycle statistics well. Simulated consumption is less volatile than output, which is typical for for developed economies. The counter cyclical movement of debt spreads and trade-balance-to-GDP ratios are also well replicated. As in data, spreads are negatively correlated with private sector consumption, investment and gross output, and positively related to trade balance.

Table 1.2: Parameters calibrated to match business cycle statistics

Calibrated Parameters		
Description	Parameters	Value
TFP loss parameter 1	κ_1	-0.700
TFP loss parameter 2	κ_2	0.790
Subjective discount factor	β	0.9825
Capital adjustment cost	ϕ	7
Fiscal rule parameter 1	ψ_1	0.5
Fiscal rule parameter 2	ψ_2	-0.02
Standard deviation of TFP shock	ε_t^z	2.75%
Standard deviation of government shock	ε_t^G	0.65%
Targeted Statistics		
Description	Data	Model
Average spread $\mathbb{E}(r - r^*)$*	4.68	4.51
Debt-to-GDP ratio $\mathbb{E}(B/Y)$*	78.6%	73.7%
Government expenditure to GDP $\mathbb{E}(G/Y)$	50.3%	48.7%
Standard deviation of output $\sigma(Y)$	11.5%	11.6%
Investment volatility $\sigma(I)/\sigma(Y)$	2.57	2.50
Correlation $\rho(r - r^*, G)$*	0.094	0.030

Notes: $r - r^*$ stands for the sovereign debt spreads. In the model, when the economy is in bad financial status, debt stock is zero, sovereign debt spread is not defined. Thus, statistics containing $r - r^*$ and B only covers the sample between 2000Q1 to 2012Q2.

Table 1.3: Other business cycle statistics from data and simulation

Description	Data	Simulation
$\rho(r - r^*, C)^*$	-0.22	-0.54
$\rho(r - r^*, I)^*$	-0.48	-0.52
$\rho(r - r^*, Y)^*$	-0.46	-0.25
$\rho(r - r^*, TBY)^*$	0.59	0.92
$\sigma(C)/\sigma(Y)$	0.93	0.79
$\rho(Y, C)$	0.85	0.63
$\rho(Y, I)$	0.90	0.68
$\rho(Y, TBY)$	-0.58	-0.26

Notes: In this table, TBY stands for trade balance to GDP ratio. Samples with * exclude default periods in data (periods after second quarter of 2012) and in simulation.

1.3.2 Typical default episodes

The changes of macroeconomic variables in default episodes are of general interest for quantitative endogenous sovereign default studies, such as Mendoza and Yue (2012). In Figure 1.1, each trajectory from the model is the averages of all simulated paths that include a default event. Default is normalized to happen at time zero. Each variable is exhibited within a window of 12 quarters before and after such a default event. For spreads and debt-to-GDP ratio the post-default periods are not included because they are not defined in bad financial status. As depicted in Figure 1.1 with red dashed lines, the Greek default is accompanied by the troughs in output, consumption and investment, by a surge in government debt-to-GDP ratio, by a peak in sovereign debt spreads, and by a fiscal consolidation in the form of government expenditure cut.

The model successfully replicates the default episodes of Greece at least in a qualitative way: the blue solid lines (from simulation) move in the similar trends as their respective red dashed lines (from data). The model predicts a decreasing government expenditure during the pre-default periods. Most importantly, as illustrated in the

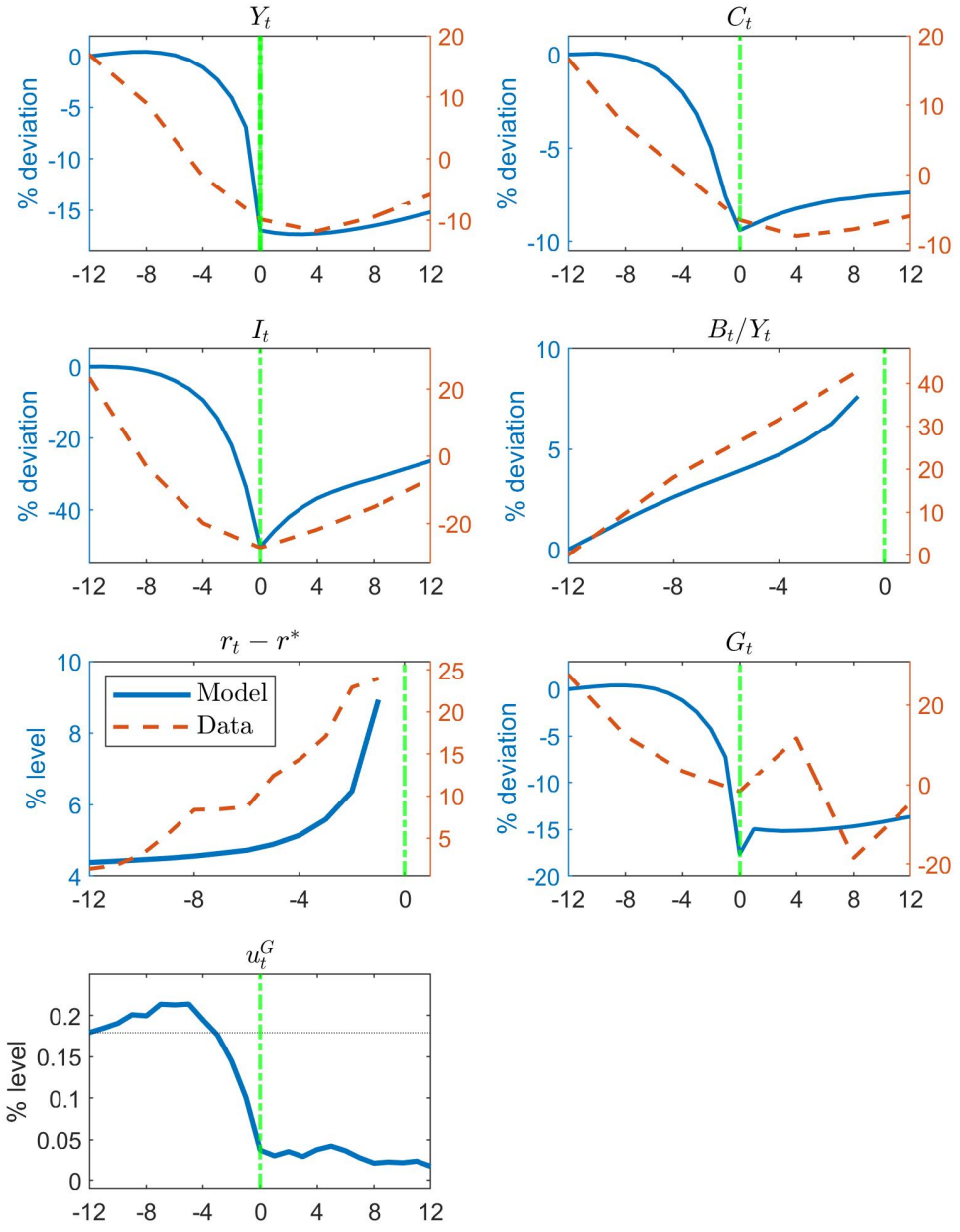

Figure 1.1: Default episodes from Greek data and model simulation. The default period is normalized to be zero and highlighted by a vertical green line. Period -4 indicates 4 quarters before the default and period 4 refers to 4 quarters after the default. The trajectories for Greek output, consumption, investment and government spending are drawn with HP-filtered.

last panel of Figure 1.1, government spending shock u_t^G experiences a sharp decline from period -5 to the default period, indicating that default is typically correlated with a fiscal austerity.

1.4 The state-dependent effects of fiscal austerity

As discussed in the introduction, the effects of fiscal austerity on the sovereign spreads are state-dependent. To be specific, the relationship between the exogenous state u_t^G and sovereign debt prices q_t depends on debt state B_t as well as exogenous productivity z_t. Figure 1.2 depicts the contour lines for the sovereign debt price schedules, $q(S, B', K')$. Holding z_t and K_t constant, the schedule is a function of only two variables, u_t^G and B_t. The "default set" illustrated in the figure corresponds to the coordinate points where default is the indebted country's optimal choice. As can be seen in the left panel where the debt outstanding is low, these contour lines are downwards sloping to the right, implying that government spending cut correlates to a higher debt prices (or lower debt spreads). However, in states of high debt levels (see the right panel of Figure 1.2) price contour lines have positive gradients. Moreover, the closer these contour lines are to the default set, the greater are the slopes. This demonstrates a converse relationship: low government shocks now correlate to low debt prices (or high spreads).

Figure 1.3 depicts debt prices as functions of government spending shock u_t^G and productivity shock z_t. In the first panel with low debt levels, a lower government shock leads to a higher debt price (or a lower spread). On coordinate points of high debt and high productivity (see the middle panel), this relationship persists but becomes weaker as the productivity goes down. At the bottom of the middle panel the contour line for price 1.11 is almost horizontal, suggesting that government shock impose little influence on debt price. Furthermore, if the economy is highly indebted and its productivity is low enough (the economy is in severe financial stress and default is very likely to happen) the above relationship will reverse. As can be seen in the last panel of Figure 1.3, the price contour lines slope downwards to the right, implying a deteriorating debt issuing price if fiscal austerity is implemented.

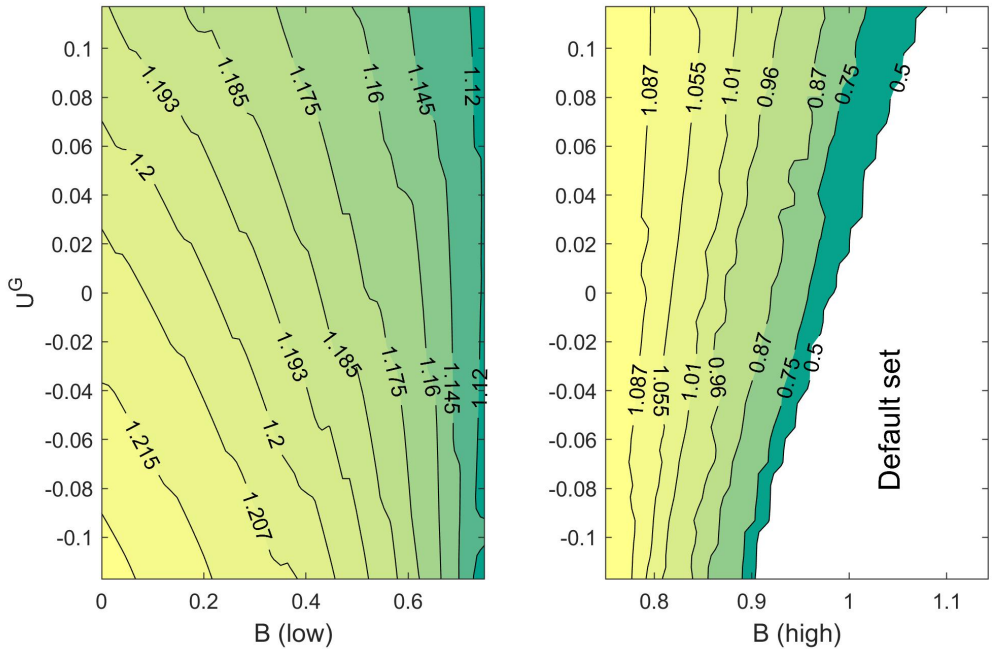

Figure 1.2: Contour lines for debt price $q(S, B', K')$, holding productivity at its unconditional mean and capital stock at its median level.

If economic fundamentals worsen further (either because of lower productivity or higher debt stock), it is optimal for the government to renege on sovereign debt obligations. The question is, how would fiscal austerity influence the borrowing country's default decision? According to the pricing rule (1.17), the expected default probability is positively related to spreads. Since it is shown that a government spending cut raises spreads in states near the default set, the default set itself should be enlarged. Figure 1.4 verifies the above conjecture: the default set D, whether defined as $D(B) = \{z : V^g \leq V^b\}$ (the left panel) or $D(K) = \{z : V^g \leq V^b\}$ (the right panel), enlarges after a low u^G shock.

In conclusion, fiscal austerity leads to lower debt spreads only if the economy is under low financial stress that features low external debt outstanding and high productivity. However, when the financial stress is high (high debt stock and low productivity) austerity becomes self-defeating: it results in lower debt issuing price, which indicates a worsening financial credibility for the borrowing country.

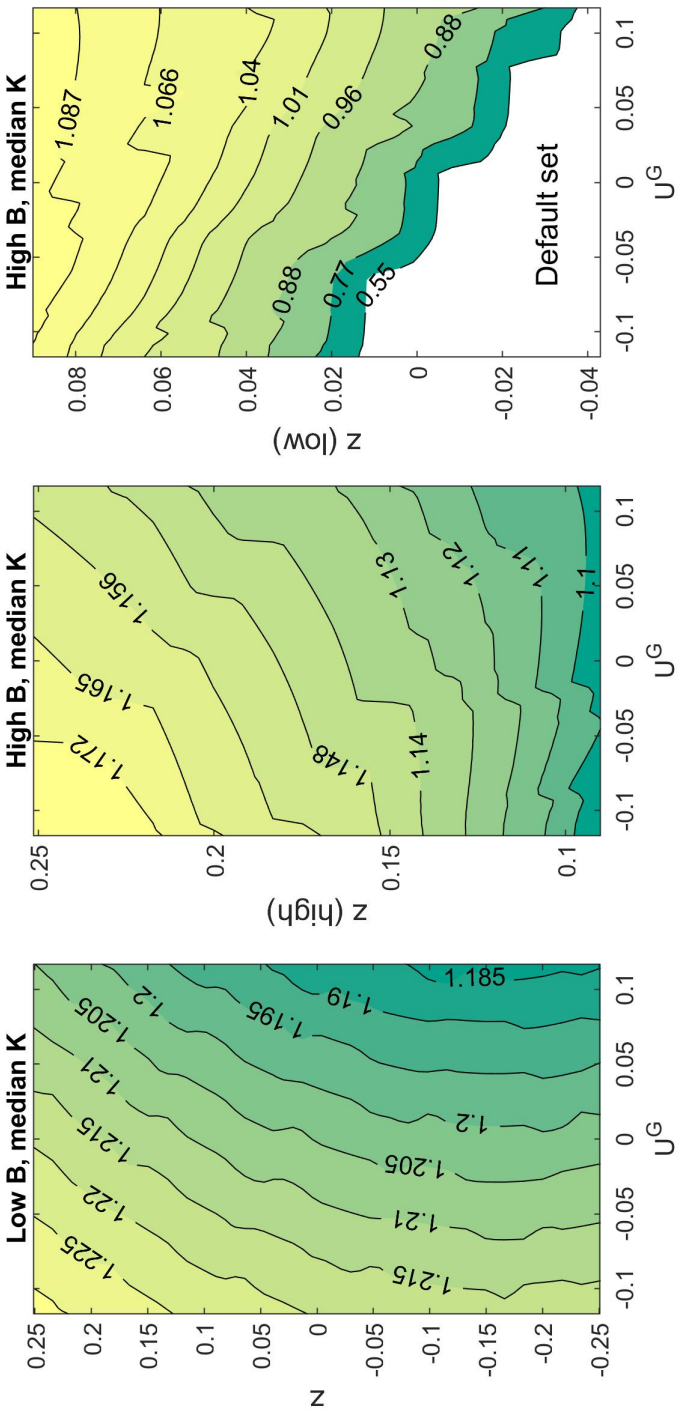

Figure 1.3: Contour lines of sovereign debt price, a function of productivity shock and government shock. Debt state fixed in each subplot (either at low or high level), capital state fixed at medium level. The first panel shows debt price contour with low debt, medium capital. (to be finished) When TFP is high, low govt shock is associated with high price (low spread). When TFP is low, low govt shock is related to low debt price (high spread).

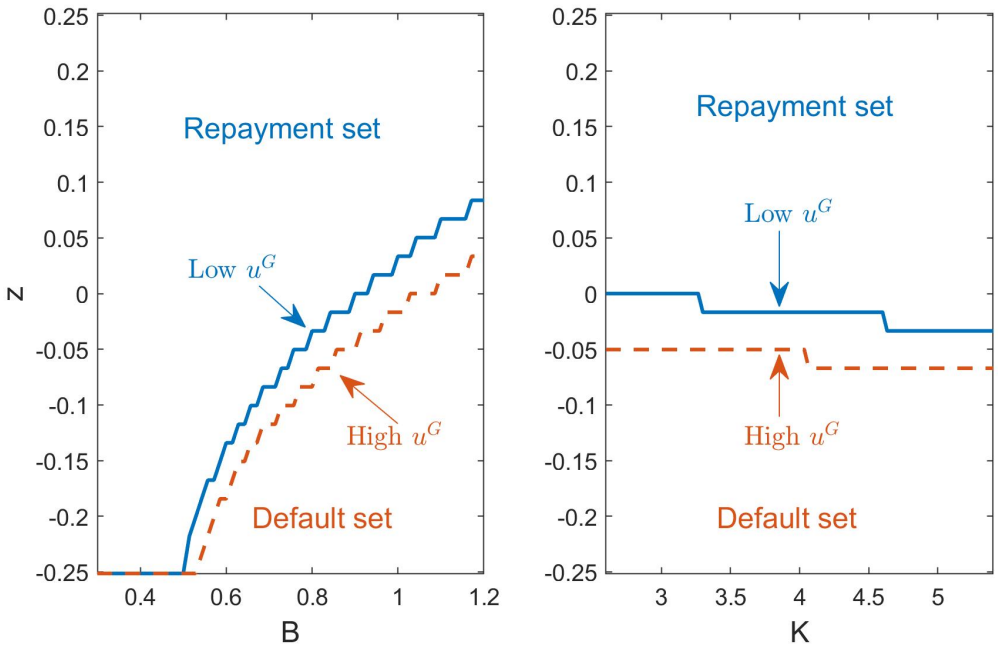

Figure 1.4: Default set as a function of TFP and debt. Low (high) govt spending shock is linked with large (small) default set. Default set as a function of TFP and capital. Low govt spending shock is linked with larger default set.

1.4.1 The role of capital

In next sections, I will explain the mechanism behind the state-dependent relationships between fiscal austerity and spreads. To begin with, it is necessary to understand how capital k and debt B influence debt prices. Figure A.1 and A.2 in the appendix depict debt prices as a function of K_t and B_t while keeping TFP and government shock u^G fixed at their respective unconditional means. We can see that higher B_t leads to lower prices, while K_t raises debt price for virtually any debt level.

We should be cautious on the interplay of capital, debt and TFP. Figure 1.5 shows the contour lines of the distinctions in value functions, $V^g - V^b$ with varying government shocks u_t^G and capital K_t. Smaller $V^g - V^b$ indicates the benevolent social planner holds stronger incentives to default and hence external creditors charge higher spreads. The upper panels show $V^g - V^b$ with debt outstanding fixed at high and low levels and TFP fixed at mean. The lower government shock reduces $V^g - V^b$ at almost everywhere but the relationship between capital state and value function difference depends on debt. At high debt levels (see the upper left panel), capital increases the difference. By contrast, at low debt levels, $V^g - V^b$ decreases with capital. There is similar state-dependence at different TFP levels if debt level is fixed. As illustrated by the lower left panel where the productivity is low, additional capital contributes to bigger distinctions in value of repayment and default. At high levels of TFP, $V^g - V^b$ decreases slowly as capital stock increases.

The role of capital could be explained using the terms from Gordon and Guerron-Quintana (2018). On the one hand, there is an "autarky channel" that under low financial stress (low debt level, high TFP level and low debt spread) capital enhances the benefit of default[10]. On the other hand, a counteracting force called "smoothing channel" kicks in when the economy suffers from high indebtedness and low productivity. Through this channel capital delays default because capital could either be

[10]The intuition of the autarky channel: If the country defaults with high capital stock, it may benefit from saving the debt repayments to external creditors and the production is not severely impaired because there is little need to borrow from external creditors to accumulate capital. Meanwhile, in modern history, physical assets in a default country's domain have not been confiscated by creditors, as documented in Tomz and Wright (2013). See Gordon and Guerron-Quintana (2018) for a detailed explanation for the autarky channel

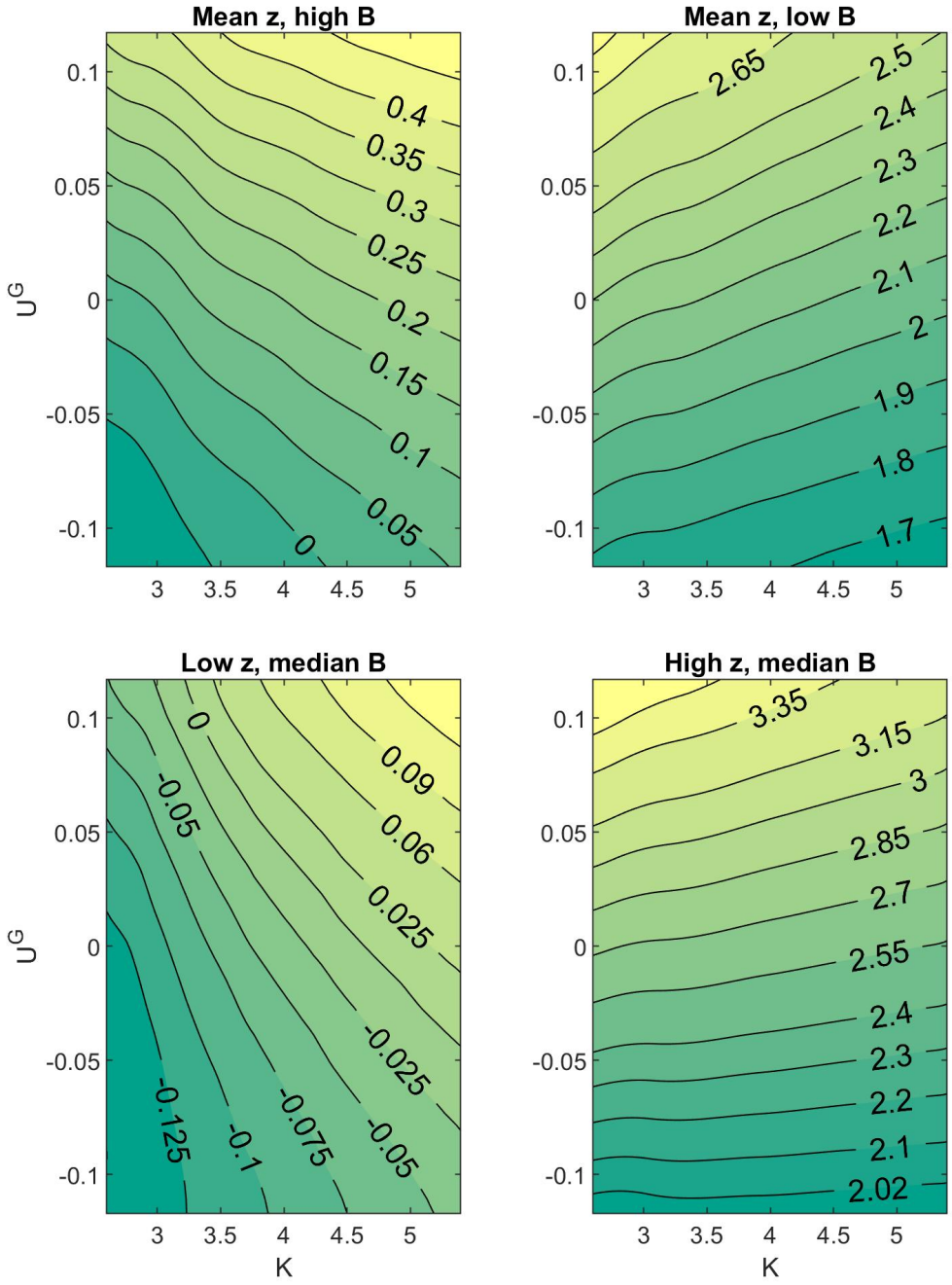

Figure 1.5: Contour lines for the differences between value functions of staying in good financial status V^g and falling to bad financial status V^b, i.e. $V^g - V^b$.

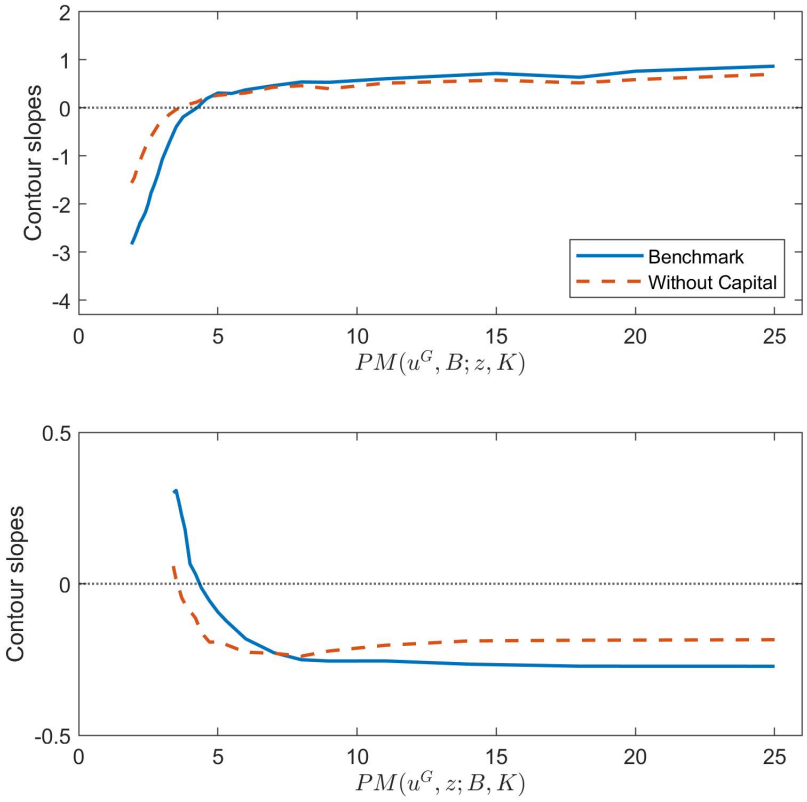

Figure 1.6: Contour lines slopes for different coordinates of states.

liquidated to fulfill repayment obligations or be invested into production to improve employment, boost production and improve the capability to repay debts. As in Gordon and Guerron-Quintana (2018), quantitatively the smoothing channel dominates the autarky channel[11] so that as shown by Figure A.1 and A.2 spreads declines as the capital stock decreases if debt outstanding is fixed at almost every level.

Comparing with the default risk channel, the capital channel plays a secondary role in determining the state-dependent relationship between spreads and austerity shock: It only reinforces the negative (positive) relationship between spreads and fiscal shock under severe (mild) financial stress. This could be verified by comparing our benchmark model with a model without capital, as illustrated in Figure 1.6. The upper

[11]Park (2017) provides an extreme case where the autarky channel is so powerful that the economy may optimally default during good times.

panel shows the spread contour slopes for states $(u^G, B; z, K)$ where productivity and capital are fixed at the levels of Figure 1.2. The blue solid line refers to the benchmark model while the red dashed line corresponds to the comparable model without capital (with productivities fixed at the same level). We can see the model without capital also displays state-dependent relationships between spreads and austerity. However, slopes for the benchmark contour are higher at high spreads but lower at low spreads, indicating that under severe (mild) financial stress the negative (positive) relationship between spreads and fiscal shock is stronger in the benchmark. Similar results are depicted for states $(u^G, z; B, K)$ (corresponding to the middle and right panels of Figure 1.3, but now the X axis is z and the Y axis is U^G. Debt states fixed at the same level): Contour slopes for the benchmark are lower (higher) than the alternative model under high (low) financial stress, indicating that austerity leads to bigger spread changes at the two extremes if capital is incorporated.

1.4.2 The role of wealth effect

The state-dependent effects of fiscal austerity is closely linked to the above mentioned state-dependent role of capital. While this link relies on wealth effect, which arises from the inclusion of KPR style utility function and government spending shock. In Figure 1.7, the impact of fiscal austerity in the form of government spending cuts is visualized by Generalized Impulse Response Functions (GIRF) that are drawn following the method of Koop et al. (1996). The GIRF refers to the average of shocked paths in simulation. As in Arellano et al. (2018), if a simulated path includes a default event in the reported 27-period window, the path will be excluded from the calculation, The response functions in blue solid lines come from the benchmark calibration model where the persistence of government spending shock ρ_G is 0.975.

Following a -1.5% government shock, the output Y_t drops immediately by nearly 1.7% from its pre shock average. The implied fiscal multiplier $\partial Y_t / \partial G_t$ is 1.5 [12], which is in the range of estimations in literature. Because of lower lump-sum tax imposed on her income, the representative household feels wealthier and decides to consume

[12]Fiscal multiplier is calculated by dividing the impulse response of Y_t by the impulse response in government spending G_t. Note that G_t is not shown in Figure 1.7.

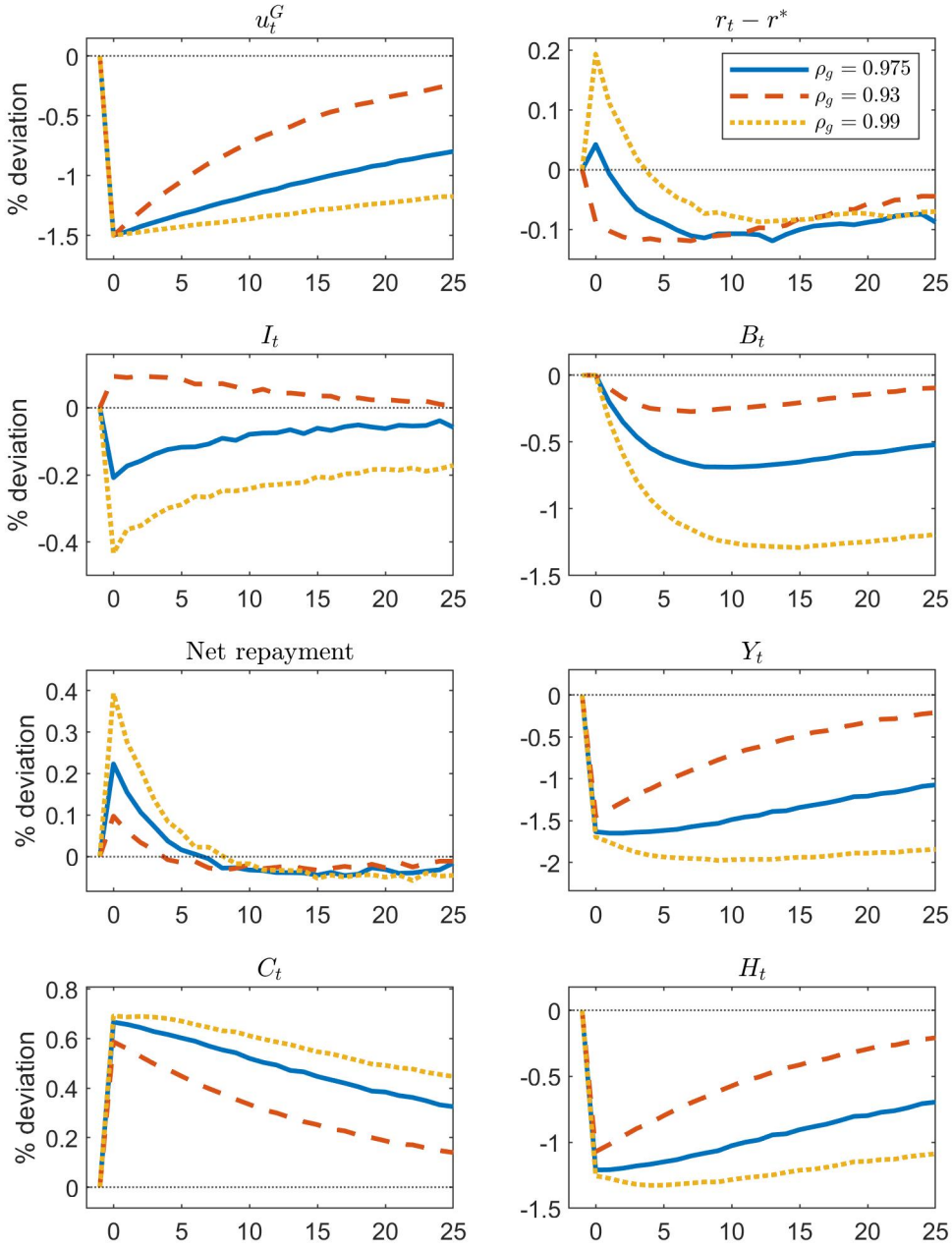

Figure 1.7: Generalized impulse response functions (IRF) for a negative 2% government spending shock. IRF for the models with different ρ_G exhibited. The benchmark ρ_G is 0.975. The innovation is normalized to hit the economy on period 0.

more ($C_t \uparrow$) and work less ($H_t \downarrow$, the definition of wealth effect). In the benchmark model wealth effect is so strong that investment must decline to satisfy the national income balance. Expecting lower capital, foreign lenders hold lower expectation about production and debt repayment and hence charge higher spreads. Meanwhile, the household would substitute cheap lump-sum tax reduction for expensive sovereign debt in financing her consumption, i.e. the "substitution effect"[13]. It is well understood that lower debt outstanding decreases debt spreads (see quantitative sovereign default models such as Arellano, 2008; Chatterjee and Eyigungor, 2012 and Mendoza and Yue, 2012) but as shown in Figure 1.7 this "indebtedness effect" is overwhelmed by the contrary influence from the smoothing channel of capital. Notice that an expected rise in spreads reinforces the decline in capital: because of lower income from debt issuance, the net repayment on debt obligations, i.e. $-q_t B_{t+1} + [\lambda + (1-\lambda)(\eta + q_t)]B_t$, would be higher. As a consequence, the borrowing country has to liquidate additional capital to fulfill the repayment.

The importance of the wealth effect could be further demonstrated by comparing the GIRFs across different values of government shock persistence, ρ_G. Ceteris paribus, higher ρ_G increases wealth effect and vice versa. Comparing with the benchmark, in the case of $\rho_G = 0.99$ the output is expected to be on a lower track, the decline of investment almost doubles, and the surges in sovereign spreads and net debt repayment are much higher. When ρ_G decreases to 0.93, wealth effect is much weaker so that the investment even rises above its pre-shock average level. Therefore, the vicious circle of the expected capital liquidation and spreads rising is absent. Notice that now although the spread decreases, net repayment still slightly increases because optimal debt issuance B_{t+1} goes down. Unlike the cases of higher wealth effect, this downward movement of B_t is not owing to higher interest rate: the increment in capital and decline in lump-sum tax jointly reduce the attractiveness of expensive external financing.

In the long run, austerity has opposite effects on spreads. In the benchmark model, spreads drop below the pre-shock level in three periods and keeps being lower in the next 23 periods. Similar long-run effects is found in the alternative calibrations. The reason is that although fiscal austerity impairs economic activities, it does adjust debt

[13]The impulse response analysis in Bianchi et al. (2019) also reveals this effect.

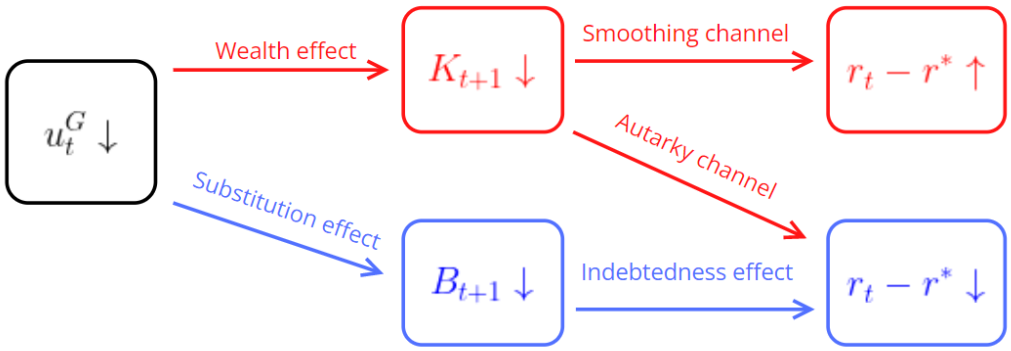

Figure 1.8: Illustration of the price change to fiscal austerity policy.

outstanding downwards and hence there is "indebtedness effect" that improves solvency. In the long term, financial stress improves because the "indebtedness effect" outweighs the weakening negative influences on production and employment.

1.4.3 Explaining state dependence

Knowing the role of wealth effect and investment, the illustrated state-dependent relationships between government spending shocks and sovereign spreads could be well explained. Figure 1.8 summarizes these effects. The blue chain refers to the case that capital is excluded from the model: Fiscal austerity is equivalent to reduction in lump-sum tax and hence there is the substitution effect that the household reduces the demand of expensive foreign borrowing B_{t+1}, while the lower expected indebtedness leads to better solvency and lower debt spreads. The inclusion of capital provides an additional mechanism as depicted in the red chain. Because of a large wealth effect, austerity decreases investment (recall the impulse response analysis) and the consequent effect depends on the competition between the smoothing channel and autarky channel. The former prevails under high financial stress and drives debt spreads higher. By contrast, the latter dominates the former for states of low financial stress and reduces spread.

Back to Figure 1.2, at high debt levels (right panel), the smoothing channel dominates the autarky channel and indebtedness effect and therefore the net effect of lower capital policy K_{t+1} and debt policy B_{t+1} is higher spreads. As shown by the upward sloping contour lines, low levels of government shock is related to low debt prices. Conversely, at low levels of debt outstanding (left panel of Figure 1.2) financial stress becomes mild and the autarky channel eventually outweighs the smoothing channel. Hence, an austerity policy is increasingly associated with a higher debt price. As depicted by the right panel those contour lines slope increasingly downward as the debt outstanding declines.

Following a similar logic, Figure 1.3 could also be well explained. With medium capital level and low TFP, the smoothing channel dominates and hence lower government shocks lead to lower capital stock and lower debt prices (see right panel). At higher levels of TFP, the autarky channel gradually takes over and as a result u_t^G reduction is increasingly associated with higher prices (see middle panel). The left panel is more complicated. At the coordinate points of low debt and high TFP (see the upper half of the left panel), financial stress is low and the autarky channel plays the leading role. Thus, at lower levels of u_t^G the associated low capital and debt policies jointly contribute to higher debt price. High productivity improves solvency so that price increases from the southeast to the northwest corner on the coordinate plane. At the lower half of the subplot, when z_t goes down financial stress increases but the autarky channel still outweighs the smoothing channel. Therefore, lower levels of capital and debt policies raise debt price and hence the contours on the lower panel bends and becomes vertical.

Now we can also rationalize the impact of fiscal austerity on default set as shown in Figure 1.4. As in most sovereign default models, the default set resides in states of high debt outstanding and low TFP and here the smoothing channel outweighs the combination of the autarky channel and indebtedness effect. Following a reduction in government shock u_t^G, the adjustment in debt is too small to cancel out the adverse effect from investment decline and hence default becomes more desirable: As verified by Figure 1.4, default sets for both $D(B)$ (left panel) and $D(K)$ (right panel) will expand.

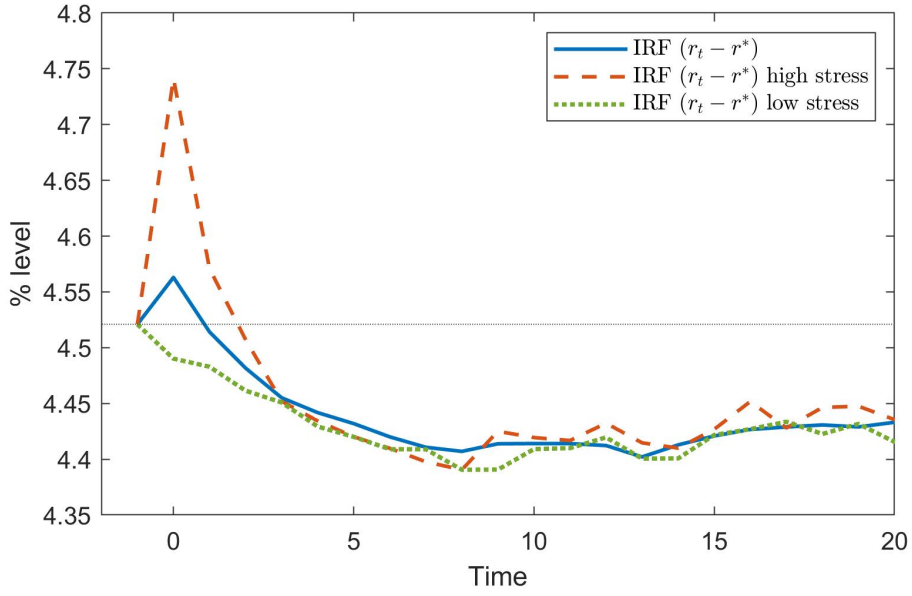

Figure 1.9: Generalized impulse response functions (IRF) for a negative 1.5% government spending shock across different levels of financial stress. The innovation hits the economy on period 0. High financial stress is defined as the states where $z \leq -0.02$ and $b \geq 0.7$, while being in low financial stress means $z \geq -0.02$ and $b \leq 0.7$. The IRF $(r_t - r^*)$ comes from the benchmark model, same as the counterpart in figure 1.7.

To further stress the state-dependence, I propose an experiment as shown by Figure 1.9. The solid blue line is the standard spread impulse response following a -1.5% government spending shock. The dashed red line depicts the debt spread in response to the same shock with an additional condition: the economy is under high financial stress that features high debt and low TFP levels. This condition excludes most of the states where the autarky channel and indebtedness take control. We should expect higher spreads because in the remaining state fiscal austerity leads to lower capital and the dominant smoothing channel increases default probability. Figure 1.9 corroborates this conjecture: comparing with the blue line, the spread surge conditional on being under high financial stress is tripled. Similarly, the green dotted IRF is conditional on the economy being under low financial stress and now the spread decreases on impact.

1.5 Sensitivity Analysis

1.5.1 Persistence of fiscal shock

From previous analysis, we know ρ_g governs the magnitude of wealth effect and hence the responses of spreads to austerity shock $-u^g$: Under high (low) financial stress, austerity tends to raise (decrease) debt spreads. In this section, We change the value of persistence of the government spending shock process, i.e. ρ_g, to see if the outcomes of fiscal austerity changes. Specifically, whether the state-dependence and the self-defeating effect still exist.

We first reset ρ_g to be 0.95 as in Anzoategui (2021), which indicates the half-life of fiscal shock shrinks from 6.5 years ($\rho_g = 0.975$) to 3 years and a quarter. Figure 1.10 illustrates the debt price contours across different outstanding debt and productivity states. When productivity and capital stock are jointly fixed at their respective median levels (upper panels), austerity (low government spending shocks) shrinks debt spreads (raises prices) if debt is initially low but enhances spreads (decreases prices) if debt outstanding is high. Meanwhile, as shown by the lower panels, state-dependence arises when debt outstanding and capital stock are jointly controlled at their respective high

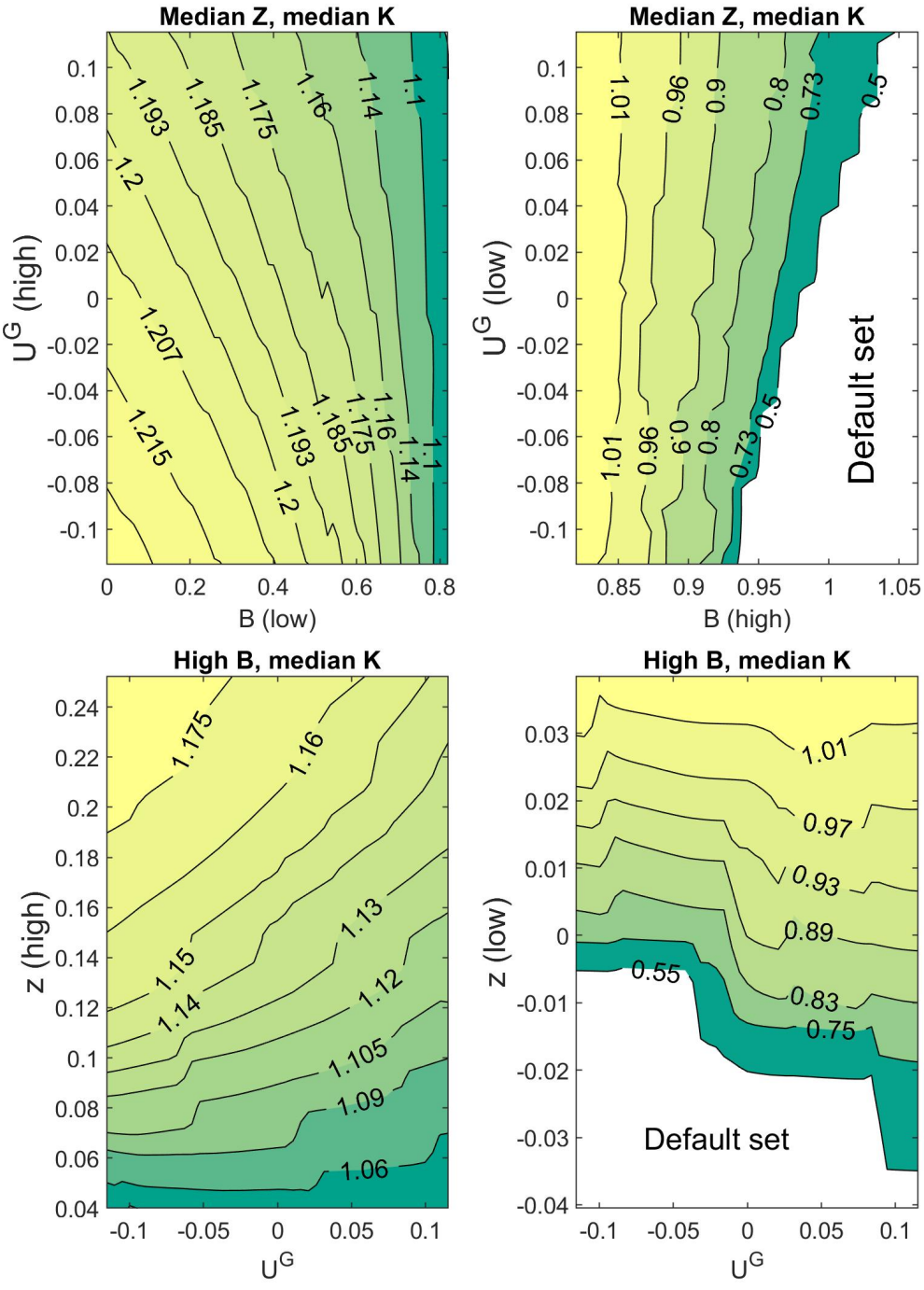

Figure 1.10: Contours of debt price, $\rho_g = 0.95$.

and median levels. Again, fiscal austerity pushes spreads up under high financial stress (lower right panel that features high debt and low productivity) but depresses spreads at higher levels of productivity.

Next we set $\rho_g = 0.93$ (as in House et al., 2020), which corresponds to a short 2-year 1-quarter half life. From the price contours (Figure 1.11), we can see that the state-dependence still exists but the positive relationship between austerity and debt spreads weakens: 1. The magnitude of the contour slopes diminishes as ρ_g decreases. 2. The supports of this relationship shrinks as ρ_g goes down. Taking the $(B(high), u^G)$ states for example, the support narrows from [0.75, 1.1] at the $\rho_g = 0.975$ case to [0.81, 1.1] at $\rho_g = 0.95$ and further to [0.9, 1.1] for the $\rho_g = 0.93$ case.

In Figure 1.12, I draw the conditional impulse response functions for $\rho_g = 0.95$ and $\rho_g = 0.93$. We can see that with lower persistence in the fiscal shock process, the spread surge under high financial stress decreases and even becomes negative when $\rho_g = 0.93$. Meanwhile, the spreads drops immediately upon the austerity shock at the average and low financial stress. In conclusion, the probability of encountering self-defeating austerity declines if the policy is (expected to be) short-term.

1.6 Discussions

Policy implications. The model provides useful policy implications: austerity could have produced better results if it had been implemented when the the economy were under mild financial stress. Similar arguments could be found in Lane (2012), Gechert and Rannenberg (2015) and Born et al. (2020). Unfortunately, the Greek fiscal consolidations packages were introduced at an awkward timing: the country was carrying a too high level of external debt outstanding and was mired in the aftermath of the Great Recession. Therefore, there is a high probability that the market perceives the harms of austerity outweighs the benefits. Another implication is to support investment, maintain employment and production and hence to enhance the capability to repay debts for those countries in distress. However, we have to be cautious with the implementation of expansionary fiscal policy during bad times. Growing government

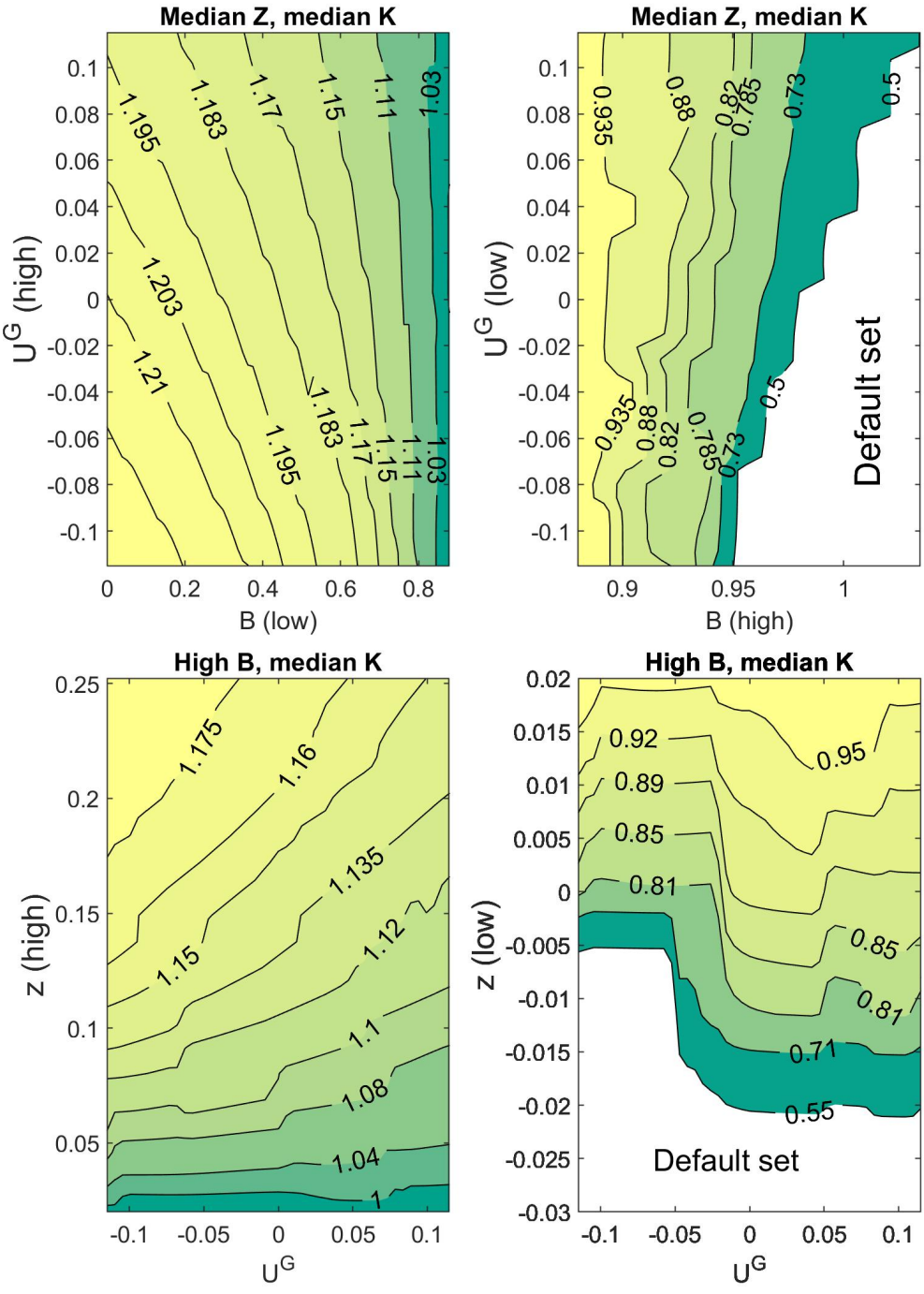

Figure 1.11: Contours of debt price, $\rho_g = 0.93$.

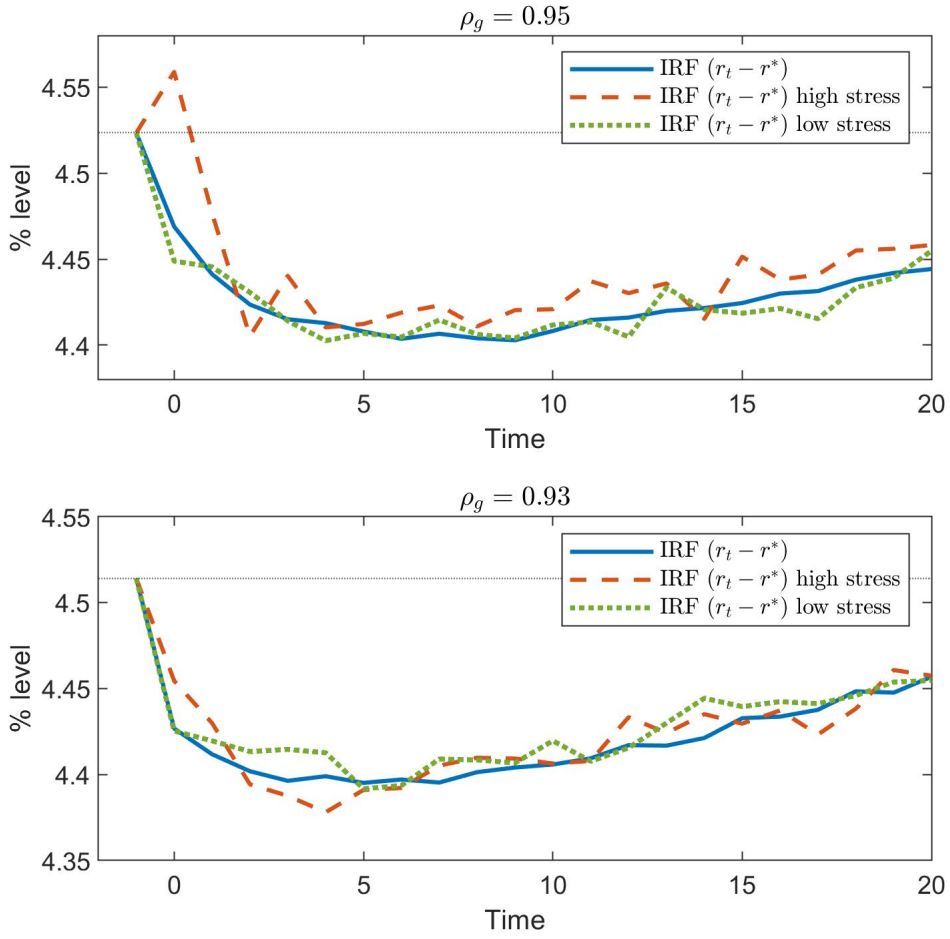

Figure 1.12: Impulse response functions to a 1.5% fiscal austerity shock conditional on different levels of financial stress. The upper panel shows the case of $\rho_g = 0.95$ while the lower panel shows the $\rho_g = 0.93$ counterparts.

spending funded by additional external debts may fuel the suspicion of deteriorating solvency, especially if markets are not convinced of its stimulative effect. In that sense, as argued in Galli (2021), an external financial support can be valuable.

Scope limitations. While contributing to studying how fiscal austerity influences sovereign debt spreads, this paper has several limitations: First, the paper does not explore the impact of spreads on fiscal austerity. In fact, the surge of spreads may induce the indebted country to implement austerity, as in Bianchi et al. (2019) and Aguiar et al. (2022). Thus, if the economy is under high financial stress (austerity leads to higher spreads), we can expect a vicious circle of spreads rising and austerity. Second, the debt pricing rule in the equation (1.17) only incorporates default risk. Other factors such as liquidity problems, inflation risks, exchange rate risks are excluded.

1.7 Conclusion

In this paper I propose an endogenous sovereign default model to study the influences of fiscal austerity on sovereign debt spreads. The model is calibrated to Greece and matches its default episodes around 2012: a typical simulated default is accompanied with austerity. The analysis of model solutions reveals state-dependent influences: when the borrowing country is highly indebted and in recession, i.e. being under high financial stress, austerity increases spreads and vice versa. Because debt crisis usually happens during such vulnerable periods, the probability of encountering self-defeating austerity would be non trivial. The mechanism for such a state-dependence relies on the existence of default risk and incorporation of capital accumulation.

The paper contributes literature in several ways: To my knowledge, it provides the first theoretical research based on endogenous default model that stresses the importance of capital accumulation to determine the outcomes of fiscal austerity. Second, it rationalizes the empirical evidence of state-dependent influences of fiscal austerity on sovereign spreads. Third, it shows that the probability of encountering self-defeating austerity is non trivial at least for countries like Greece. Fourth, it reveals that the high degree of persistence of austerity plans is crucial to the adverse effects.

Chapter 2

Matlab-Based GPU Computation of Sovereign Default Models

2.1 Introduction

This paper discusses the efficient numerical solving for non-linear macroeconomic models. Discretized Value Function Iteration (DVFI) method has been widely applied to this type of problems because it is suitable to address the inherent kinks and endogenous choice dependent variables in such models. To implement DVFI, the state space should be discretized into grid points and integration is in terms of probability weighted average (addition). Endogenous sovereign default models[1] in the Eaton and Gersovitz (1981) framework belong to this strand of models: the option to default leads to kinks and the equilibrium debt price depends on policies. Hence, such models need to be solved via DVFI[2]. However, solving via the DVFI is typically slow because this method usually leads to large-scale matrix multiplication and hundreds of iterations. This problem worsens when more state variables are included and hence the number of

[1] Also called equilibrium default model or quantitative default model.

[2] Local solution based on perturbation method, such as first-order approximation in Uhlig (1995) and Sims (2002) as well as higher order approximation in Schmitt-Grohé and Uribe (2004), is not feasible for endogenous sovereign default models. Readers are referred to the second section of this paper for an detailed explanation.

grid points grows exponentially. Meanwhile, calibrating means such models need to be repeatedly solved. Therefore, accelerating the DVFI is of interest to macroeconomic researchers using sovereign default models as well as other non-linear models, such as the heterogeneous agents model, as workhorses.

This paper proposes a method to achieve the acceleration of solving with DVFI: to implement DVFI on the Matlab Parallel Computing Toolbox with GPU (Graphic Processing Unit). The advantages for choosing this platform is twofold. First, most macroeconomists currently use Matlab programming language (Coleman et al., 2021). Besides, Matlab's parallel computation toolbox has always been well maintained, updated and optimized by professionals. Moreover, this GPU language is easy to write. The intuition behind GPU acceleration is that this device is designed to employ large amount of processors [3] to accomplish mathematical computation in a synchronized manner. Hence, GPU has been intensively used in high-performance computation like deep learning. While CPU (Central Processing Unit) is a generalized processor that cannot handle parallelization as efficiently as a GPU. Second, parallelization with GPU is accessible at home. Nowadays personal computers (even laptops for home use) that possess a discrete NVIDIA GPU are easy-to-find and affordable. CPUs with a large number of processors are expensive and usually installed in supercomputers.

The endogenous sovereign default models discussed in the paper includes the one-period bond model as in Arellano (2008) and the long-maturity bond model from Chatterjee and Eyigungor (2012). The long-maturity case is more complicated in calculation and hence it provides a good example for exploring the relationship between computation efficiency improvement and complexity of codes. We find that the improvement from GPU could reach tenfold. Although this paper focuses on solving sovereign default models, the GPU parallel coding could be easily adapted to solve other complex dynamic stochastic general equilibrium (DSGE) models. In the latter part of the paper, I apply the Matlab GPU computation to solve a classic neoclassical growth model. The time consumed in solving shows that the GPU approach provides even larger efficiency improvement (over 20 times) for such a simpler DSGE model. In this paper, the efficiency improvement is defined by comparing the time consumed for

[3]For example, the GPU device used in this paper, NVIDIA RTX 3060 Laptop Version, has 3,840 cores while the CPU device, Intel Core 11800H, has only 8 cores.

solving a model in GPU approach with the non parallelized CPU approach[4].

The paper contributes to the efficient computation of endogenous sovereign default models in several aspects. First, it provides a comparison of three algorithms that implement the DVFI method to solve sovereign default models. The record of time consumed in solving dislikes the frequently used Full Vectorization (FV) algorithm but favours the use of a single loop, i.e., the Looping Over Exogenous Shocks (LOES) algorithm. In LOES, only the grid points for the exogenous shock (in this paper this shock is the endowment income for debt issuing country) are in the loop index. The Looping Over All States (LOAS) algorithm, where the loop indices cover all grid points of the state variables (in this paper, these variables are endowment and debt outstanding), requires two layers of loop and it is the slowest among all 3 algorithms. This result not only holds for the CPU computation but is also robust to the GPU approach[5]. Apart from being slower than LOES, the FV algorithm is much easier to encounter the out-of-memory problem[6]. The likelihood of encountering this problem is much larger if the model has more than one endogenous state, for example when capital accumulation is incorporated. Like the LOES, the LOAS algorithm effectively avoids the memory trap but its speed is usually lower than FV[7].

Second, the efficiency improvement from switching to GPU on Matlab is similar to the application of GPU with Julia via Julia CUDA. When GPU computation is accompanied with the LOES algorithm on Matlab to solve the one-period debt sovereign default model, it takes only 30 percent of the time spent in solving the same model

[4]In the scope of this paper, GPU computation denotes to using the "gpuArray()" command to distribute array elements to the GPU memory and hence enable the GPU parallel computing. The CPU computation refers to the execution of code on Matlab without using the CPU-based parallel command, i.e. "parfor".

[5]Usually, efficient algorithms for CPU also work well for GPU device. See Mathwork® web page Measure and Improve GPU Performance for detailed discussion.

[6]More specifically, the size of data that Matlab sent to a random access memory (RAM) exceeds the limit in MATLAB Workspace Preferences (usually very close to the upper limit of the RAM)

[7]Matlab is an interpreted language and hence using multiple layers of loops in Matlab significantly reduces computation efficiency. Compiled languages like C/C++ and FORTRAN are way more efficient in using LOAS algorithm.

with Julia CUDA, which is reported in Guerrón-Quintana (2021)[8]. Overall, comparing with CPU, the speed-ups from using GPU on Matlab could be near 10 times, very close to the acceleration from applying GPU computation in Julia. Therefore, switching to Julia does not seem to be more attractive than Matlab in terms of the benefit from GPU devices. Comparing with Matlab, the macroeconomist community is still less familiar with Julia. Last but not least, with 25% more efficient CPU, this paper reports a solving with Matlab that is 3 times faster than the reported Julia CPU results.

In terms of the third contribution, the speed enhancement of GPU computation relative to CPU depends on the complexity of applied algorithm. Incorporating taste shocks to facilitate solving long-maturity debt default models leads to more complicated codes and higher computation workload, which decreases the efficiency improvement from 10 times to 7 times. To further explore this point, I write Matlab codes to solve the neoclassical growth model that is much simpler to solve than sovereign default models: 1. only a single value function needs to be updated during each iteration[9]; 2. sovereign debt price depends on the expected difference between value functions while the neoclassical growth model does not have such computation workload. The time records of solving such a simpler model show that the acceleration from GPU could be as high as 21 times.

This paper is closely related to the literature on solving macroeconomics with GPU computation. Guerrón-Quintana (2021) implement Julia CUDA to solve a sovereign default model with one-period debt. They also discuss Julia specific acceleration techniques and coding recommendations. The magnitudes of Julia GPU speed-up relative to Julia CPU could reach tenfold, which is similar to this paper. However, the comparable time spent in solving via either Julia CPU or GPU is significantly higher than the respective Matlab results in this paper. Aldrich et al. (2011) show that using CUDA C, a dialect of C/C++ that enables using NVIDIA GPU, to solve a neoclas-

[8]For floating-point performance, the GPU device used for this paper (NVIDIA RTX 3060 Laptop Version) outperforms that in Guerrón-Quintana (2021) (NVIDIA RTX 2060 Laptop Version) by 90% (8.76 TFLOPS vs 4.61 TFLOPS). Hence, under the same programming language, the time spent in GPU computation on my laptop should theoretically take more than 50% of the time spent on their laptop.

[9]For sovereign default model, two new value functions need to be computed — the value of repayment (and hence being in good financial status) V^G and the value of default (and hence falling into bad financial status) V^B.

sical growth model provides huge speed improvement comparing with utilizing CPU. However, macroeconomists are usually unfamiliar with C/C++ and mastering this language requires a steep learning curve. Fernández-Villaverde and Valencia (2018) provides pedagogical guidance for using CPU and GPU parallel computation to solve a life-cycle model. Although they implement the computation on many different platforms, such as Julia, Matlab, R, Python, C++, their codes are not optimized to each of these languages and hence the computation speed comparison should be interpreted with caution. Coleman et al. (2021) test the efficiency of solving neoclassical growth model with DVFI method on Matlab, Python, Julia[10]. They parallelize the computation on CPU and find the speed across three platforms similar. However, the speed for any of the three languages they report fall significantly behind the counterparts in this paper.

The rest of this paper is organized as follows. In Section 2, I test LOES, FV and LOAS algorithms on both CPU and GPU devices to solve sovereign default models with one-period and long-maturity debt. I find the LOES prevails and with that algorithm applying GPU could provide tenfold acceleration over CPU. I also replicate the Julia solve model in Guerrón-Quintana (2021) on my Matlab to compare the speed of the two languages. Section 3 delivers a robustness test: I use neoclassical growth model to evaluate the computing speed as in Section 2. I find that as code complexity and computational workload increase, the speed advantage of the GPU deteriorates. I draw the conclusion in Section 4.

2.2 Endogenous Sovereign Default Models

In this section I discuss 3 algorithms to solve endogenous sovereign default models à la Eaton and Gersovitz (1981) with either one-period or long term sovereign debt. I first show that solving with a single loop (the LOES algorithm) over all grid points of the exogenous state is faster than the conventional full vectorization method as well as a double loop method (LOAS). Second, I show that GPU computation provides a significant solving acceleration over the CPU for both the short-term and long-term

[10]This strand of results is illustrated in Table 3 of Coleman et al. (2021).

debt models. Third, we can see that incorporating long-term debt to the endogenous default framework results in higher computation workloads and hence slows down the solving with either CPU or GPU and deteriorates the speed-up benefits of GPU over CPU.

2.2.1 The Model with One-Period Debt

The sovereign default model with one-period debt follows Arellano (2008). In each period the economy receives an exogenous endowment income y that follows an AR(1) motion law:

$$\log(y) = \rho_y \log(y) + \varepsilon^y, \quad \varepsilon^y \sim i.i.N(0, \sigma^y) \tag{2.1}$$

The social planner solves the following optimization problems to determine debt issuance b' and whether to default $\mathcal{D}$. To begin with, the value of repaying debts and hence maintaining good financial status is denoted as

$$V^G(y, b) = \max_{b' \geq 0,\, c \geq 0} u(c) + \beta \mathbb{E}_{y'|y} V(y', d') \tag{2.2}$$

subject to budget constraint

$$c = y - b + q(y, b')b' \tag{2.3}$$

where b is the outstanding sovereign debt, b' is the debt issuance (policy) and $q(y, b')$ is the issuing price of debt. The value of default and therefore falling into bad financial status is

$$V^B(y) = u(y - L(y)) + \beta \mathbb{E}_{y'|y} \Big[(1 - \mu) V^B(y) + \mu V(y', 0) \Big] \tag{2.4}$$

where $L(y)$ is the endowment cost owing to the bad financial status. It follows the quadratic loss function as in Chatterjee and Eyigungor (2012):

$$L(y) = \max \left\{ 0, \kappa_1 y + \kappa_2 y^2 \right\} \tag{2.5}$$

where μ is an exogenous probability to re-enter the international financial market if the country is already in bad financial status. Notice that at the re-entry period, the

country is exempted from previous debt obligations. Finally, the social planner decides whether to default by comparing the value of repayment to that of default:

$$V(y,b) = \max_{\mathcal{D}=0,1}(1-\mathcal{D})V^G(y,b) + \mathcal{D}V^B(y) \tag{2.6}$$

If $V^G - V^B > 0$, the social planner chooses not to default, i.e. $\mathcal{D}(y,b) = 0$. If $V^G - V^B \leq 0$, default becomes the optimal choice, i.e. $\mathcal{D}(y,b) = 1$. Debt issuing price is determined by risk-neutral foreign lenders:

$$q(y,b') = \mathbb{E}_{y'|y}\Big[1 - D(y',b')\Big]/(1+r^*) \tag{2.7}$$

where r^* denotes the world risk-free interest rate.

Definition 2 (Recursive equilibrium)**.** Given endowment y and debt outstanding b, a recursive equilibrium of the sovereign default model with one-period bond has following elements:

1. A set of value functions $V^G(y,b)$, $V^B(y)$ and $V(y,b)$
2. Debt issuance $b'(y,b)$ and default decision $\mathcal{D}(y,b)$.
3. A debt price function $q(y,b')$ such that
   (a) Given bond price $q(y,b')$ and budget constraint equation (2.3), the value functions (2.6), (2.2) and (2.4) solve the social planner's problem and provides the default rule $\mathcal{D}(y,b)$.
   (b) Given $\mathcal{D}(y,b)$ the price of sovereign bond satisfies the risk-neutral rule (2.7).
   (c) The bond price solves problem (2.6) and the debt issuing policy solves (2.2).

The solutions to such sovereign default model are numerically derived via the discretized value function iteration (DVFI) method. To implement such method, the state space is discretized into candidate grid points, expectation is the probability weighted sum of discrete states while the value functions and debt price function are based on the coordinates of grid points. In other words, this paper does not use off-the-grid methods to find the debt policy. Readers interested in off-the-grid methods

are referred to Hatchondo et al. (2010) where the robustness of Chebyshev collocation and spline interpolation methods are discussed.

Perturbation methods, or local approximation methods, are not suitable to solve sovereign default models (Guerrón-Quintana, 2021). Reasons are as follows. First, the optimization problems are different between the good and bad financial status. Therefore, the value $V(y, b)$ and policy $\mathcal{D}$ have kinks, which makes the problem not differentiable at the default threshold. Second, the debt price is a function of expected default decision $\mathcal{D}$, which is a function of expected debt issuance and itself is an endogenous variable. Hence, we need a global optimization approach like DVFI to solve the model and time-saving local perturbation methods are not feasible. The above-mentioned second problem adds additional difficulties to the convergence of solving. For example, Arellano et al. (2016) report that solving endogenous default model with envelop condition method (ECM), which provides huge speed improvement than DVFI for neoclassical growth model, easily runs into convergence problems. Convergence becomes more difficult if long-maturity debt is incorporated.

2.2.1.1 Algorithms for Discretized Value Function Iteration

In this section I compare three algorithms to apply the DVFI method to either CPU or GPU. It should be noted that all models are solved using the one-loop method[11] as defined in Hatchondo et al. (2010) That is, value functions and bond price are simultaneously updated in each iteration. To begin with, I show the general DVFI algorithm for one-period debt sovereign default model, as in Algorithm 1.

There are three versions of codes to implement DVFI. The first version is referred to as the full vectorization method (FV) that is used in Arellano (2008). In the FV, all candidate coordinate points for the value and price functions are vectorized in the "while" loop. Specifically, the $V_0^G(y, b)$, $V_0^B(y, b)$ and $q_0(y, b')$ functions are reformulated to be $V_0^G(y \times b, b')$, $V_0^B(y \times b, b')$ and $q_0(y \times b, b')$ such that each row index of the matrices corresponds to a combination of y and b states while each column

[11] As reported in Hatchondo et al. (2010), this one-loop approach is significantly more time-saving than the two-loop method that is widely used in earlier default models.

Algorithm 1: FV algorithm for DVFI

Data: Initial guesses for value functions V_0^B, V_0^G, V_0, debt price q_0, a tolerance threshold tol and Δ such that $\Delta > tol$

Result: The value functions V^B, V^G, V, debt policy B' and debt price q.

Initialization;

while $\Delta > tol$ **do**

Given debt price q_0, derive consumption c with equation (2.3) and value functions for being in good V^G and bad financial status V^B with equation (2.8), (2.2) and (2.4);

Calculate the default indicator as $\mathcal{D}(y, b) = V^G - V^B$ and the risk-neutral price $q(y, b')$ as in equation (2.7);

Calculate the aggregate maximum norm Δ between the old and new value functions and debt prices $\Delta = \| V^G - V_0^G \| + \| V^B - V_0^B \| + \| q - q_0 \|$;

Set $V^G = \max\{V^G, V^B\}$, $V_0^G = V^G$, $V_0^B = V^B$, $V_0 = V^G(y, 0)$ and $q_0 = q$; otherwise, end the loop;

end

index relates to a grid point of the candidate debt choice. The number of grid points for debt choice is the same as debt state. Hence, all the matrices fed into 2.4 and 2.2 are $(N_y \times N_b, N_b)$ matrices if the numbers of grid points for y and b states are respectively N_y and N_b. In consequence, the updated $V^G(y,b)$, $V^B(y,b)$ and $q(y,b')$ will be $(N_y \times N_b, 1)$ column vectors because the debt policy b'^* has been found. They should be reshaped into (N_y, N_b) matrices for the next iteration within the "while" loop. For Matlab, matrix operation would automatically utilize multiple CPU cores and hence using FV algorithm benefits from that.

The second algorithm features a naive "looping over all states" (LOAS) that uses multiple loops to separately visit the grid points of all state variables. In the scope of this paper, this method incorporates two loops within the "while" loop: the outer loop operates on the grid points of endowment y while the inner loop iterates on the grids of debt outstanding b. Hence, for each pair of grid points the state variables (y_i, b_i), we evaluate a $(1, N_b)$ welfare vector, i.e. $u + \beta \mathbb{E}_{y'|y} V_0^G$, to obtain the updated value functions and policy. The pseudo code listed in Algorithm (2) provides a detailed explanation. In the illustration, $\mathbb{Y}$ and $\mathbb{B}$ respectively denote the set of grid points for exogenous state y and endogenous state b. LOAS algorithm is straightforward and widely used in coding with complied languages, such as C/C++ and FORTRAN. It is less used in Matlab (an interpreted language) because of its inefficiency in executing multiple lays of loops.

The third method is called the "looping over exogenous shocks" (LOES) algorithm. Within the "for" loop, grid points for the endowment y_i are sequentially visited and at each visit the corresponding value and price functions $V^G(y_i, b)$ and $q(y_i, b')$ are evaluated. For each grid point of y we need to calculate an (N_b, N_b) welfare matrix to find out the value function V^G and the corresponding debt policy B'. All value and policy functions are $(1, N_b)$ vectors in the "for" loop and these vectors are integrated into (N_y, N_b) matrices to execute the next iteration in the outer "while" loop. Therefore, the LOES algorithm could be regarded as a mix of FV and LOAS. The details of LOES are illustrated in 3.

Algorithm 2: LOAS algorithm for DVFI

while $\Delta < tol$ **do**

  for *Each grid point of* $\mathbb{Y}$, y_i **do**

    for *Each grid point of* $\mathbb{B}$, b_i **do**

      $c = b' \times q(y_i, b') - b_i + y_i$;

      $[V^G(y_i, b_i), B'(y_i, b_i)] = \max\{u(c) + \beta \mathbb{E}_{y'|y_i} V_0^G\}$;

    end

  end

  $V^B(y, b) = u(y - L(y)) + \beta \mathbb{E}_{y'|y}(\mu V_0 + (1 - \mu) V_0^B)$;

  if $V^G(y_i, b_i) > V^B(y_i, b_i)$ **then**
    $\mathcal{D}(y_i, b_i) = 0$

  else
    $\mathcal{D}(y_i, b_i) = 1$

  end

  $q(y, b') = (1 - \mathbb{E}_{y'|y} \mathcal{D}(y, b))/(1 + r^*)$;

  Calculate Δ and update value functions, debt price and debt policy;

end

Algorithm 3: LOES algorithm for DVFI

while $\Delta < tol$ **do**

  for *Each grid point of* $\mathbb{Y}$, y_i **do**

    $c = b' \times q(y_i, b') - b + y_i$;

    $[V^G(y_i, b), B'(y_i, b)] = \max\{u(c) + \beta \mathbb{E}_{y'|y_i} V_0^G\}$

  end

  All else the same as in Algorithm (2);

end

2.2.1.2 The Results of One-Period Debt Model

In the quantitative implementation, the utility function follows the standard constant relative risk aversion (CRRA) form:

$$u(c) = \frac{c^{1-\sigma} - 1}{1 - \sigma} \tag{2.8}$$

For the calibration, the risk aversion parameter σ is 2 and the discount factor β takes 0.90. The endowment loss parameters are $\kappa_1 = -0.35$, $\kappa_1 = 0.44$. The risk-free interest rate is set to $r^* = 0.01$. Following Uribe and Schmitt-Grohé (2017), the endowment process is characterized by $\rho_y = 0.93165$ and $\sigma^y = 0.03696$[12] to match the Argentina default in 2001. The AR(1) process for endowment is approximated via a probability transition matrix $\mathbb{E}_{y'|y}$ that is drawn following the Tauchen (1986) method. $\mathbb{Y}$ consists of 25 equally spaced grid points within the 4.2 standard deviations above and below the unconditional mean of endowment process. The probability of re-entering international financial market is fixed at 0.0385 (Chatterjee and Eyigungor, 2012) indicating a 6.5-year exclusion on average. Debt outstanding relative to the unconditional mean of endowment is in the interval of $\mathbb{B} \in [0, 2]$. The tolerance threshold for the value function iteration, i.e. tol, is set to be $1e^{-7}$.

The grid points for debt policy are equally discretized within the debt state $\mathbb{B}$. Several numbers of grid points for b are used to implement the solving: 200, 600, 1500, 3000, 6000. As argued by many quantitative researches on sovereign default model such as Hatchondo et al. (2010), this number should be large enough to provide a good approximation. For single endogenous state (debt) case, using 400 grid points seems to be satisfactory (Uribe and Schmitt-Grohé, 2017). However, if two endogenous states are incorporated the corresponding total number of grid points for state variables could be very large. For example, using 50 grids for debt as well as capital results in

[12] See the Chapter 13 of Uribe and Schmitt-Grohé (2017).

$50 \times 50 = 2500$ grids in total[13] and we need to search throughout the 2500 grid points to locate the best policy that maximizes the debt issuing country's welfare. Therefore, it is of interest to explore the case of large set of grid points for debt in this single-endogenous-state sovereign default model to shed light on the case of multiple endogenous states.

Table 2.1: Speed Comparison, 3 Algorithms for CPU, One-period Debt Model

Debt Points	LOES	FV	LOAS
200	0.887	2.437	5.038
	(0.3424)	(0.9410)	(1.9452)
600	10.484	25.94	37.15
	(3.666)	(9.069)	(12.989)
1500	91.17	163.24	201.84
	(30.800)	(55.149)	(68.190)
3000	394.36	N.A.	651.30
	(131.45)	(N.A.)	(217.10)
6000	1654.66	N.A.	2273.23
	(528.64)	(N.A.)	(726.27)

Notes: The time spent in solving is in seconds. Figures in brackets represent the average solving time multiplied by 100. The Full Vectorization (FV) algorithm results for debt points 3000 and 6000 are not available because the computer will run out of memory.

The remaining of this section provides following findings: First, as shown in Table 2.1, I compare the performance of above-mentioned three algorithms performed on CPU. Second, I pick the best performing LOES algorithm[14] to be executed on Matlab

[13]For example, Park (2017) discretizes debt and capital state spaces respectively into 200 and 800 grid points. He uses parallel computing with 30 CPU cores to handle such large computation workload. Na et al. (2018) uses 200 grids for debt and 150 grids for lagged real wage as two endogenous state variables and solving that model requires 189,650 seconds on a desktop with an Intel Xeon 3.5 GHz CPU and 256GB RAM, which is far more powerful than the personal laptop used as an experimental platform for this paper.

[14]GPU computation with LOAS algorithm is not reported because it is much slower than FV and LOES.

Parallel Computation Toolbox with GPU devices and compare its performance with the CPU approach. The results are reported in Table 2.2. Finally, for the GPU computation, the FV method is faster than LOES for small numbers of debt grid points but falls behind LOES when the number of debt grids goes larger (See Table 2.3). We measure the speed of computation by the time consumed in executing the outer "while" loop in each case.

Before reporting the results, it is necessary to clarify the experimental platform. All computing performance experiments are conducted on a Dell G15 5511 Laptop with Windows 11 operating system. The CPU used is an Intel® Core™ i7-11800H with 2.30 GHz and the Random Access Memory (RAM[15]) is 2×8 GB with 3200 MHz. The discrete Graphic card is a NVIDIA® GeForce RTX™ 3060 (Laptop version) with 6 GB memory. The GPU computation mentioned in this paper uses double precision to be in line with CPU, although that device is designed to be more efficient when operating at single precision[16]. All versions of programs run on the 2021b version of Matlab software.

As can be seen in Table 2.1, for CPU computation the LOES algorithm is superior to the frequently used FV algorithm in endogenous sovereign default studies, such as Aguiar and Gopinath (2006), Arellano (2008) and Na et al. (2018), etc. On the one hand, the computation time consumed by the FV method is about 2 times bigger than the LOES counterpart. On the other hand, the LOES method effectively avoids the out-of-memory problem that the FV method easily encounters when the number of debt grid points exceeds 1500. The reason is that the value function to evaluate is an $(N_y \times N_b, N_b)$ matrix in the FV method. With LOES, for each grid point of y_i the value matrix to evaluate is of (N_b, N_b) size and this matrix is rewritten (thus the memory is reused) for the next stride y_{i+1}. The LOAS method also use small size of value matrices $((1, N_b))$ but it falls behind of LOES. This drawback is mainly attributed to that Matlab is an interpreted and untyped language and hence it has to read the "max" function, check the inputs and outputs of a function each time it is called. While the function is call N_y times in the LOES but $N_y \times N_b$ times in the LOAS. Therefore,

[15]The size and memory frequency of RAM significantly influences the performance of CPU computation.

[16]For computer, the the largest ϵ that makes equation $1 + \epsilon = 1$ hold is smaller than $1e^{-16}$ under double precision. For single precision, the largest ϵ would be $1e^{-8}$.

LOAS spend much more time in reading and checking the functions. Notice that this speed difference narrows down with the expansion grid points of debt: $\frac{LOAS}{LOES}$ is 5.68 at $N_d = 200$ but $\frac{LOAS}{LOES}$ falls to 1.37 at $N_d = 6000$.

Table 2.2: Speed Comparison, LOES Algorithm, One-Period Debt Model

Debt Points	CPU	GPU	$\frac{\text{CPU}}{\text{GPU}}$
200	0.887	3.386	0.262
	(0.3424)	(1.3074)	-
600	10.688	5.428	1.969
	(3.7371)	(1.8978)	-
1500	91.17	16.06	5.677
	(30.800)	(5.4251)	-
3000	394.36	47.23	8.349
	(131.45)	(15.744)	-
6000	1654.66	178.35	9.278
	(528.64)	(56.98)	-
12000	7263.60	1185.82	6.125
	(2194.44)	(358.25)	-

Notes: The time spent in solving the One-Period Debt Model is in seconds. Figures in brackets represent the average solving time multiplied by 100. GPU compuation with LOAS algorithm are not reported because they are very slow on Matlab. For a comparision between LOES and FV algorithm, please find it in Table 2.3.

Next, the model is solved via GPU basing with the LOES algorithm. A comparison of efficiency between CPU and GPU is reported in Table 2.2. For small number of debt grid points, i.e. $N_b = 200$, applying GPU does not pay off. As N_b grows larger, the speed improvement from GPU significantly increases. At $N_b = 600$, GPU computation is 2 times faster than CPU. At $N_b = 6,000$, the acceleration from GPU reaches the peak of 9.3 times. If the N_b keeps growing, the advantage of GPU seems to wane but the scale of speed-up is still over 6 times. Overall, under LOES algorithm, the GPU has significant advantage in solving one-period debt sovereign default model with a

large number of grid points.

Table 2.3: Speed Comparison, FV Algorithm, One-Period Debt Model

Debt Points	CPU	GPU	$\frac{\text{CPU}}{\text{GPU}}$	$\frac{\text{GPU(FV)}}{\text{GPU(LOES)}}$
200	2.437	1.056	2.307	0.312
	(0.9410)	(0.4079)	-	-
600	25.94	4.086	6.349	0.753
	(9.069)	(1.4285)	-	-
1500	163.24	27.46	5.946	1.710
	(55.149)	(9.2758)	-	-

Notes: The time spent in solving the One-Period Debt Model is in seconds. Figures in brackets represent the average solving time multiplied by 100. The Full Vectorization (FV) algorithm results for debt points higher than 1500 are not available because in that cases the computer run out of memory.

Finally, I investigate the efficiency difference between GPU and CPU when the FV algorithm is applied. FV consumes longer time than LOES if we use CPU computation. From Table 2.3, we can see that utilizing GPU device with LOES underperforms GPU with FV for small numbers of grid points, i.e. $N_b = 200$ and $N_b = 600$. However, as the number expands to 1500, the LOES algorithm becomes more efficient. Meanwhile, the speed-up from GPU with the FV algorithm seems to hit the upper limit at $N_d = 600$ and then drops to 5.95 times at $N_d = 1,500$. This further supports using LOES algorithm to implement GPU computation. The results of LOAS are not reported because under that algorithm GPU computation is much slower than CPU as LOAS has multiple layers of "for" loops. Intuitively, GPU's better performance over CPU comes from synchronization while too many "for" loops significantly increases the number of serial operations.

Table 2.4: Speed Comparison, Matlab v.s. Julia, One-Period Debt Model

Debt Points	CPU(Matlab)	$\frac{\text{CPU(Matlab)}}{\text{CPU(Julia)}}$	GPU(Matlab)	$\frac{\text{GPU(Matlab)}}{\text{GPU(Julia)}}$
100	0.1070	8.47%	1.4470	87.2%
	(0.0378)	-	(0.5113)	-
500	2.0206	18.64%	1.5788	43.4%
	(0.7140)	-	(0.5579)	-
1000	6.3850	17.3%	2.5766	39.4%
	(2.2562)	-	(0.9105)	-
5000	268.38	32.3%	27.42	32.7%
	(95.17)	-	(9.7247)	-

Notes: The time spent in solving the One-Period Debt Model is in seconds. Figures in brackets represent the average solving time multiplied by 100. CPU (Matlab) and GPU (Matlab) respectively denotes the time spent under the LOES algorithm on Matlab with CPU and GPU, while CPU (Julia) and GPU (Julia) respectively corresponds to the Julia CPU and GPU run time reported in the Figure 11 of Guerrón-Quintana (2021).

2.2.1.3 Comparing with Julia

In this section, I compare the Matlab CPU/GPU solving efficiency with the results reported in Guerrón-Quintana (2021), whose experiments are performed with Julia and Julia CUDA. For comparability, I replicate the one-period debt sovereign default model and the corresponding calibration in their paper: now the endowment after default loss is $(1-\tau)y$ where τ is a constant parameter taking the value 0.15. The endowment process takes the same form as equation (2.1) but is calibrated as $\rho_y = 0.9$, $\sigma_y = 0.025$. Debt state is equally discretized with $\mathbb{B} \in [0, 1]$ and $N_y = 7$. Apart from that, subjective discount rate is $\beta = 0.953$, world risk-free interest rate is $r^* = 0.017$, re-entry probability is $\mu = 0.28$.

It should be noted that the CPU and GPU device in this paper outperforms those used in Guerrón-Quintana (2021) by respectively 63% and 90% [17]. We can see that with 5,000 grid points for candidate debt policies, the Matlab CPU computation outperforms Julia CPU by 210% (1/32.3% - 1) while for GPU computation Matlab defeats Julia CUDA by 206% (1/32.7% - 1). These magnitudes of outperforming significantly exceed the theoretical computation enhancement from the evolution of CPU/GPU devices between two papers. Overall, applying GPU computation on Matlab to solve the sovereign default model is at least as efficient as on Julia.

2.2.2 The Model with Long-Term Debt

The model with long-maturity debt follows the Chatterjee and Eyigungor (2012). The issuer is obligated to pay coupon rate $\eta > 0$ for each unit of debt outstanding. In each period, a λ share of debt outstanding matures while the remaining $1-\lambda$ share does not. Overall, the model is similar to the version with one-period debt, except for the budget constraint for being in good financial status

$$c = y + q(y, b')b' - \Big[\lambda + (1-\lambda)(\eta + q(y, b')\Big]b \tag{2.9}$$

[17] The CPU speed is measured by Cinebench R23 (Multi-Core) performance. GPU performance is measured with floating point operations per second (FLOPS), as indicated by the footnotes in the Introduction section.

and the risk-neutral pricing rule

$$q(y,b') = \frac{\mathbb{E}_{y'|y}(1-\mathcal{D}(y',b'))\Big[\lambda + (1-\lambda)(\eta + q(y,b')\Big]}{1+r^*} \tag{2.10}$$

The loss function takes the same form as in equation (2.5) but the calibration is different: $\kappa_1 = -0.18819$, $\kappa_1 = 0.24558$. The probability of re-entering international financial market is still 0.0385 in each period after default. Coupon rate $\eta = 0.03$ and the reciprocal of average maturity length is $\lambda = 0.05$. The calibration for the endowment process, which follows equation (2.1), is borrowed from Gordon (2019) where $\rho_y = 0.9485$ and $\sigma_y = 0.027092$. As in the one-period debt model, the set $\mathbb{Y}$ equally discretized with 25 grids. The grid points for debt outstanding is equally spaced within $b \in [0, 1.4]$ and the number of $\mathbb{B}$ varies from 200 to 6,000. The tolerance threshold *tol* is still $1e^{-7}$.

As mentioned, endogenous sovereign default models may suffer from convergence problem in solving. When long-maturity debt is incorporated into such a model, naive DVFI method generally does not deliver convergence and hence we need more sophisticated algorithm which in turn leads to heavier computation workload and slower computation. Chatterjee and Eyigungor (2012) and Gordon and Guerron-Quintana (2018) mitigates the convergence problem by incorporating continuous iid transitory income shocks. In this paper, I adopt a simpler method from Gordon (2019) that introduces taste shocks to both debt issuance and default decision to induce convergence for the DVFI approach. This taste shock method has been used in several recent quantitative sovereign default papers, such as Arellano et al. (2020). The mathematical details of this algorithm are explained in the appendix. Briefly speaking, we need to assign probabilities to each choice of default and debt issuance to smooth the expected value functions and hence to facilitate the global maximum search, as shown in Algorithm 4.

To implement Algorithm 4, the critical value for debt policy ε_b and default choice $\varepsilon_{\mathcal{D}}$ are set to be $5e^{-4}$ and $2e^{-4}$, respectively. Since we use double precision ($\epsilon = 1e^{-16}$), the ε_b equals $5e^{-4} \times \log(\epsilon)$, while the $\varepsilon_{\mathcal{D}}$ is numerically equivalent to $2e^{-4} \times \log(\epsilon)$. If the log odd ratio for debt policy, i.e. $W(y_i, b_j, b') - V^G(y_i, b_j)$, is smaller than ε_b then the debt policy b' is treated as highly unlikely and the probability assigned to such policy is zero.

Algorithm 4: LOES algorithm for DVFI, Long-Maturity Debt Model

while $\Delta < tol$ **do**

for *Each grid point of* $\mathbb{Y}$, y_i **do**

$c = b' \times q(y_i, b') - (\lambda + (1-\lambda) \times (\eta + q(y_i, b'))b + y_i$;

$W(y_i, b, b') = u(c) + \beta \mathbb{E}_{y'|y_i} V_0^G$;

$[V^G(y_i, b), B'(y_i, b)] = \max\{W\}$;

if $W(y_i, b, b') - V^G(y_i, b) > \varepsilon_b$ **then**

$W(y_i, b, i') = W(y_i, b, b')$

else

$W(y_i, b, i') = -\inf$

end

Calculate the probability of debt policy i, i.e. $\mathbb{P}(b' = i|y_i, b)$, with equation (B.4) in the appendix;

$V^B(y_i, b) = u(y_i - L(y_i)) + \beta \mathbb{E}_{y'|y_i}(\mu V_0 + (1-\mu)V_0^B)$;

if $V^B(y_i, b) - V^G(y_i, b) > \varepsilon_{\mathcal{D}}$ **then**

$V(y_i, b) = V^B(y_i, b)$

else

$V(y_i, b) = -\inf$

end

Calculate $\mathbb{P}(\mathcal{D} = 0|y, b) = \frac{\exp[V(y_i, b, \mathcal{D}=0) - V^G(y_i, b)]}{\exp[V(y_i, b, \mathcal{D}=0) - V^G(y_i, b)] + \exp[V(y_i, b, \mathcal{D}=0) - V^B(y_i, b)]}$ or equivalently equation (B.6).

end

Calculate debt price via equation (B.7);

All else the same as in Algorithm (2);

end

Similarly, for log odd ratio $V^B(y_i, b_j) - V^G(y_i, b_j)$ smaller than $\varepsilon_{\mathcal{D}}$, default risk related to state (y_i, b_j) will be deemed to be negligible. This choice of taste shocks ensures the convergence of solving the long-maturity debt default model with DVFI within 1000 iterations. Readers may have noticed that the taste shock method described in the appendix is naturally incompatible with FV method: for each exogenous state y_i, the accumulative probability for all debt policy grids or default decisions is required to be one unit and hence looping over $\mathbb{Y}$ is necessary. Therefore, in addition to the previously mentioned speed and memory drawbacks, being incompatible with taste shocks and hence not suitable for solving long-maturity debt model is another limitation of the FV method.

Table 2.5: Speed Comparison, Long-Term Debt Model

Debt Points	CPU	GPU	$\frac{\text{CPU}}{\text{GPU}}$
200	2.529	13.058	0.194
	(0.7640)	(3.9451)	-
600	27.043	18.005	1.502
	(8.1947)	(5.4561)	-
1500	367.27	73.19	5.025
	(69.43)	(13.83)	-
3000	1902.85	279.22	6.803
	(293.20)	(43.02)	-
6000	9674.41	1369.07	7.067
	(1175.51)	(166.35)	-

Notes: The time spent in solving the Long-Term Debt Model is in seconds. Figures in brackets represent the average solving time multiplied by 100. The algorithm applied to both CPU and GPU is the LOES.

Table 2.5 reveals several facts on the computational efficiency. First of all, the improvement from applying GPU parallel computation becomes more obvious as the number of grid points for debt (policy) grows larger. With 200 grid points, CPU computation is even faster than GPU. At $N_b = 600$ the time consumed by CPU is

1.5 times bigger than the GPU counterpart. For $N_b = 1500$ the ratio of time elapsed for CPU over GPU grows to 5. At $N_b = 6000$, the GPU only consumes 14.14% of the time spent in CPU. By exploring the GPU computation for solving long-maturity debt model, I also wish to find out if a higher complexity in algorithm would lead to a different magnitude of efficiency improvement. This could be answered by comparing Table 2.5 with the results from one-period debt model (Table 2.2), both using the LOES coding. The higher complexity in solving long-maturity debt model decreases the efficiency improvement from utilizing GPU. The potential reason is that CPU is more efficient at dealing with general operations while GPU provides the biggest improvement in conducting simple numerical calculations like matrix multiplication and addition. Calculating probability weighted integrals in discrete time, which takes a large part of time consumed in this paper, is one of the advantages of GPU. Later, we will see that GPU provides much larger efficiency enhancement in solving a simple neoclassical growth model.

2.3 Neoclassical Growth Model for Comparison

In this section I illustrate the speed improvement from switching to GPU in calculating the numerical solutions of a standard neoclassical growth model. We consider a dynamic programming problem of finding the value function V and capital policy k' to solve the Bellman equation below:

$$V(z,k) = \max_{c\geq 0,\, k'} u(c) + \beta \mathbb{E}_{z'|z} V(z',k') \tag{2.11}$$

where β is the subjective discount factor. The budget constraint for this problem is

$$c = e^z k^\alpha + (1-\delta)k - k' \tag{2.12}$$

where c, k and z denote consumption, capital stock and productivity respectively. δ is the depreciation rate of capital stock. The stochastic productivity z follows an AR(1) law:

$$z' = \rho_z z + \varepsilon^z, \quad \varepsilon^z \sim i.i.N(0,\sigma^z) \tag{2.13}$$

The primes on variables denote next period and $\mathbb{E}_{z'|z}V(z',k')$ is the expected value conditional on state (z,k) and the probability transition law of z. The utility function takes the same form as in equation 2.8. For the calibration, $\beta = 0.95$, $\sigma = 2$, $\alpha = 0.33$, $\delta = 0.1$, $\rho_z = 0.9$ and $\sigma^z = 0.01$. The probability transition matrix for z is drawn by the Tauchen (1986) method with 25 equally spaced grid points. Capital k is equally discretized between 25% and 400% of its steady state and the number of grid points N_k varies from 200 to 6000.

Algorithm 5: FV algorithm, neoclassical growth model

while $\Delta < tol$ **do**

$c = \exp(z)k^\alpha + (1-\delta)k - k'$;

Calculate $u(c)$ with equation (2.8) and replicate $u(c)$ in row by N_k times;

$EV = \mathbb{E}_{z'|z} \times V_0$, then replicate EV in row by N_k times;

Find the column index (debt policy K'): $[V, K'] = \max\{u(c) + \beta EV\}$;

$\Delta = \max(|V - V_0|)$;

$V_0 = V$;

end

Algorithm 5 and 6 respectively describe the FV and LOES methods to solve the neoclassical growth model. We can see that compared with previous sovereign default models, these algorithms are much simpler: On the one hand, in each "while" loop for solving sovereign default models, two value functions (V^G and V^B) and hence two probability weighted averages (expected values in discrete time) need to be calculated. For the neoclassical growth model, only one value function and expected value need to be computed. On the other hand, debt prices should be updated in each "while" loop for sovereign default models but no such computation is required for the neoclassical growth model. Overall, the workload for solving neoclassical growth model is significantly smaller than sovereign default models.

As can be seen in Table 2.6, GPU provides huge improvement relative to conventional CPU computation under the FV algorithm. For $N_k = 600$, the acceleration exceeds 15 times. This magnitude grows to 21.7 at 1,500 grid points for capital stock.

Algorithm 6: LOES algorithm, neoclassical growth model

while $\Delta < tol$ **do**

  for *Each grid point of* $\mathbb{Z}$, z_i **do**

    $c = \exp(z_i)k^{\alpha} + (1-\delta)k - k'$;

    Calculate $u(c)$ with equation (2.8);

    $EV = \mathbb{E}_{z'|z_i} \times V_0$;

    Find the column index (debt policy K'): $[V, K'] = \max\{u(c) + \beta EV\}$;

    $\Delta = \max(|V - V_0|)$;

    $V_0 = V$;

  end

end

Table 2.6: Speed Comparison, neoclassical growth model via FV

Debt Points	CPU	GPU	$\frac{\text{CPU}}{\text{GPU}}$	$\frac{\text{GPU(FV)}}{\text{GPU(LOES)}}$
200	2.386	0.702	3.399	0.132
	(0.6629)	(0.1950)	-	-
600	25.05	1.575	15.905	0.218
	(6.9581)	(0.4376)	-	-
1500	152.65	7.034	21.702	0.398
	(42.402)	(1.9539)	-	-

Notes: The time spent in solving the neoclassical growth model is in seconds. Figures in brackets represent the average solving time multiplied by 100. To be in line with previous tables, the Full Vectorization (FV) algorithm results for debt points higher than 1,500 are not reported. In fact, for $N_k = 2,000$ the computation with FV is still free from the out-of-memory problem. $\frac{GPU(FV)}{GPU(LOES)}$ represents the ratio of time spent with FV over LOES, with GPU devices applied for both algorithms.

The FV method performed with GPU devices also dominates the LOES algorithm in efficiency (see the fifth column of Table 2.6). For example, at $N_k = 600$ the time elapsed under FV takes only 21 percent of LOES. However, the $\frac{GPU(FV)}{GPU(LOES)}$ ratio grows as the number of capital grid points enlarges and the out-of-memory problem is still there.

Table 2.7: Speed Comparison, neoclassical growth model via LOES

Debt Points	CPU	GPU	$\frac{\text{CPU}}{\text{GPU}}$
200	1.1609	3.6250	0.320
	(0.4739)	(1.4796)	-
600	10.1067	4.9178	2.055
	(4.1252)	(2.0073)	-
1500	80.53	12.02	6.70
	(32.87)	(4.905)	-
3000	340.69	34.01	10.02
	(139.06)	(13.88)	-
6000	1386.82	139.76	9.92
	(566.05)	(57.05)	-

Notes: The time spent in solving the neoclassical growth model is in seconds. Figures in brackets represent the average solving time multiplied by 100. The algorithm applied to both CPU and GPU is the LOES. Notice that the number of iteration for LOES is different from that of FV: the former uses 246 iterations while the latter needs 361. However, the derived value and policy functions are the same across two algorithms.

In the next, I solve the neoclassical growth model with LOES and test the improvement from utilizing GPU devices. The first finding is that CPU computation with LOES algorithm is faster than FV. As for GPU, if the number of grid points is small (200, 600 and 1,500), solving with LOES algorithm underperforms FV. For higher levels of N_b, GPU with LOES offers 10-times speed-up over the CPU but this magnitude of improvement is much smaller than the FV counterpart. The $\frac{GPU(FV)}{GPU(LOES)}$ ratios reported in Table 2.6 are well below 1 unit. As been explained, the workload in solving neoclassical growth model is significantly smaller than solving sovereign default

models. In the meantime, the LOES algorithm forces GPU to execute the solving in a partially sequential manner while the FV fully utilizes the built-in parallelization advantage between GPU cores. To sum up, the efficiency improvement from switching to GPU is significant but it is negatively correlated with the complexity of algorithm.

2.4 Conclusion

This paper discusses the efficient solving with discretized value function iteration (DVFI) method. Although this method is generally slow, it is robust and irreplaceable for many non-linear macroeconomic models, Accelerating DVFI is therefore of interest to macroeconomic modellers. The paper uses endogenous sovereign default models to evaluate the efficiency improvement in solving non-linear models by switching from CPU (and no parallelization) to GPU parallel computation. These experiments are conducted on Matlab with its Parallel Toolbox for GPU. The time consumed in solving is compared with the Matlab CPU counterpart.

The paper provides several findings. First of all, the Looping Over Exogenous Shocks (LOES) algorithm is significantly faster than the commonly used Full Vectorization (FV) algorithm as well as the straightforward Looping Over All States (LOAS) approach, either for CPU or GPU computation. We also find that for the sovereign default model with one-period debt, the efficiency improvement of GPU over CPU could reach tenfold. This relative speed-up is at least as good as the results from applying Julia CUDA (GPU computation with Julia language). The GPU acceleration is negatively correlated with the complexity of DVFI algorithm: For a neoclassical growth model, which is much simpler than the one-period debt model, the speed enhancement could reach 21 times. However, if long-maturity debt is incorporated into the sovereign default framework, which means additional complexity and hence higher workload in the algorithm, the speed-up from GPU degenerates to 7 times relative to CPU. In conclusion, the Matlab Parallel Toolbox with GPU parallelization provides significant and convenient efficiency gains in solving sovereign default models. This advantage could be applied to solving other non-linear macroeconomic models via the DVFI approach.

Chapter 3

Sovereign Debt Pricing with Shifting Long-run Growth Expectations[1]

3.1 Introduction

The far-reaching Eurozone debt crisis since 2009 has caused default concerns in the European debt market and drawn attention to the determinants of sovereign debt spreads. At that time, fundamentals such as debt-to-GDP ratio, fiscal deficits seemed not to be the sole driving force of spreads. For example, De Grauwe and Ji (2013) demonstrate that spreads surge is associated with negative self-fulling market sentiments. The role that output expectation plays has been highlighted by Durdu et al. (2013). In their sovereign default model, agents learn total factor productivity (TFP) growth via noisy news. Bad news leads to underestimated output growth and therefore decreases expected probability to repay and increases spreads. In this article, we document new evidence on the relationship between spreads and output expectation: the

[1]This chapter is based on joint work with Dr. Pei Kuang and Prof. Kaushik Mitra.

potential growth rate forecasts and sovereign debt spreads[2] are negatively correlated. The correlation coefficient is -0.63 for GIIPS countries[3] and -0.47 for non-GIIPS Eurozone economies. These correlations are also non-linear: the negative relationship is stronger at lower potential growth forecasts and vice versa.

Existing equilibrium sovereign default models struggle to explain this documented new evidence. Aguiar and Gopinath (2006) incorporate trend shocks in their model and assume full information rational expectation (FIRE) on trend knowledge. However, quantitative results show that the correlation between trend growth rates and spreads is insignificant. Durdu et al. (2013) do not distinguish trend growth rate and hence provide no rationale. In this paper, we provide a solution by relaxing the FIRE assumption for trend growth. Agents possess imperfect knowledge on trend and they form subjective beliefs into infinite horizon to make optimal decisions, including debt issuance and whether to default. Following the quantitative default framework à la Eaton and Gersovitz (1981), the government issues debts to risk-neutral foreign lenders who incorporate default risk into yield spreads. Default is endogenously made to maximize household's utility.

Why incorporating learning about trend is important to the rationale of new evidence? On the one hand, when the model is built upon a FIRE hypothesis, existing estimations show that trend shock only take a very small portion of the total variance of TFP shocks, i.e. the trend-TFP variance ratio is low, especially when financial friction is considered[4]. Apart from productivity shocks, Garcia-Cicco et al. (2010) let TFP shocks, which include trend and transitory components, compete with interest-rate shocks, preference shocks and government spending shocks. The estimated trend-TFP variance ratio is only 2.4%. In Gordon et al. (2018) default risk, another form of financial friction, is included and the estimated trend-TFP variance ratio is only

[2]The potential growth rate forecast data comes from the European Economic Forecast published by the European Commission. Following literature, sovereign debt spreads are measured as the premiums in the 10-year government bonds over the German counterpart. The sample of spreads includes 10 Eurozone countries between 2004 and 2016: Austria, Belgium, France, Finland, Greece, Ireland, Italy, Netherlands, Portugal, Spain.

[3]The GIIPS countries include Greece, Ireland, Italy, Portugal and Spain, all severely affected by the Eurozone debt crisis.

[4]In a frictionless neoclassical framework, Aguiar and Gopinath (2007) estimate that trend shock takes 40% of the TFP variance for Canada. Uribe and Schmitt-Grohé (2017) provide thorough critiques on the relative importance of trend shocks.

1.3%. As verified in the later part of this paper, with a trivial importance of trend shocks, assuming FIRE in an sovereign default framework makes the simulated correlation coefficient between debt spreads and trend beliefs insignificant. On the other hand, Boz et al. (2011) embed learning about trend shocks into a small open economy framework[5] and the ratio of trend-TFP variance is estimated to be 20% for a case of developed economy. We develop their learning model by incorporating endogenous default risk. With calibrated 6.5% trend-TFP variance ratio, the simulated correlation coefficient matches GIIPS data.

There are two channels contribute to the non-trivial impact of subjective trends on spreads. The first one is related to the belief updating system and we refer to it as the *learning channel*. This channel arises from the updating of subjective trend shocks. The TFP consists of transitory and trend components, both of which are unobservable. Trend beliefs are updated via a Bayesian system, with observed TFP shocks and noisy signals about the trend as inputs. Therefore, agents usually have difficulty in distinguishing the trend and transitory shocks. Statistics results show the perceived trend is positively correlated with the perceived transitory shock, which is the main driver of expected output, debt issuance, default and hence spreads.

The second channel, denoted as the *belief channel*, is associated with how agents taking subjective beliefs into account. Decisions are based on infinite horizon forecasts, while the probability distribution of future states is deeply influenced by perceived trend growth rates. Intuitively, beginning at the steady state of the FIRE model, lower (higher) trend/transitory shock leads to lower (higher) expected output, lower (higher) capability to repay maturing debt and hence foreign lenders charge higher (lower) spreads. The previously mentioned learning channel exaggerates shocks: the perceived trend growth is usually below (above) real trend during economic downturn (booming). Therefore, pessimism (optimism) over trend growth results in underestimated (overestimated) output, overestimated (lower) default probability Accordingly, debt spreads raise higher than levels determined by fundamentals.

We show that our learning model also generates much more volatile debt market

[5]Similar to Schmitt-Grohé and Uribe (2003), the small open economy faces external debt-elastic interest-rate premium, which represents a simple way to introduce financial friction.

variables compared to its FIRE counterpart. The default frequency and standard deviation of spreads are respectively 10 and 4 times higher. Because of the much larger probability of default, simulated average spreads in the learning model is 3.2 times larger. This improvement in debt-relevant statistics is closely related to the movements of trend beliefs. As confirmed by a generalized impulse response analysis in Koop et al. (1996) style, upon a negative transitory productivity shock, trend growth becomes underestimated and spreads immediately rise up. For the FIRE model, agents know that trend growth is independent with transitory shocks so that spreads stay unaffected in this scenario. We also prepare typical default analysis as in Mendoza and Yue (2012) and the results resemble the Greek default in 2012. More importantly, as the typical default event approaches, the learning model delivers a deeper reduction in subjective trend growth estimates and a greater surge in spreads than FIRE.

This paper is related to two strands of literature. The first strand of literature incorporates learning behaviour into macroeconomic models in a range of wide applications. Such as Preston (2005), Eusepi and Preston (2011), Adam et al. (2012), Kuang (2014). Agents behave as econometricians who update parameters when new data are available, make infinite horizon forecasts and solve their optimization problems. This method could also be regarded as the "anticipated utility" approach in Kreps (1998). Following that, each of the perceived trend growth rates corresponds to a specific set of policy functions and debt price. Trend belief is acquired via a Boz et al. (2011) style Bayesian updating rule[6] where agents estimate the trend and transitory components of TFP shock. Kuang and Mitra (2016) show that potential GDP growth forecasts is a crucial ingredient in understanding business cycle fluctuations, while Kuang and Mitra (2021) document the systematic forecast errors for Eurozone potential GDP growth rates. Inspired by these papers, we wish to see if beliefs of potential growth are correlated with sovereign debt markets during recent Eurozone debt crises.

The second steam of literature is on quantitative sovereign debt default models in Eaton and Gersovitz (1981) style where default is endogenous. Various researches

[6]In fact, the Bayesian updating rule in Boz et al. (2011) is embedded into the first-order linear solutions of their model, see the chapter 5 of Uribe and Schmitt-Grohé (2017) for detail. Such algorithm is unable to be applied to sovereign default model because of the non-linearity.

have investigated how economic fluctuations influences default risk/sovereign debt pricing and vice versa. A short list includes Arellano (2008), Mendoza and Yue (2012), Chatterjee and Eyigungor (2012), Na et al. (2018), etc. Specifically, our FIRE model resembles Aguiar and Gopinath (2006), where the TFP shock has both permanent and transitory components. The most relevant paper is Durdu et al. (2013), which incorporates imperfect knowledge on productivity shock to study the relationship between news and default risk. We advance on these two studies by introducing subjective trend growth. Sovereign default literature exploring the self-fulfilling default crisis, i.e. belief that default is possible could accelerate default, is also relevant. For example, Bocola and Dovis (2019) find this nonfundamental risk played a role in the crisis. Galli (2021) show the vicious circle of pessimism beliefs in repayment, substituting borrowing with taxation, and hence lower growth and higher default risk.

The remainder of this paper proceeds as follows: Section 2 exhibits the new evidence on the relationships between Eurozone sovereign debt spreads and potential growth forecasts; Section 3 explains the learning model as well as its comparative full information model; Section 4 shows the calibration and quantitative analysis of our model; in Section 5, we conduct sensitivity analysis by changing the trend belief calibrations and considering long-maturity sovereign debt; Section 6 draws the conclusion.

3.2 New evidence

This section presents new evidence on Eurozone sovereign debt crisis. We firstly document evidence on the relationship between sovereign bond spreads and potential GDP growth forecasts. The former is measured as the difference in the 10-year government bond yields for sampling countries against Germany. The latter is the average of growth rate of real potential GDP forecast over year t to $t+3$ made in Spring or Autumn of year t. Forecasts are taken from the annual macroeconomic database published in European Economic Forecast by the European Commission (EC) that covers

data vintages from 2004 Autumn to 2016 Spring[7]. This dataset has been computed consistently across countries by the EC using a uniform estimation methodology for potential output. Quarterly sovereign bond yields are from Datastream. Using the data between 2004 Autumn and 2016 Spring, Table 3.1 reports the correlation coefficients between 10-year government bond yield spreads and average forecasts of growth rates of real potential GDP over next four years for ten Eurozone countries. There are negative correlation coefficients for the potential output growth forecasts and government bond spreads. The coefficients range from -0.53 to -0.84, all statistically significant at 1% confidence level.

Table 3.1: Correlation between spreads and potential GDP growth forecasts

Country	$\rho(\tilde{\gamma}, r - r^*)$	p-value
Greece	-0.78	0.000
Ireland	-0.81	0.000
Italy	-0.82	0.000
Portugal	-0.80	0.000
Spain	-0.84	0.000
Belgium	-0.65	0.001
France	-0.77	0.000
Netherlands	-0.68	0.000
Austria	-0.53	0.008
Finland	-0.60	0.002

Notes: $r - r^*$ stands for the spread of 10-year government bond, i.e. the bond yield to maturity r minus risk-free rate r^*, which is Germany 10-year government bond yield to maturity. $\tilde{\gamma}$ denotes potential GDP growth forecast. $\rho(\tilde{\gamma}, r - r^*)$ is the correlation coefficient between trend growth forecast and sovereign debt spread.

Upper panel of Figure 3.1 plots pooled sovereign bond spread data in vertical axis

[7]We use European Economic Forecast data because it is an expert forecast. In our learning model, although agents only possess imperfect information on trend growth, they estimate the trend in an optimal manner. Hence, we argue that European Economic Forecast is a good match with our model setup.

against pooled average of real potential output growth rate forecasts in horizontal axis. Data comes from GIIPS countries that were most severely influenced by the recent crisis. The correlation coefficient of these two variables is -0.63. The lower panel of Figure 3.1 plots the same relationship for all 10 Eurozone countries mentioned in Table 3.1 and the correlation coefficient is -0.55. For the pooled data for 5 non-GIIPS countries, the correlations coefficient is -0.47.

Notice that the above-mentioned relationships are not linear. To illustrate this, We fit the pooled data for both GIIPS and all 10 Eurozone countries with a linear model:

$$\tilde{\gamma}_t = \beta_1 + \beta_2(r_t - r^*) + \varepsilon_t \tag{3.1}$$

as well as a non-linear model

$$\tilde{\gamma}_t = \beta_1 \cdot \exp\left[\beta_2 \cdot (r_t - r^*)\right] + \varepsilon_t \tag{3.2}$$

We estimate parameters β_1 and β_2 for both models with the debt spread data $(r_t - r^*)$ as dependent variable and potential GDP growth forecast data $\tilde{\gamma}_t$ as independent variable. Estimation results are reported in table 3.2, which indicates that the non-linear model outperforms the linear model. Specifically, given that $\hat{\beta}_1$ and $\hat{\beta}_2$ for both models are significant in 1% confidence level, the information criteria and the sum of squared errors of the non-linear model are lower than those of the linear model.

As shown in Figure 3.1, this non-linear relationship indicates that when the trend forecast falls, the negative correlation between spreads and forecasts becomes stronger. By contrast, at optimistic levels of trend forecasts, this correlation is much weaker. As will be explained, the equilibrium default model with learning mechanism could replicate the negative correlation coefficient between spreads and trend beliefs but also the non-linearity of this relationship.

Finally, we draw the movements of sovereign debt spread and GDP potential growth rate forecast for Greece during its default episodes around the second quarter of 2012. As shown in Figure 3.2, it is clear that the projected potential GDP growth exhibits continued decline prior to the default. In the meantime, Greek 10-year government bond spread experiences dramatic increase. After 2012, sovereign spread stays at a

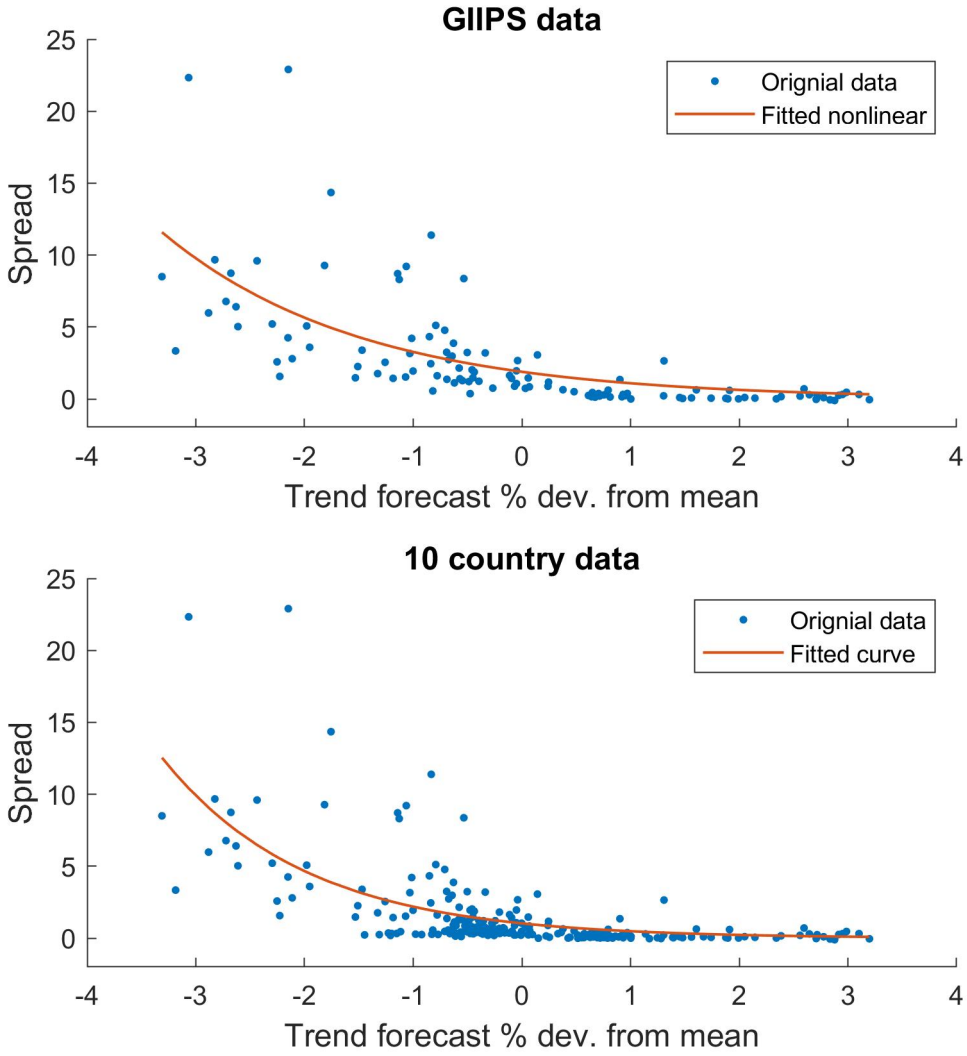

Figure 3.1: Debt spreads and trend forecasts data, 2004-2016, from GIIPS and 10 Eurozone countries. Trend forecast is the deviation from each country's mean level.

Table 3.2: Data-Based Estimation of linear and non-linear relationships

	GIIPS		10 Eurozone	
Statistics	Non-linear	Linear	Non-linear	Linear
$\hat{\beta}_1$	1.893	2.623	1.032	1.492
	(0.3064)	(0.2763)	(0.1433)	(0.160)
$\hat{\beta}_2$	-0.547	-1.482	-0.754	-1.307
	(0.0684)	(0.1686)	(0.0569)	(0.1282)
SSE	984.21	1081.3	1181.9	1469.1
AIC	595.07	608.35	1065.7	1119.9
BIC	600.64	613.93	1072.7	1126.9
Sample size	120	120	240	240

Notes: SSE is sum of squared error of estimation; AIC is Akaike's Information Criteria; BIC means Bayesian Information Criteria. Numbers in brackets are standard errors in parameter estimation. All 8 estimated coefficients are statistically significant in 1% confidence level.

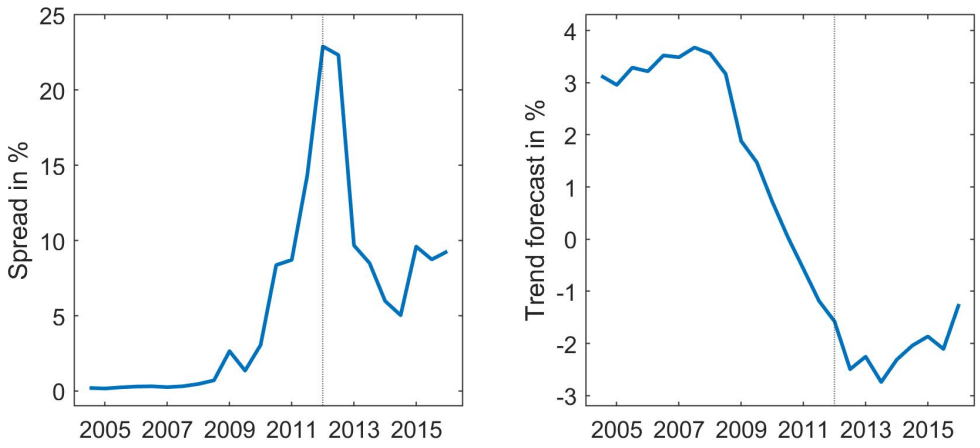

Figure 3.2: Debt spreads and trend forecast in recent Greece sovereign debt crisis. Spread data is from 10-year government bond spread, trend growth rate forecast comes from European Economic Forecast, both two times series are in semi annual frequency. Vertical dotted line indicates default time. In March 2012, Greece and its private creditors completed a debt restructuring, so we define the first half of 2012 as default time.

lower platform, while the trend growth forecast stops decreasing and stabilizes. In summary, the negative correlation between trend growth forecast and sovereign bond spread is a non negligible feature for the recent Eurozone debt crisis.

3.3 The model

In this section, we explain the sovereign default model built upon imperfect knowledge on trend growth rate. We begin with the model where agents have full knowledge on the permanent and transitory components of the TFP, or equivalently Full Information Rational Expectation (FIRE) model.

3.3.1 The FIRE model

Three types of agents resides in the economy: the representative household, firm and government. The household aims to maximize the sum of expected discounted utility

$$E_0 \sum_{t=0}^{\infty} \beta^t u(C_t, h_t) \tag{3.3}$$

C_t is consumption, h_t denotes working hours. Utility function follows the commonly used Greenwood–Hercowitz–Huffman (GHH) form (Greenwood et al., 1988) in equilibrium sovereign default literature. It is adjusted to be compatible with the stationarity of h_t:

$$u(C_t, h_t) = \frac{1}{1-\sigma}\left[\left(C_t - \frac{1}{\omega}\Gamma_{t-1} h_t^{\omega}\right)^{1-\sigma} - 1\right] \tag{3.4}$$

Household consumption is financed by wage income $W_t h_t$, dividend income Π_t and government transfer payment F_t, as shown in the budget constraint:

$$C_t = W_t h_t + \Pi_t + F_t \tag{3.5}$$

The firm seeks to maximise profit Π_t by producing real goods and hiring optimal amount of labour:

$$\max_{h_t}\{\Pi_t\} = \max_{h_t}\{Y_t - W_t h_t\} \tag{3.6}$$

Real goods are produced with following function (Aguiar and Gopinath, 2006):

$$Y_t = e^{z_t}\Gamma_t h_t^{1-\alpha} \tag{3.7}$$

where z_t stands for the transitory component of TFP and follows an AR(1) process:

$$z_t = \rho_z z_{t-1} + \varepsilon_t^z \tag{3.8}$$

with $|\rho_z| < 1$ and $\varepsilon_t^z \sim i.i.N(0, \sigma_z^2)$. Γ_t represents the cumulative product of the permanent component of TFP:

$$\Gamma_t = \gamma_t \Gamma_{t-1} = \prod_{s=0}^{t} \gamma_t \tag{3.9}$$

where the trend growth γ_t follows

$$\log(\gamma_t) = (1-\rho_\gamma)\log(\overline{\gamma}) + \rho_\gamma \log(\gamma_{t-1}) + \varepsilon_t^\gamma \tag{3.10}$$

with $|\rho_\gamma| < 1$ and $\varepsilon_t^\gamma \sim i.i.N(0, \sigma_\gamma^2)$. The TFP shock is $A_t = e^{z_t}\Gamma_t$ and its growth rate in logarithm is:

$$\Delta \log(A_t) \equiv \log\left(\frac{e^{z_t}\Gamma_t}{e^{z_{t-1}}\Gamma_{t-1}}\right) = z_t - z_{t-1} + \log(\gamma_t) \tag{3.11}$$

The benevolent government issues foreign debt D_{t+1} at price q_t if the country maintains good financial status, i.e. $\mathcal{I}_t = 1$. All net governmental borrowings are transferred to the household:

$$F_t = \mathcal{I}_t\Big(q_t D_{t+1} - D_t\Big) \tag{3.12}$$

Default is another endogenous choice: all external debts not recognised and all due

repayments are transferred to the household[8]. After default, the country immediately falls into bad financial status ($\mathcal{I}_t = 0$) where it cannot issue sovereign debt. In each period of bad financial status, there is a constant probability θ that the country returns to good financial status and regain access to foreign lending, see equation (3.17). Debt issuance price q_t is determined in a buy-side market where buyers are risk-neutral and equate the price to the expected value of repayment:

$$q_t = \frac{\mathbb{E}_t \mathcal{I}_{t+1}}{1 + r^*} \tag{3.13}$$

where r^* is the risk-free rate. In bad financial status, the sovereign debt price does not exist [9].

Apart from financial autarky, the country also suffers from an output loss $L(y_t)$ in bad financial status. As argued in Arellano (2008) and quantitatively shown in Uribe and Schmitt-Grohé (2017), default cost is important to generate low default frequency. In this article, we adopt an ad hoc quadratic productivity loss function similar to Chatterjee and Eyigungor (2012):

$$L\left(\exp(z_t)\right) = \max\left\{0, \delta_1 \exp(z_t) + \delta_2[\exp(z_t)]^2\right\} \tag{3.14}$$

Trend shock γ_t is not included into the productivity loss, in line with the empirical findings in Borensztein and Panizza (2009) that output loss of default is short-lived. The transitory shock after default cost is $\exp(z_t^{aut}) = \exp(z_t) - L\left(\exp(z_t)\right)$. Detrended output in bad financial status y^{aut} is assumed to be a function of variable z^{aut} and the unconditional mean of trend growth as a parameter:

$$y_t^{aut} = y(z_t^{aut}; \overline{\gamma}) \tag{3.15}$$

Similarly, the equilibrium labour in bad financial status is $h_t^{aut} = h(z_t^{aut}; \overline{\gamma})$[10]

[8] See Yue (2010) for an example of debt renegotiation.

[9] Readers interested in the shadow price of domestic debt are referred to Na et al. (2018) equation (21). We do not explore the shadow price in this paper.

[10] We treat trend growth as parameter in y_t^{aut} and h_t^{aut} for the convenience of incorporating anticipated learning about trend growth rate. Using γ_t in y_t^{aut} and h_t^{aut} casts little influence on the results but significantly complicates the learning model.

3.3.1.1 Recursive Representation of the FIRE Model

Let $s_t = (z_t, \gamma_t)$ denotes the set of exogenous variables, d_t stands for the endogenous state variable debt. Define V as the detrended[11] value function. The value corresponding to good financial status is V^g, while V^b corresponds to being in bad financial status. Social planner maximizes V^g by choosing optimal consumption, working hours and debt policy d_{t+1}, given s_t:

$$V^g(s,d) = \max_{c,h,d'} \left\{ u(c,h) + \tilde{\beta}\mathbb{E}_{s'|s} V^o(s',d') \right\} \tag{3.16}$$

where $\tilde{\beta} = \beta\gamma^{1-\sigma}$. The optimization of V^g is subject to the consumption constraint in good financial status, as replicated from equation (C.11):

$$c = y - d + \gamma q d'$$

The value function corresponding to being in bad financial status is

$$V^b(s) = u\left(c^{aut}, h^{aut}\right) + \tilde{\beta}\mathbb{E}_{s'|s}\Big[\theta V^o(s',0) + (1-\theta)V^b(s')\Big] \tag{3.17}$$

The V^o in above two value functions denotes the value of the default option:

$$V^o(s,d) = \max\left\{ V^g(s,d), V^b(s) \right\} \tag{3.18}$$

The default indicator $\mathcal{I}_t$ depends on the value of staying in good financial status or falling into bad financial status:

$$\mathcal{I} = \begin{cases} 1, & \text{if } V^g(s,d) > V^b(s). \\ 0, & \text{otherwise.} \end{cases} \tag{3.19}$$

The face value of sovereign bond is assumed to be one unit. Risk-neutral lenders equalize q_t and default risk adjusted discounted value of expected future repayment $E_{s'|s}\mathcal{I}'$:

$$\mathcal{I}\left[q(s,d') - \frac{\mathbb{E}_{s'|s}\mathcal{I}(s',d')}{1+r^*} \right] = 0 \tag{3.20}$$

[11] For the derivation of detrended equations equilibrium conditions of RE model, see Appendix A.

The yield to maturity of bond is $r_t = 1/q_t$. Sovereign spread is defined as the difference between the yield to maturity and risk free rate, $r_t - r^*$.

Definition 3 (Model equilibrium, FIRE Model)**.** Given exogenous shocks s_t and debt state d_t, a recursive equilibrium for the FIRE model consists of the policy functions of default $\mathcal{I}_t$, output y_t, consumption c_t, working hours h_t, debt issuance d_{t+1}, and the value functions for different financial status, $V^g(s,d)$, $V^b(s)$, $V^o(s,d)$ and bond price q_t, such that

1. Given price q_t, the policy functions and value functions (3.16), (3.17), (3.18) solve the social planner's optimization problem.
2. Given optimal default rule $\mathcal{I}_t$, bond price q_t satisfies the risk-neutral rule (3.20).
3. y_t, c_t and h_t depend on default loss functions and other equilibrium conditions.

3.3.2 Learning about Trend

We has shown the empirical evidence of non-linear negative relationship between sovereign debt spreads and trend growth forecasts. This evidence is rationalized with a quantitative sovereign default model where agents have imperfect information on trend growth rates. We refer to this model, to be explained in this section, as the "learning model".

The agents cannot observe z_t and γ_t so that they can only learn the transitory and trend shocks, i.e. $\tilde{z}_t$ and $\tilde{\gamma}_t$, to make decisions. The belief formation is based on observed TFP growth $\Delta \log(A_t)$ and a noisy signal n_t about the trend growth:

$$n_t = \log(\gamma_t) + \varepsilon_t^n \tag{3.21}$$

where $\varepsilon_t^n \sim i.i.N(0, \sigma_n^2)$ is a noise that measures the deviation of signal from true trend shock. The structures of $\Delta \log(A_t)$ (3.11) and n_t are assumed to be known to agents. The *observation equation* summarizes the construction of observed TFP and

trend signal in state space representation $\mathbf{Y}_t = \mathbf{Z}_t\boldsymbol{\alpha}_t$, or equivalently:

$$\begin{bmatrix} \Delta \log(A_t) \\ n_t \end{bmatrix} = \begin{bmatrix} 1 & -1 & 1 & 0 \\ 0 & 0 & 1 & 1 \end{bmatrix} \cdot \begin{bmatrix} z_t \\ z_{t-1} \\ \log(\gamma_t) \\ \varepsilon_t^n \end{bmatrix} \tag{3.22}$$

Another equation called *transition equation* describes the evolution of unobserved variables $\boldsymbol{\alpha}_t = (z_t, z_{t-1}, \log(\gamma_t), \varepsilon_t^n)^T$ on the left hand side of equation (3.22): $\boldsymbol{\alpha}_t = \mathbf{T}\boldsymbol{\alpha}_{t-1} + \mathbf{C} + \mathbf{R}\boldsymbol{\eta}_t$, or equivalently:

$$\begin{bmatrix} z_t \\ z_{t-1} \\ \log(\gamma_t) \\ \varepsilon_t^n \end{bmatrix} = \begin{bmatrix} \rho_z & 0 & 0 & 0 \\ 1 & 0 & 0 & 0 \\ 0 & 0 & \rho_\gamma & 0 \\ 0 & 0 & 0 & 0 \end{bmatrix} \begin{bmatrix} z_{t-1} \\ z_{t-2} \\ \log(\gamma_{t-1}) \\ \varepsilon_{t-1}^n \end{bmatrix} + \begin{bmatrix} 0 \\ 0 \\ (1-\rho_\gamma)\log(\overline{\gamma}) \\ 0 \end{bmatrix} + \begin{bmatrix} 1 & 0 & 0 \\ 0 & 0 & 0 \\ 0 & 1 & 0 \\ 0 & 0 & 1 \end{bmatrix} \begin{bmatrix} \varepsilon_t^z \\ \varepsilon_t^\gamma \\ \varepsilon_t^n \end{bmatrix} \tag{3.23}$$

where $\boldsymbol{\eta}_t \sim i.i.N(0, \mathbf{Q})$, $\mathbf{Q}$ is the variance-covariance matrix for the three independent shocks. As $\sigma_n \to +\infty$, the signal provides less information on trend growth. As $\sigma_n \to 0$, the signal becomes more accurate.

Given equation (3.22) and (3.23), a Bayesian updating rule provides the best estimation $\mathbf{a}_t$ for the unobserved variables, $\boldsymbol{\alpha}_t$. The prior estimator is determined by $\mathbf{a}_{t|t-1} = \mathbf{T} \cdot \mathbf{a}_{t-1} + \mathbf{C}$ while the posterior $\mathbf{a}_t$ is a linear combination of the prior beliefs and observations such that

$$\mathbf{a}_t = \kappa^1 \mathbf{a}_{t|t-1} + \kappa^2 \mathbf{Y}_t \tag{3.24}$$

where $\kappa^1 = [\mathbf{I} - \mathbf{P}\mathbf{Z}'(\mathbf{Z}\mathbf{P}\mathbf{Z}')^{-1}\mathbf{Z}]$ and $\kappa^2 = \mathbf{P}\mathbf{Z}'(\mathbf{Z}\mathbf{P}\mathbf{Z}')^{-1}$ are the gain parameters [12]. $\mathbf{I}$ is a 4×4 identity matrix. We denote the vector $\mathbf{a}_t$ as $[\tilde{z}_t, \tilde{z}_{t-1}, \log(\tilde{\gamma}_t), \tilde{\varepsilon}_t^n]^T$. Notice that rule (3.24) only governs the perceptions of exogenous shocks. In Boz et al. (2011), a similar updating rule is embedded into the linear solutions of their model so that agents will anticipate this learning rule. Readers interested in the details of their method are referred to the chapter 5 of Uribe and Schmitt-Grohé (2017). However,

[12] $\mathbf{P}_t$ is the covariance matrix of estimation error. $\mathbf{P}_t \equiv \mathbb{E}\left[(\boldsymbol{\alpha}_t - \mathbf{a}_t)(\boldsymbol{\alpha}_t - \mathbf{a}_t)'\right]$ with an updating rule called *Raccati equation*, which is is written as $\mathbf{P}_{t+1} = \mathbf{T}\mathbf{P}_t\mathbf{T}' - \mathbf{Z}\mathbf{P}_t\mathbf{Z}'(\mathbf{Z}\mathbf{P}_t\mathbf{Z}')^{-1}\mathbf{Z}\mathbf{P}_t\mathbf{T}' + \mathbf{R}\mathbf{Q}\mathbf{R}'$. To obtain the steady state of $\mathbf{P}_t$, we run iterations given an initial guess $\mathbf{P}_0$ until the absolute value norm of the difference between $\mathbf{P}_{t+1}$ and $\mathbf{P}_t$ is smaller than a tolerance rate.

such an asymptotic method should not be applied to sovereign default model because of its built-in kink: different financial statuses deliver different optimization problems.

For dynamic programming problems like the equilibrium sovereign default model, a natural method to introduce imperfect information is the "anticipated utility" approach in Kreps (1998). Policy functions are updated in each period using current posterior of the parameters of interest. To solve the optimization problem, agents treat the learnt parameters as constant into infinite future. Under this approach, trend uncertainty are accounted for but learning itself is not anticipated, as discussed in Koulovatianos et al. (2009). Incorporating anticipated learning in sovereign default model is intractable, but anticipated utility approach provides a reasonable alternative.

The solutions of the learning model is as follows In the FIRE model, the perceptions of transitory growth $\tilde{z}_t$ and trend growth $\tilde{\gamma}_t$ coincide with the true realizations. However, in the learning model, $\tilde{z}_t$ and $\tilde{\gamma}_t$ generally deviate from the true shocks. $\tilde{\gamma}_t$ is treated as constant parameter when the dynamics programming problems are being solved. $\tilde{z}_t$ is still treated as a stochastic shock. We define x_t as the set of control variables, $x_t = (c_t, y_t, h_t, q_t, y_t^{aut}, h_t^{aut}, \mathcal{I}_t)$. For each trend belief $\tilde{\gamma}_t$, we obtain a unique *decision equation* that governs the evolution of control variables:

$$x_t = g(\tilde{z}_t, d_t; \tilde{\gamma}_t) \tag{3.25}$$

and a motion law of the endogenous state:

$$d_{t+1} = h(\tilde{z}_t, d_t, x_t; \tilde{\gamma}_t) \tag{3.26}$$

Beliefs $\tilde{z}_t$ and $\tilde{\gamma}_t$ evolves as the Bayesian updating rule in 3.24.

3.3.2.1 Recursive Representation of the Learning Model

In the learning model, given belief $\tilde{z}_t$, social planner treat $\tilde{\gamma}_t$ as a parameter to solve her optimization problem. Value function in good financial status is:

$$V^g(\tilde{z}, d; \tilde{\gamma}) = \max_{\{c,h,d'\}} \Big\{ u(c,h) + \tilde{\beta}\mathbb{E}_{\tilde{z}'|\tilde{z}} V^o(\tilde{z}', d'; \tilde{\gamma}) \Big\} \tag{3.27}$$

value function in bad financial status is:

$$V^b(\tilde{z}; \tilde{\gamma}) = u\Big(c(\tilde{z}^{aut}; \overline{\gamma}), h(\tilde{z}^{aut}; \overline{\gamma})\Big) + \tilde{\beta}\mathbb{E}_{\tilde{z}'|\tilde{z}} \Big[\theta V^o(\tilde{z}', 0; \tilde{\gamma}) + (1-\theta) V^b(\tilde{z}'; \tilde{\gamma}) \Big] \tag{3.28}$$

and the value of default option is:

$$V^o(\tilde{z}, d; \tilde{\gamma}) = \max \Big\{ V^g(\tilde{z}, d; \tilde{\gamma}), V^b(\tilde{z}; \tilde{\gamma}) \Big\} \tag{3.29}$$

The non-default indicator is now $\tilde{\mathcal{I}} = \mathcal{I}(\tilde{z}, d; \tilde{\gamma})$, and the risk-neutral pricing rule of sovereign debt becomes:

$$\mathcal{I}(\tilde{z}, d; \tilde{\gamma}) \cdot \left[q(\tilde{z}, d'; \tilde{\gamma}) - \frac{\mathbb{E}_{\tilde{z}'|\tilde{z}} \mathcal{I}(\tilde{z}', d'; \tilde{\gamma})}{1 + r^*} \right] = 0 \tag{3.30}$$

The difference in $\mathcal{I}(s, d)$ and $\mathcal{I}(\tilde{z}, d; \tilde{\gamma})$ plays an important role in replicating the evidence of negative correlation between sovereign bond spread and trend growth rate forecast. Recall that social planner chooses to default if and only if V^b is bigger than V^g. When trend growth belief is pessimistic ($\tilde{\gamma} < \gamma$), $y(s)$ is more likely to be higher than $y(\tilde{z}; \tilde{\gamma})$. So that for the imperfect information case, the production difference between bad and good financial status, $y^{aut}(\tilde{z}; \overline{\gamma}) - y(\tilde{z}; \tilde{\gamma})$, is more likely to be overestimated relative to the corresponding difference from the full information case, i.e., $y^{aut}(z; \overline{\gamma}) - y(s)$. This indicates that the gap between the value functions of bad and good financial status, $V^b - V^g$, is likely to be overestimated in the imperfect information case. As a result, expected default probability $[1 - \mathbb{E}_{\tilde{z}'|\tilde{z}} \mathcal{I}(\tilde{z}', d'; \tilde{\gamma})]$ will be overestimated (underestimated) if the social planner holds pessimistic (optimistic) perceptions on trend growth. Accordingly, the risk-neutral pricing rule (3.30) delivers

lower (higher) sovereign bond price $q(\tilde{z}, d'; \tilde{\gamma}) < q(s, d')$ $(q(s, d') < q(\tilde{z}, d'; \tilde{\gamma}))$ in the imperfect information case compared with the full information case. For the algorithm that solves this learning model, readers are referred to appendix C.2.

Definition 4 (Model equilibrium, learning model)**.** Given state $\tilde{z}_t$ and d_t, and current trend belief $\tilde{\gamma}_t$, a recursive equilibrium for the learning model consists of policy functions of default choice $\tilde{\mathcal{I}}_t$, output y_t, consumption c_t, working hours h_t, debt issuance d_{t+1}, value functions $V^g(\tilde{z}, d; \tilde{\gamma})$, $V^b(\tilde{z}; \tilde{\gamma})$, $V^o(\tilde{z}, d; \tilde{\gamma})$ and bond price q_t, such that

1. Given bond price q_t, the policy functions, value functions (3.16), (3.17) and (3.18) solve the economy's optimization problem.
2. Given default decision $\tilde{\mathcal{I}}_t$, bond price q_t satisfies risk-neutral pricing rule (3.30).
3. y_t, c_t and h_t depend on default loss functions and other equilibrium conditions.

3.4 Calibration and Computation

The learning model is calibrated to match the average of GIIPS economies' quarterly business cycle statistics between the first quarter of 2000 and the fourth quarter of 2018. The FIRE model takes the same calibration, except that there is no parameter relevant to the learning mechanism. The calibration is summarized in Table 3.3 and could be classified into three strands. The first strand relates to the trend belief updating: The standard deviation of error term for transitory shock process σ_z, trend growth σ_γ and signal noise σ_n. To calibrate standard deviation of signal noise process error term σ_n, we set the signal to noise ratio σ_γ/σ_n to be 23%. The autoregressive coefficient of transitory shock process ρ_z is 0.90 as commonly used in literature. Given the variance of TFP

$$Var\Big[\log(\Delta A_t)\Big] = Var\Big[\log(\gamma_t) + z_t - z_{t-1}\Big] = \frac{\sigma_\gamma^2}{1-\rho_\gamma^2} + \frac{2\sigma_z^2}{1+\rho_z} \tag{3.31}$$

the variance of trend shock could be derived as the following equation:

$$\sigma_\gamma^2 = \frac{V_\gamma/V_A}{1 - V_\gamma/V_A} \cdot \frac{2\sigma_z^2(1-\rho_\gamma^2)}{1+\rho_z} \tag{3.32}$$

We pick σ_z and V_γ/V_A such that the standard deviation of Hodrick–Prescott filtered simulated output matches the average of GIIPS countries' GDP data, 2.5%. See the sensitivity analysis in later section for alternative values for V_γ/V_A. Similar small V_γ/V_A could be found in Garcia-Cicco et al. (2010) and Gordon et al. (2018) where financial frictions are incorporated. The choice of σ_γ and σ_n makes the difference between the simulated maximum and minimum quarterly trend growth belief to be 0.88%, close to the documented trend forecast range for GIIPS counties, 1.08%.

The second strand of calibration consists of structural parameters for a typical equilibrium default model. β is lower than the commonly used values in RBC models but within the range of sovereign default literature. A low β is needed to generate reasonable default frequency and sovereign bond spread. The value of productivity loss parameters δ_1 and δ_2 are selected to make simulated output loss conditional on being in bad financial status equal 7%, as in Na et al. (2018). β, δ_1 and δ_2 are jointly calibrated to deliver average bond spread of 2.02% to match the average sovereign bond spread for GIIPS countries in sample. The resulting average debt-to-output ratio from our model is 32% that is in line with literature on sovereign default but falls below the average government debt to GDP ratio for the GIIPS countries.

The third strand relates to the discretization of state spaces. we approximate the processes for z_t, γ_t and $\tilde{z}_t$ with the method in Tauchen (1986). The maximum and minimum deviations from the unconditional means is set to be 4.2 standard deviations. Notice the structure of perceived transitory process $\{\tilde{z}_t\}$ is generally different in structure from the true process $\{z_t\}$. To account for this difference, simulated $\tilde{z}_t$ is used to estimate the AR(1) parameters of $\{\tilde{z}_t\}$ process for the learning model. The estimated serial correlation parameter is 0.9475, while the estimated standard deviation of error term is 0.94%. Both $\tilde{z}$ and $\tilde{\gamma}$ are discretized into 101 equally spaced grid points. Debt state is equally spaced into 200 grids within $[0, 80\%]$, and the upper bound is never visited during the simulation. Overall, our learning model has $101 \times 101 \times 200$ coordinate points of states. Ceteris paribus, the FIRE model has 51 grid points for both

Table 3.3: Calibration, the Learning Model

Parameters	Value	Description
$1-\alpha$	0.68	Share of labour
β	0.913	Subjective discount factor
σ	2	Coeff. of relative risk aversion
θ	0.1	Probability of reentry
r^*	0.01	Risk free rate
ω	1.455	Labour supply curvature
δ_1	-0.6919	Loss function parameter
δ_2	0.7477	Loss function parameter
ρ_z	0.90	Serial correlation of z_t
σ_z	0.96%	Standard deviation of ε_t^z
$\overline{\gamma}$	1.005	Unconditional mean of trend
ρ_γ	0.21	Serial correlation of γ_t
σ_γ	0.254%	Standard deviation of ε_t^γ
σ_n	1.13%	Std of trend growth signal noise
V_γ/V_A	0.065	Relative variance of trend
σ_γ/σ_n	0.23	Signal-to-noise ratio
Discretization		
$[n_{\tilde{z}}, n_z]$	[101, 51]	Number of $\tilde{z}_t$ and z_t grids
$[n_{\tilde{\gamma}}, \gamma_z]$	[101, 51]	Number of $\tilde{\gamma}_t$ and γ_t grids
$[\underline{d}, \overline{d}]$	[0, 0.800]	Range of debt grids
$[\log(\underline{\tilde{\gamma}}), \log(\overline{\tilde{\gamma}})]$	[0.057%, 0.938%]	Range of trend belief grids

Notes: θ follows Aguiar and Gopinath (2006), indicating average autarky duration of 2.5 years. α, σ and ω values are common in small open economy literature. ρ_γ follows the Boz et al. (2011) estimation for developed economies.

exogenous shocks. The value functions for good financial status, bad financial status and bond price are iterated until the aggregate maximum norm between two adjacent steps is below $1.0e-6$.

3.5 Results

3.5.1 Quantitative results

Table 3.4 reports business cycle statistics of interest from data and simulations. The first column shows the results from data, all calculated as the average of individual GIIPS countries' respective statistics. The second column exhibits simulated moments from our learning model. The third column shows moments from the FIRE model. To compute the moments from two models, we run 500 independent chains of simulation with each chain containing 1200 quarters. We drop the first 200 quarters in each chain to obtain stationarity. The reported moments takes the median value of statistics across all 500 chains.

As we can see from the Table 3.4, the learning model generally matches business cycle data well. Most importantly, it produces highly negative correlation coefficient between trend growth beliefs and sovereign spreads, i.e. $\rho(r-r^*,\gamma)=-0.62$, which is very close to the coefficient in data -0.63. Meanwhile, the FIRE model only produces weak correlation (absolute value lower than 0.1) between perceived trend growth rates and sovereign spreads. The reason of low correlation for FIRE model is that the unconditional variance of trend growth process is very low while the changes in spreads are dominated by transitory shocks. In this article, we are able to rationalize the evidence of tight correlation between trend growth beliefs and sovereign debt spreads, even though the true trend may not be important to explain spreads.

There are two channels contributing to the match of coefficient of $\rho(r-r^*,\tilde{\gamma})$. The first is referred to as the "learning channel": trend growth perceptions are positively correlated with transitory growth beliefs. Under belief updating rule described

Table 3.4: Statistics from Data and Simulation

	Data	Learning	FIRE
Default frequency	-	4.4%	0.4%
$\mathbb{E}(r - r^*)$	2.03	2.02	0.64
$\sigma(r - r^*)$	0.026	0.027	0.007
$\sigma(y)$	0.025	0.025	0.024
$\sigma(c)/\sigma(y)$	0.9	1.30	1.34
$\rho(r - r^*, y)$	-0.42	-0.47	-0.59
$\rho(r - r^*, tby)$	0.45	0.71	0.82
$\rho(r - r^*, \tilde{z})$	-	-0.51	-0.56
$\rho(r - r^*, \tilde{\gamma})$	-0.63	-0.62	-0.07

Notes: Default frequency is calculated as the frequency of default event in 400 quarters. $r - r^*$ stands for the spread of sovereign debt, i.e. the yield of sovereign bond minus risk-free rate. y denotes HP-filtered GDP. *tby* denotes net export, or trade balance to GDP ratio. c stands for HP-filtered consumption. $\tilde{z}$ stands for the perceived transitory shock. $\tilde{\gamma}$ is the perceived trend growth rate.

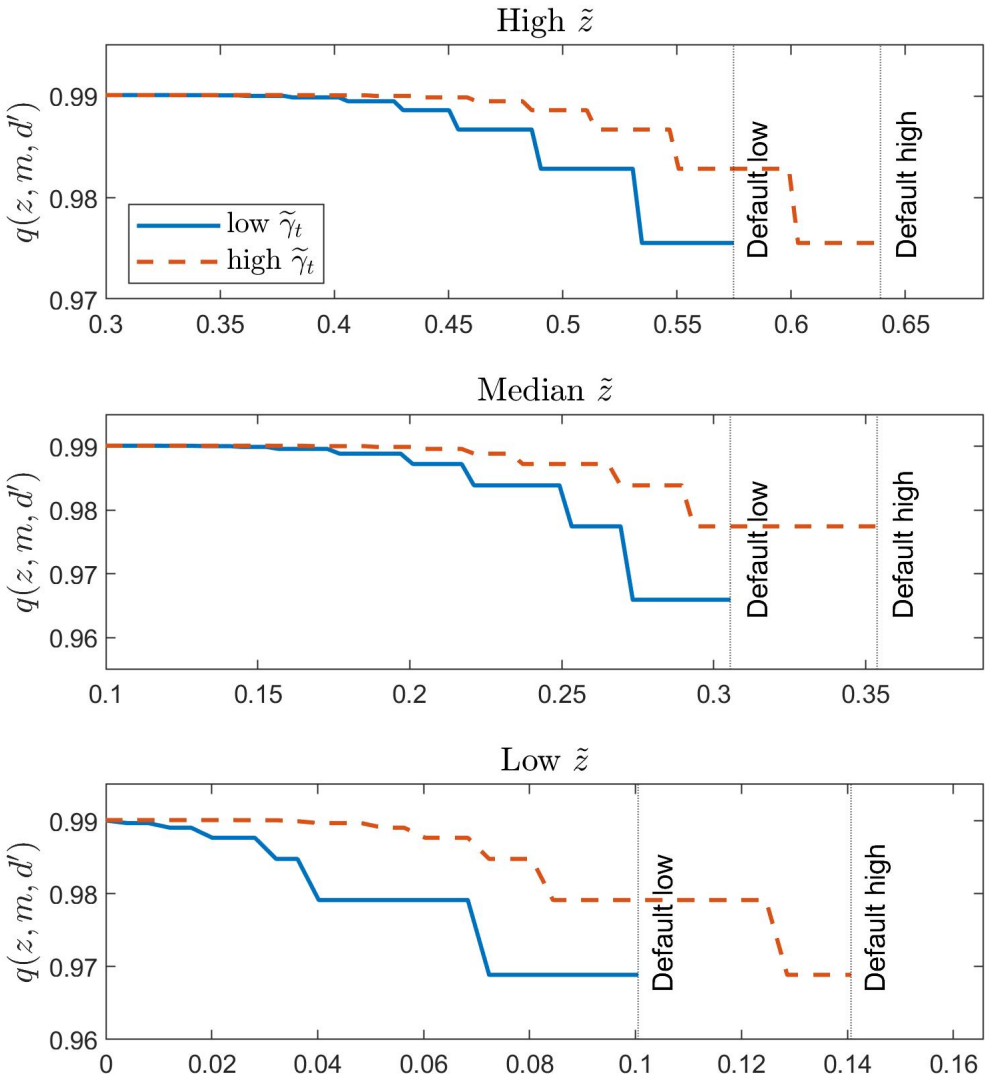

Figure 3.3: Bond price as functions of debt states. The blue solid lines correspond to 0.2% quarterly $\tilde{\gamma}$; red dashed lines correspond to 0.6% quarterly $\tilde{\gamma}$. $\tilde{z}$ is 0.056 in the high case (top panel), 0 in the median case (medium panel) and -0.056 in the low case (bottom panel). Prices only resides in good financial status. Lower $\tilde{z}$ results in fewer price supporting debt states. In the high and median $\tilde{z}$ case, the bond prices corresponding to zero debt outstanding are 0.99. Price lines are truncated for the convenience of illustration. "Default low" denotes the default sets associated with low perceived trend, while "Default high" relates to the high perceived trend.

by equation (3.24), trend belief comoves with the observed TFP, whose fluctuations are mainly ascribed to transitory shocks. Since debt price and most endogenous variables in the model is driven by transitory shocks, the correlation between spreads and transitory shocks will be strong. As verified by simulation, the correlation coefficient between $\tilde{\gamma}$ and $\tilde{z}$ is 0.42, while the correlation coefficient between $\tilde{\gamma}$ and $r_t - r^*$ is -0.62.

The second channel is named as the "belief channel". It comes from the fact that the perceived trend growth rate is taken into agents' infinite horizon expectation and hence influences their choices. As discussed in a previous section, the underestimation of trend growth leads to an overestimation of the value function gap $V^b - V^g$, which implies that repaying debt is becoming suboptimal because the future income and consumption are more likely to be lower. Observing this, the risk neutral foreign lenders takes the higher default probability into account and hence charge a higher spread over the country's sovereign debts. This relationship is verified by the debt price schedules as shown in Figure 3.3. We can see that for all three fixed levels of transitory growth beliefs, the prices (spreads) of sovereign debt corresponding to low trend belief is lower (higher) than the prices (spreads) corresponding to higher trend beliefs, across all shared debt states.

Comparing with the FIRE model, assuming imperfect knowledge on trend not only delivers higher default frequency but also a default frequency that is larger than average spread[13]. The reason is twofold. First, the default set resides on the downside of trend beliefs. Consider an imaginary threshold $\overline{\gamma}$ below which default is optimal. Lower trend belief leads to higher probability of $\gamma_t < \overline{\gamma}$. While higher trend belief makes the economy further away from default. Eventually the distribution of perceived trend is more dispersed than the real trend, as a result the default set $\{\gamma : \gamma \leq \overline{\gamma}\}$ enlarges. Second, trend belief is treated as a constant each time agents solve the optimization problems so that for an γ_t lower than $\overline{\gamma}$ the probability of $\gamma_t < \overline{\gamma}$ is zero (According to equation 3.30, debt price and spread is related to expected γ_t). Hence, the setup of anticipated utility negatively influences spreads. Overall, there is larger chance that the average spread falls below default frequency in the learning model.

[13]As discussed in Uribe and Schmitt-Grohé (2017), for equilibrium default model with one period debt, the simulated default frequency usually falls below the average debt spread.

Table 3.5: Simulation-Based Estimation of linear and non-linear relationships

	Simulation		GIIPS Data	
Statistics	Non-linear	Linear	Non-linear	Linear
$\hat{\beta}_1$	1.724	2.105	1.893	2.623
	(0.0748)	(0.0701)	(0.3064)	(0.2763)
$\hat{\beta}_2$	-2.016	-4.684	-0.547	-1.482
	(0.0825)	(0.1990)	(0.0684)	(0.1686)
SSE	3639.5	3846.5	984.21	1081.3
AIC	3767.0	3816.7	595.07	608.35
BIC	3776.6	3826.1	600.64	613.93
Sample size	1000	1000	120	120

Notes: SSE is sum of squared error of estimation; AIC is Akaike's Information Criteria; BIC means Bayesian Information Criteria. Numbers in brackets are standard errors of respective estimation. All 4 estimated coefficients are statistically significant in 1% confidence level.

Our learning model also replicates the non-linearity in the relationship between spreads and trend growth forecasts. As shown in Table 3.5, the sum of squared errors and information criteria for the non-linear model is much smaller than those for the linear model. Figure 3.4 visualizes the curve fitting. Data points in this figure is taken from an arbitrary chain of the 500 simulated chains. As in data, the simulated negative correlation is stronger at lower levels of trend belief. Regarding the intuition behind this non-linear relationship, note that default is a tail risk and default set is on the left-hand side of the probability density curve of the perceived TFP distribution. Below some threshold of TFP (keeping the debt state fixed), default would be an optimal choice. When the perceived trend growth is low, the density curve of perceived TFP moves to the left. Hence, the area below the density curve and to the left of the TFP threshold increases exponentially. This means if the perceived trend growth drops, the probability of default grows exponentially, and therefore the spread rises up with an increasing speed.

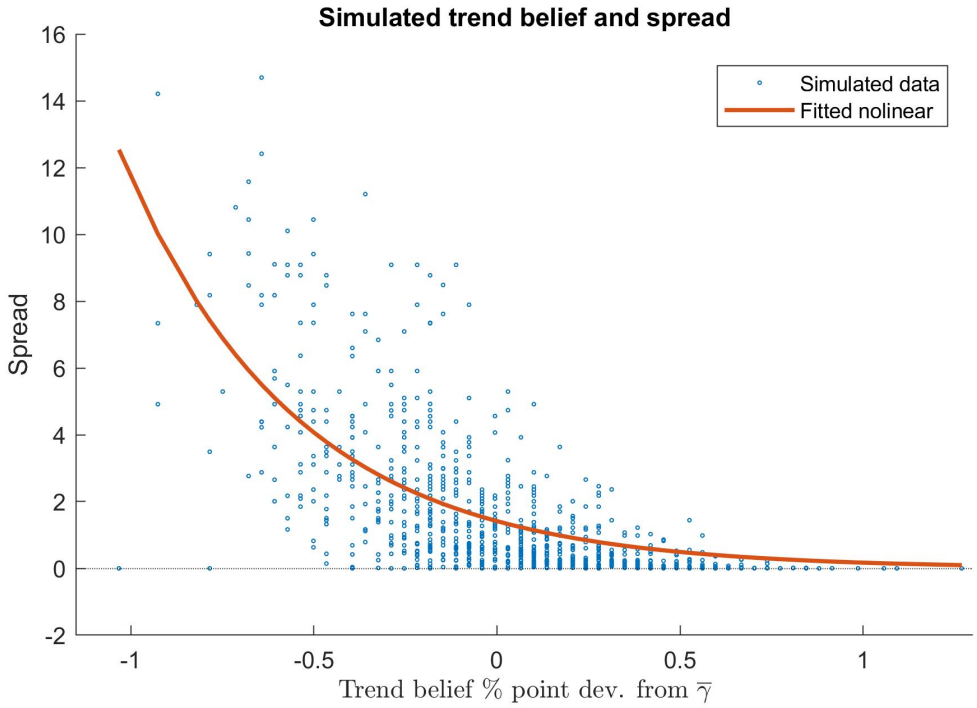

Figure 3.4: Debt spreads and trend forecasts from the learning model's simulation.

3.5.2 Impulse Response Analysis

In this section we conduct impulse response analysis to show how a negative transitory shock (transitory shock takes 96.5% of the TFP shock variance) influences exogenous beliefs and other variables. Considering the non-linear nature of sovereign default model, we follow Koop et al. (1996) and Arellano et al. (2018) to draw generalized impulse response functions. We simulate two bunches of 5000 independent paths, each path includes 320 periods.

The first bunch is called *shocked path*s. From time 1 to 320, true transitory shocks z_t are randomly generated following the underlying Markov chain, while trend estimation error ε_t^{γ} and trend signal noise ε_t^{n} follows their respective IID distribution. Given z_t, ε_t^{γ} and ε_t^{n}, perceived exogenous shocks $\tilde{z}_t$ and $\tilde{\gamma}_t$ are generated following the belief updating rule (3.24). The first 300 periods are used to get rid of the influence of initial value. The shocked time is 301, which is normalised to be time 0 in Figure 3.5: z_t is adjusted downwards by 1 percent in each path, but ε_t^{γ} and ε_t^{n} stay unchanged. From

time 301 on, z_t evolves under its conditional Markov chain while $\tilde{z}_t$ and $\tilde{\gamma}_t$ continue to update under rule (3.24).

For each shocked path, there is a *unshocked paths*, which is the same as the corresponding shocked path before time 301. From time 301 on, the unshocked path is not influenced by the 1% transitory shock. Hence, we obtain 5000 pairs of shocked and unshocked paths. Impulse response functions for variables with trend (such as output and consumption) take the average of the percentage differences between shocked and unshocked paths. For stationary variables such as exogenous shocks, sovereign spread and debt-to-GDP ratio, impulse response functions are simply the difference between two paths. Impulse response functions are plotted in Figure 3.5. Periods 1 to 300 are truncated. Any path with default event in the remaining 20 periods is discarded, as in Arellano et al. (2018).

In the $\tilde{z}$ panel of Figure 3.5, the magnitude of perceived transitory shock $\tilde{z}$ change in learning model (in blue solid line) is smaller than the size of the perceived change (which coincides with z) in FIRE model. This underestimation comes from learning rule (3.24) that a part of the true shock z is allocated to a downward adjustment in trend belief in the learning model. As illustrated by the $\tilde{\gamma}$ panel, trend belief for the learning model decreases on impact, while the belief for FIRE model is always $\overline{\gamma}$ because agents know that γ is independent with transitory shock. The $r - r^*$ panel shows that debt spreads for both models rise up immediately at the time of impact. The magnitude of the movement for the learning model is significantly larger than FIRE model (2.55% v.s. 0.70%). The spread change is also very short-lived: the surges drop sharply after time 0 and become very close to pre-shock levels on time 3. Since the change in trend belief is also transitory these impulse response functions verifies the negative $\rho(r - r^*, \tilde{\gamma})$ for the learning model.

Spread movement is accompanied with quick adjustment of debt. As shown in the d/y panel, debt-to-GDP ratios slightly rise up on time 0 and bottoms at time 3. A reduction in debt-to-GDP ratio decreases social planner's incentives to default, which is widely documented in sovereign default literature (e.g. Arellano (2008)) and revealed in Figure 3.3 that higher debt states are associated with lower prices (higher

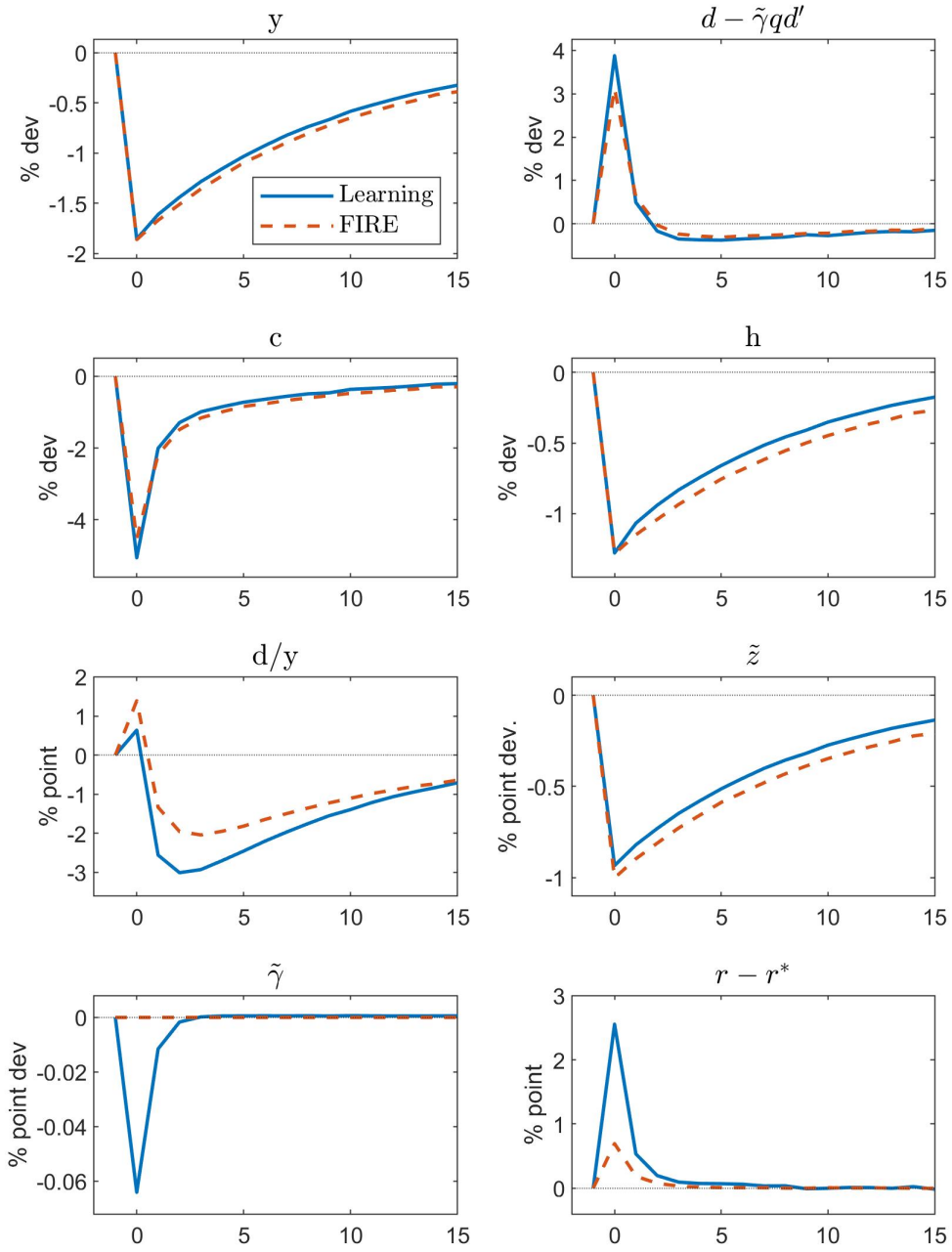

Figure 3.5: Impulse response functions to 1% decline in true transitory shock at time 0. $d - qd'$ denotes net debt repayment, h is working hours, d/y stands for debt-to-GDP ratio. Debt-to-GDP ratio d/y and spreads $r - r^*$ are the percentage point deviations from respective steady states.

spreads). Quick adjustment of borrowing results in swift recovery of spreads [14]. The upward movement in debt-to-GDP ratio at time 0 is due to the decline in output: d_0 is determined at time -1 at time 0 it is on the pre-shock level. y_0 is determined in period 0 and y_{-1} is at steady state because it is an endogenous variable that is determined at time -1. Since $y_0 < y_{-1}$ and $d_0 = d_{-1}$, d_0/y_0 will be higher than d_{-1}/y_{-1}.

In the y and h panel of Figure 3.5, output and working hours drop in similar scales for both models because the change in perceived TFP for the learning model ($\tilde{\gamma}$ plus $\tilde{z}$ equals -0.997%) is very close to FIRE model (-1%). Since period 1, output for learning becomes slightly higher because its $\tilde{z}$ is higher than the true size z while the difference between $\tilde{\gamma}$ and $\overline{\gamma}$ is negligible. The percentage growth of net export on GDP ratio is larger in learning model, as shown in the top right panel of Figure 3.5. For learning model, the obviously larger increment in debt spread means its net debt repayment $d_0 - \tilde{\gamma}_0 q_0 d_1$ must be lower. Therefore, higher trade balance is needed to finance a larger capital inflow reduction. Hence, consumption will be more adversely affected.

3.5.3 Typical Default Episodes

In this section we discuss typical default episodes, a topic generally of interest in equilibrium sovereign default literature (Mendoza and Yue, 2012, Gordon et al., 2018 and Na et al., 2018). Figure 3.6 shows the averages of all simulated paths around default events. The blue solid lines depict the learning model, while red dashed lines belong to the FIRE model. Default is normalized to happen at time 0. Time -2 indicates two periods before a typical default, while 2 denotes two periods after default. For trend belief, debt-to-GDP ratio and debt spread the windows end at 0, because in bad financial status sovereign debt does not exist, debt spread is not defined while trend belief is assumed to be on steady state.

As in most literature, defaults typically happen during "bad times" the features low

[14] If capital is involved in a sovereign default model, the response of spreads to a technology innovation will be much more persistent. For example, in Arellano et al. (2018), spreads revert to steady state in 25 periods following a -0.5% productivity innovation.

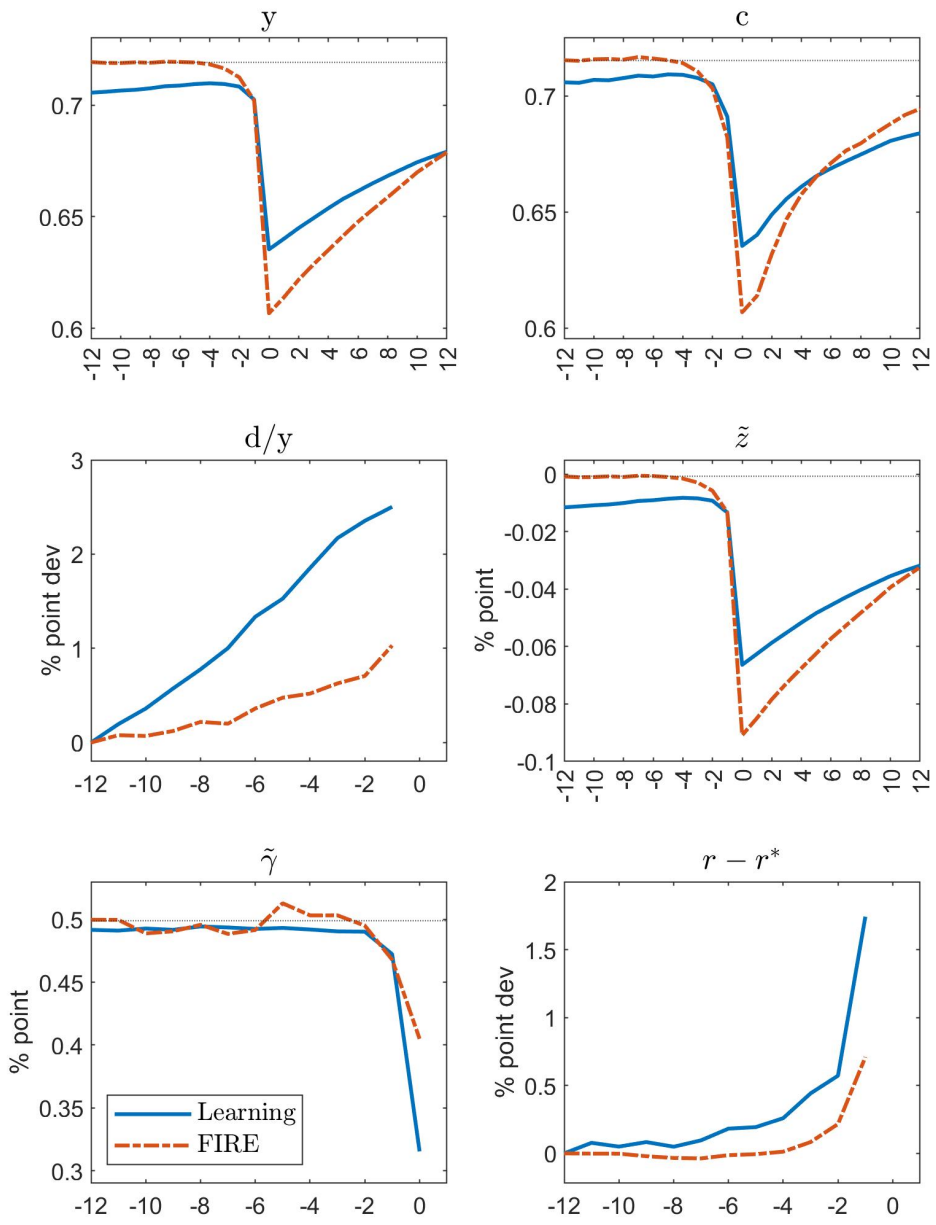

Figure 3.6: Typical default episodes for main variables. Debt-to-GDP ratio d/y and spreads $r - r^*$ are the percentage point deviations from respective steady states.

productivity, consumption and output[15]. As can be seen in the $\tilde{z}$ subplot of Figure 3.6, transitory shock in both models (FIRE model in red dashed line and the learning model in blue solid line) sharply drop down 2 periods before default. $\tilde{z}$ in the learning model is slightly higher because under the belief updating rule (3.24) part of the true transitory shock is allocated to trend belief. The fact of $\tilde{z} > z$ at default time results in output and consumption in the learning model being higher than FIRE model, which indicates that imperfect information on trend increases default tendency. The debt-to-GDP ratios for the two models both exhibit an upward trend, qualitatively in line with the Greek default documented in the Figure 8 of Na et al. (2018).

In the $\tilde{\gamma}$ panel, perceived trend growth for the learning model decreases since time -4 and this decline accelerates as the default time approaches. Trend growth for FIRE model drops down in a magnitude smaller than learning model. In the bottom right panel, sovereign bond spread rises in both models but the learning model has a larger scale of surge: since time -12, the increment in the spread is 1.74% for the learning model and only 0.71% for the FIRE. The above movements in contrary directions during typical default episodes is similar to the Greek data as illustrated in Figure 3.2. Meanwhile, the different magnitudes indicates that the learning model will deliver a more non-linear relationship between spreads and trend beliefs.

3.5.4 Output loss

In this section we provide a different perspective on the mechanisms of belief channel: Output loss is underestimated in the learning model when agents are pessimistic about trend growth, which in turn leads to higher default probability and spreads. The output in bad financial status before adjusting for productivity loss is denoted as y, while the output in bad financial status after productivity loss is labeled as y^{aut}. Output loss is defined as y^{aut}'s percentage deviation from y: $(y - y^{aut})/y \times 100$.

[15]Readers interested in defaults during "good times" may find Durdu et al. (2013) and Park (2017) useful. The former incorporates news shock so that bad news during good times could incur default; the later includes capital so that default may become optimal if high levels of capital is accumulated, even if the economy is in "good times".

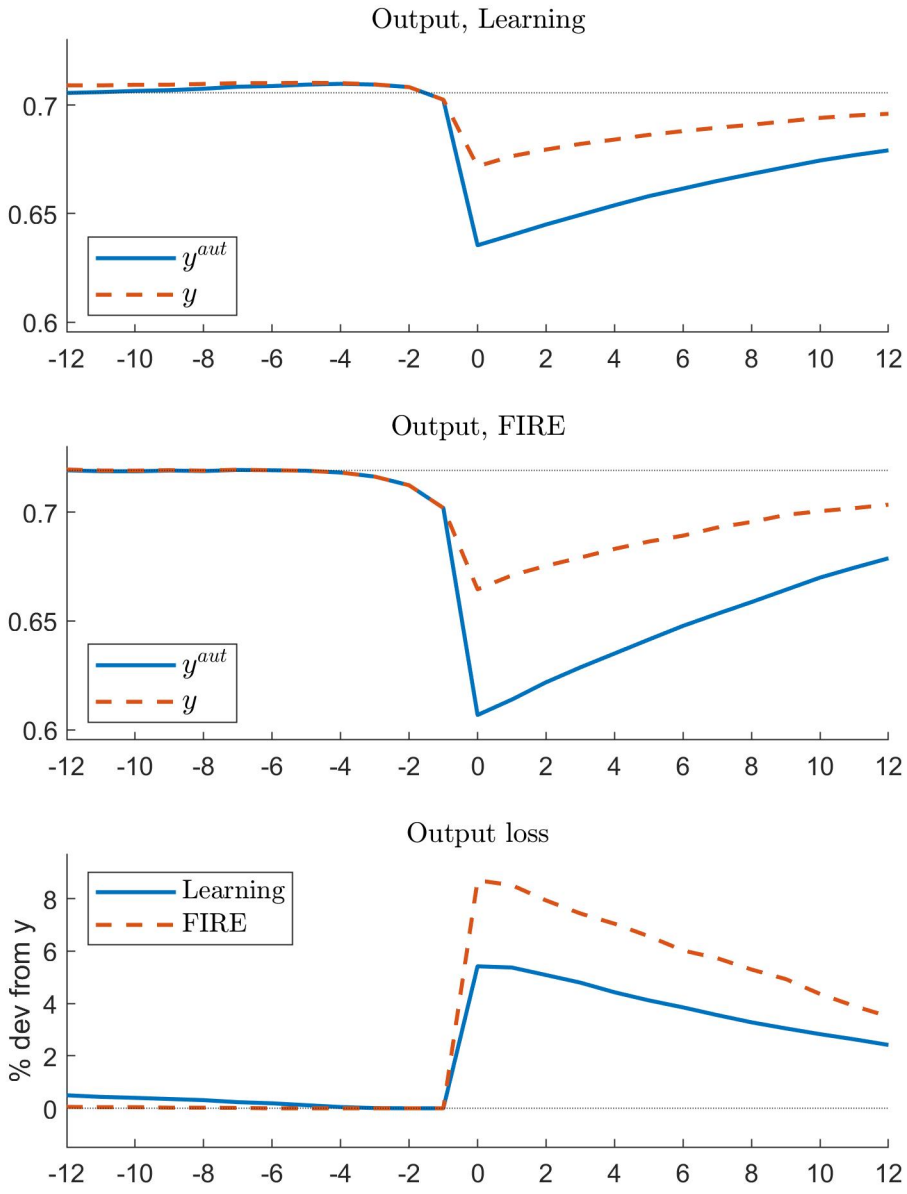

Figure 3.7: Different levels of output loss from the FIRE and Learning model.

The top and middle panel of Figure 3.7 show y and y^{aut} around a typical default event for the learning and FIRE model, respectively. Default is normalized to happen at time 0. The difference between y and y^{aut} becomes obvious after the default. Productivity cost defined in equation (3.14) sets an upper bound of productivity for bad financial status, resulting in y^{aut} being lower than y As highlighted by the bottom panel, the magnitude of output loss (calculated as y minus y^{aut}) for the learning model is smaller than that of FIRE model: at time 0, default cost is 8.80% in the former case but 5.42% in latter case.

The lower default cost in the learning model comes from the structural design: productivity loss is exogenously imposed and is independent of agents' trend beliefs. After a sequence of adverse TFP shocks, agents become pessimistic about trend growth (see learning rule 3.24). That is, $y^{aut}(z^{aut};\overline{\gamma})$ is more likely to be higher than $y(z^{aut},\tilde{\gamma})$, and hence $y(z^{aut},\tilde{\gamma}) - y^{aut}(z^{aut};\overline{\gamma})$ is more likely to be smaller. This means default cost tends to be underestimated during bad times in the learning model, which in turn delivers high incentives of borrowing and reneging.

3.6 Sensitivity analysis

3.6.1 Size of Errors about Trend Belief

In this section, we perform sensitivity analysis to see how the main results would alter with the different levels of trend growth uncertainty. Table 3.6 reports the results. In the benchmark model, the ratio of trend growth variance (V_γ) over TFP variance (V_A), i.e. V_γ/V_A, is calibrated to be 0.065 and the signal noise ratio σ_γ/σ_n is set to be 23%. Now we use alternative values for V_γ/V_A and σ_γ/σ_n to see how the simulated statistics would change. As shown in Table 3.6, for those alternative calibrations, the correlation coefficients $\rho(r-r^*,\gamma)$ lie in interval $[-0.47,-0.73]$. In other words, the negative correlation between trend growth beliefs and sovereign spreads still holds.

Case (6) to case (11) show adjustments in signal-to-noise ratio of trend (σ_γ/σ_n).

Table 3.6: Sensitivity analysis of trend uncertainty.

	$\sigma(r-r^*)$	$\rho(r-r^*,y)$	$\rho(r-r^*,tby)$	$\rho(r-r^*,z)$	$\rho(r-r^*,\tilde{\gamma})$
(1) Data	0.026	-0.42	0.45	N.A.	-0.63
(2) Benchmark	0.027	-0.47	0.71	-0.51	-0.62
Signal-to-noise ratio ($\sigma_\gamma/\sigma_n = 0.23$)					
(6) $\sigma_\gamma/\sigma_s = 0.11$	0.024	-0.47	0.72	-0.50	-0.73
(7) $\sigma_\gamma/\sigma_s = 0.16$	0.026	-0.47	0.71	-0.51	-0.69
(8) $\sigma_\gamma/\sigma_s = 0.21$	0.026	-0.47	0.71	-0.50	-0.64
(9) $\sigma_\gamma/\sigma_s = 0.25$	0.027	-0.46	0.71	-0.50	-0.61
(10) $\sigma_\gamma/\sigma_s = 0.30$	0.029	-0.47	0.70	-0.51	-0.57
(11) $\sigma_\gamma/\sigma_s = 0.45$	0.036	-0.45	0.67	-0.51	-0.47
Trend shock to TFP ($V_\gamma/V_A = 0.065$)					
(12) $V_\gamma/V_A = 0.05$	0.046	-0.45	0.62	-0.53	-0.57
(13) $V_\gamma/V_A = 0.06$	0.031	-0.46	0.69	-0.52	-0.60
(14) $V_\gamma/V_A = 0.07$	0.024	-0.46	0.72	-0.49	-0.63
(15) $V_\gamma/V_A = 0.08$	0.019	-0.45	0.74	-0.45	-0.66
(16) $V_\gamma/V_A = 0.09$	0.017	-0.43	0.75	-0.42	-0.67

Notes: Ratios in brackets show the calibration of benchmark model.

Lower ratios indicate noisier trend signals so that agents form their trend beliefs relying heavier on the observed TFPs. In case (6), $\rho(\tilde{\gamma}, \tilde{z}) = 0.51$ is higher than benchmark ($\rho(\tilde{\gamma}, \tilde{z}) = 0.42$). Recall that transitory shock takes the dominant part of TFP variance and is the main driver of spreads, thus $\rho(r - r^*, \gamma)$ is also higher in magnitude than the benchmark. For case (11), trend signal becomes more reliable as its variance of noise is smaller. The corresponding $\rho(\tilde{\gamma}, z) = 0.27$ is significantly lower than that of the benchmark, resulting in the correlation $\rho(r - r^*, \tilde{\gamma})$ as low as -0.47.

Case (12) to (16) explore different unconditional variance ratios for trend shock over TFP (V_γ/V_A). The low ratio in case (12) leads to a low variance in trend ($\log(\tilde{\gamma}_t)$ is in the interval of $[0.14\%, 0.86\%]$, while for the benchmark case the corresponding interval is $[0.06\%, 0.94\%]$). Low variance in trend leads to smaller magnitude in the correlation between spreads and trend beliefs. Case (12) also delivers high variance of bond spreads because the unconditional variance of perceived transitory shock is 0.096%, larger than the 0.063% in case (16) and the 0.078% in the baseline. By contrast, a larger V_γ/V_A ratio in case (16) delivers a wider range of trend growth beliefs and bigger magnitude in $\rho(r - r^*, \tilde{\gamma})$.

3.6.2 Long-Maturity Debt

In this section we investigate whether the main results still hold if the government issues long-maturity debts. Compared with one-period debt in the benchmark model, long-maturity debt facilitates hedging against income risks because the it provides state-contingent payoffs. If income risk is better insured, would trend beliefs still be significantly related to sovereign spreads? Following Chatterjee and Eyigungor (2012), the government pays coupon $\eta > 0$ in the form of final output for every unit of sovereign bond outstanding D_t. On each period, λ share of bond outstanding matures while the remaining $1 - \lambda$ share does not. The repayment of maturing bond's principal and coupon equals $[\lambda + (1 - \lambda)\eta]D_t$, while the income from issuing bonds is $q_t D_{t+1}$. The transfer payment to household at period t is

$$F = qD' - [\lambda + (1 - \lambda)(\eta + q')]D \tag{3.33}$$

The debt pricing rule is in the following form

$$\mathcal{I} \cdot \left[q(z, d'; \gamma) - \frac{\mathbb{E}_{z'|z} \mathcal{I}' \Big[\lambda + (1-\lambda) \Big(\eta + q(z', a(z', d'; \gamma); \gamma \Big) \Big]}{1 + r^*} \right] = 0 \tag{3.34}$$

where $a(z', d'; \gamma)$ is the policy rule of d_{t+1}. There is convergence difficulty in solving this type of dynamic programming problem. Following Gordon (2019), I use taste shock on both default and debt issuance decisions to facilitate convergence. This algorithm is also used in Arellano et al. (2020) and Galli (2020). Details of this algorithm are attached in the Appendix.

Discount rate β, productivity loss parameter δ_1 and δ_2 and true transitory shock error term σ_z are calibrated to match average spreads 2.05%, output loss 7% and standard deviation of output 2.5%. All other variables remain the same as the benchmark learning model. We also formulate the comparable FIRE model. The learning model delivers correlation coefficient between spreads and trend beliefs $\rho(r - r^*, \gamma) = -0.47$, a huge improvement than FIRE model where $\rho(r - r^*, \gamma) = -0.10$. Figure C.1 shows the long-maturity bond price schedules for different trend beliefs and transitory shocks. We can see that bond prices (spreads) are lower (higher) if trend belief decreases. Figure C.2 depicts the impulse functions to negative transitory shock. It is clear to see that in learning model transitory shock leads to underestimation of trend growth and bigger spreads surge. Figure C.3 illustrates typical default event. For the learning model, the pre-default trend belief decline is more consistent and the spreads rising is much higher. Both figure C.2 and C.3 are similar to the benchmark learning model with one-period debt.

3.7 Conclusion

Fundamentals seemed not to be the sole determinant of sovereign debt spreads during the recent Eurozone debt crisis. Contributing to this field of research, this paper documents new evidence on the role of potential output expectation: the correlation

between sovereign debt spreads and potential GDP growth forecasts is significantly negative and non-linear for Eurozone countries. Existing sovereign default models built on full information rational expectation (FIRE) hypothesis that agents know the true trend growth rates have hard time in explaining this new evidence. To provide a rationale, we augment the equilibrium sovereign default framework à la Aguiar and Gopinath (2006) by relaxing the FIRE: agents only have imperfect information on trend growth and therefore they need to learn about it to make optimal decisions about debt issuance and whether to default or repay. Beliefs on the transitory and trend components of TFP shocks are updated via an Bayesian updating rule. Each new trend belief is taken into infinite future when agents solve their optimization problems. Simulation results show the model replicates the documented new evidence: the correlation coefficient between spreads and trend beliefs is -0.62, very close to the -0.63 in GIIPS countries' data. Meanwhile, this relationship exhibits the significant non-linearity as in data: the negative correlation grows stronger at lower levels of trend beliefs. Impulse response analysis and the simulated typical episodes of default, which resembles the Greek default data around 2012, support the comovement between spreads and trend beliefs. We also explain the mechanisms of the above rationale: the learning channel relates the transitory shocks to the perceived trend beliefs. Meanwhile, the belief channel delivers debt price schedules that vary with trend beliefs.

Bibliography

Adam, K., Kuang, P., and Marcet, A. (2012). House price booms and the current account. *NBER Macroeconomics Annual*, 26(1):77–122.

Aguiar, M., Chatterjee, S., Cole, H., and Stangebye, Z. (2022). Self-fulfilling debt crises, revisited. *Journal of Political Economy*, 130(5):1147–1183.

Aguiar, M. and Gopinath, G. (2006). Defaultable debt, interest rates and the current account. *Journal of international Economics*, 69(1):64–83.

Aguiar, M. and Gopinath, G. (2007). Emerging market business cycles: The cycle is the trend. *Journal of political Economy*, 115(1):69–102.

Aldrich, E. M., Fernández-Villaverde, J., Gallant, A. R., and Rubio-Ramírez, J. F. (2011). Tapping the supercomputer under your desk: Solving dynamic equilibrium models with graphics processors. *Journal of Economic Dynamics and Control*, 35(3):386–393.

Anzoategui, D. (2021). Sovereign spreads and the effects of fiscal austerity. Technical report, Morgan Stanley Research.

Arellano, C. (2008). Default risk and income fluctuations in emerging economies. *American Economic Review*, 98(3):690–712.

Arellano, C. and Bai, Y. (2017). Fiscal austerity during debt crises. *Economic Theory*, 64(4):657–673.

Arellano, C., Bai, Y., and Mihalache, G. (2018). Default risk, sectoral reallocation, and persistent recessions. *Journal of International Economics*, 112:182–199.

Arellano, C., Bai, Y., and Mihalache, G. P. (2020). Monetary policy and sovereign risk in emerging economies (nk-default). Technical report, National Bureau of Economic Research.

Arellano, C., Maliar, L., Maliar, S., and Tsyrennikov, V. (2016). Envelope condition method with an application to default risk models. *Journal of Economic Dynamics and Control*, 69:436–459.

Bi, H. (2012). Sovereign default risk premia, fiscal limits, and fiscal policy. *European Economic Review*, 56(3):389–410.

Bianchi, J., Ottonello, P., and Presno, I. (2019). Fiscal stimulus under sovereign risk. Technical report, National Bureau of Economic Research.

Bocola, L. and Dovis, A. (2019). Self-fulfilling debt crises: A quantitative analysis. *American Economic Review*, 109(12):4343–77.

Borensztein, E. and Panizza, U. (2009). The costs of sovereign default. *IMF Staff Papers*, 56(4):683–741.

Born, B., Müller, G. J., and Pfeifer, J. (2020). Does austerity pay off? *Review of Economics and Statistics*, 102(2):323–338.

Boz, E., Daude, C., and Durdu, C. B. (2011). Emerging market business cycles: Learning about the trend. *Journal of Monetary Economics*, 58(6-8):616–631.

Chambers, J. and Gurwitz, Z. (2014). Default study: Sovereign defaults and rating transition data, 2013 update. *RatingsDirect, Standard and Poor's*.

Chatterjee, S. and Eyigungor, B. (2012). Maturity, indebtedness, and default risk. *American Economic Review*, 102(6):2674–99.

Coleman, C., Lyon, S., Maliar, L., and Maliar, S. (2021). Matlab, python, julia: What to choose in economics? *Computational Economics*, 58(4):1263–1288.

Corsetti, G., , and Müller, G. (2012). Has austerity gone too far? *VoxEU. org*.

Corsetti, G., Kuester, K., Meier, A., and Müller, G. J. (2013). Sovereign risk, fiscal policy, and macroeconomic stability. *The Economic Journal*, 123(566):F99–F132.

Cottarelli, C. (2012). Fiscal adjustment: Too much of a good thing? *VoxEU. org*.

David, A. C., Guajardo, J., and Yepez, J. F. (2022). The rewards of fiscal consolidations: Sovereign spreads and confidence effects. *Journal of International Money and Finance*, 123:102602.

De Grauwe, P. and Ji, Y. (2013). Self-fulfilling crises in the eurozone: An empirical test. *Journal of International Money and Finance*, 34:15–36.

Durdu, C. B., Nunes, R., and Sapriza, H. (2013). News and sovereign default risk in small open economies. *Journal of International Economics*, 91(1):1–17.

Eaton, J. and Gersovitz, M. (1981). Debt with potential repudiation: Theoretical and empirical analysis. *The Review of Economic Studies*, 48(2):289–309.

Eusepi, S. and Preston, B. (2011). Expectations, learning, and business cycle fluctuations. *American Economic Review*, 101(6):2844–72.

Fernández-Villaverde, J. and Valencia, D. Z. (2018). A practical guide to parallelization in economics. Technical report, National Bureau of Economic Research.

Galli, C. (2020). Inflation, default risk and nominal debt. *UCL manusript*.

Galli, C. (2021). Self-fulfilling debt crises, fiscal policy and investment. *Journal of International Economics*, 131:103475.

Garcia-Cicco, J., Pancrazi, R., and Uribe, M. (2010). Real business cycles in emerging countries? *American Economic Review*, 100(5):2510–31.

Gechert, S. and Rannenberg, A. (2015). The costs of greece's fiscal consolidation. *Vierteljahrshefte zur Wirtschaftsforschung*, 84(3):47–59.

Gordon, G. (2019). Efficient computation with taste shocks. Technical report, Federal Reserve Bank of Richmond.

Gordon, G., Guerron-Quintana, P., et al. (2018). A quantitative theory of hard and soft sovereign defaults. Technical report, Federal Reserve Bank of Richmond.

Gordon, G. and Guerron-Quintana, P. A. (2018). Dynamics of investment, debt, and default. *Review of Economic Dynamics*, 28:71–95.

Greenwood, J., Hercowitz, Z., and Huffman, G. W. (1988). Investment, capacity utilization, and the real business cycle. *The American Economic Review*, pages 402–417.

Guerrón-Quintana, P. (2021). Parallel computation of sovereign default models. *Available at SSRN 3912677*.

Hatchondo, J. C., Martinez, L., and Sapriza, H. (2010). Quantitative properties of sovereign default models: solution methods matter. *Review of Economic dynamics*, 13(4):919–933.

House, C. L., Proebsting, C., and Tesar, L. L. (2020). Austerity in the aftermath of the great recession. *Journal of Monetary Economics*, 115:37–63.

Kanellopoulos, K. and Kousis, M. (2018). Protest, elections and austerity politics in greece. *Living under austerity: Greek society in crisis*, pages 90–112.

King, R. G., Plosser, C. I., and Rebelo, S. T. (1988). Production, growth and business cycles: I. the basic neoclassical model. *Journal of monetary Economics*, 21(2-3):195–232.

Koop, G., Pesaran, M. H., and Potter, S. M. (1996). Impulse response analysis in nonlinear multivariate models. *Journal of Econometrics*, 74(1):119–147.

Koulovatianos, C., Mirman, L. J., and Santugini, M. (2009). Optimal growth and uncertainty: learning. *Journal of Economic Theory*, 144(1):280–295.

Kreps, D. M. (1998). Anticipated utility and dynamic choice. *Econometric Society Monographs*, 29:242–274.

Kuang, P. (2014). A model of housing and credit cycles with imperfect market knowledge. *European Economic Review*, 70:419–437.

Kuang, P. and Mitra, K. (2016). Long-run growth uncertainty. *Journal of Monetary Economics*, 79:67–80.

Kuang, P. and Mitra, K. (2021). Potential output pessimism and austerity in the european union. Technical report, University of Birmingham.

Lane, P. R. (2012). The european sovereign debt crisis. *Journal of economic perspectives*, 26(3):49–68.

Leeper, E. M., Plante, M., and Traum, N. (2010). Dynamics of fiscal financing in the united states. *Journal of Econometrics*, 156(2):304–321.

Mendoza, E. G., Tesar, L. L., and Zhang, J. (2014). Saving europe?: The unpleasant arithmetic of fiscal austerity in integrated economies. Technical report, National Bureau of Economic Research.

Mendoza, E. G. and Yue, V. Z. (2012). A general equilibrium model of sovereign default and business cycles. *The Quarterly Journal of Economics*, 127(2):889–946.

Na, S., Schmitt-Grohé, S., Uribe, M., and Yue, V. (2018). The twin ds: Optimal default and devaluation. *American Economic Review*, 108(7):1773–1819.

Park, J. (2017). Sovereign default and capital accumulation. *Journal of International Economics*, 106:119–133.

Peterman, W. B. (2016). Reconciling micro and macro estimates of the frisch labor supply elasticity. *Economic inquiry*, 54(1):100–120.

Preston, B. (2005). Learning about monetary policy rules when long-horizon forecasts matter. *International Journal of Central Banking*.

Schmitt-Grohé, S. and Uribe, M. (2003). Closing small open economy models. *Journal of international Economics*, 61(1):163–185.

Schmitt-Grohé, S. and Uribe, M. (2004). Solving dynamic general equilibrium models using a second-order approximation to the policy function. *Journal of economic dynamics and control*, 28(4):755–775.

Sims, C. A. (2002). Solving linear rational expectations models. *Computational economics*, 20(1-2):1.

Tauchen, G. (1986). Finite state markov-chain approximations to univariate and vector autoregressions. *Economics Letters*, 20(2):177–181.

Tomz, M. and Wright, M. L. (2013). Empirical research on sovereign debt and default. *Annu. Rev. Econ.*, 5(1):247–272.

Uhlig, H. (1995). A toolkit for analyzing nonlinear dynamic stochastic models easily. *CentER Discussion Paper*, 1995.

Uribe, M. and Schmitt-Grohé, S. (2017). *Open Economy Macroeconomics*. Princeton University Press.

Yue, V. Z. (2010). Sovereign default and debt renegotiation. *Journal of international Economics*, 80(2):176–187.

Appendix A

Appendix to Chapter 1

A.1 Deriving Optimal Consumption and Labour

Assume a social planner who knows all the information of the economy wishes to maximize household's utility $u(C, H)$. Combining the budget constraints for the household and government, respectively equation (1.3) and (1.10), and the government spending rule (1.9), we obtain the post-tax budget constraint for the household:

$$C_t + \tilde{I}_t + u_t^G = (1 - \psi_1)Y_t + q_t B_{t+1} - (\psi_2 + q_t^1)B_t$$

where $q_t^1 = \lambda + (1-\lambda)(\eta + q_t)$. Then we can build a Lagrangian to derive the necessary conditions for the social planner's problem:

$$\mathcal{L}_t = \ln(C_t) - \theta \frac{H_t^{1+\chi}}{1+\chi} - \Lambda_t \Big[C_t - (1 - \psi_1)Y_t + \tilde{I}_t + u_t^G - q_t B_{t+1} + (\psi_2 + q_t^1)B_t \Big]$$

Optimization yields the following first order conditions for consumption and working hours:

$$\frac{1}{C_t}(1 - \psi_1)e^{z_t} K_t^{\alpha}(1 - \alpha)H_t^{-\alpha} = \theta H_t^{\chi+\alpha}$$

then we can derive

$$Y_t = \frac{\theta C_t H_t^{1+\chi}}{(1-\psi_1)(1-\alpha)}$$

Substituting the above equation into the post-tax budget constraint for the household, we can write working hours as a function of variables determined by states and candidate policies:

$$H_t = \Big[\frac{1-\alpha}{\theta}\Big(1+\frac{s_t}{C_t}\Big)\Big]^{\frac{1}{\chi+1}}$$

where $s_t = \tilde{I}_t + u_t^G - q_t B_{t+1} + (\psi_2 + q_t^1)B_t$. q_t is treated as given for the social planner because the debt price is determined in a buy-side international financial market, as shown in equation (1.17). Now the budget constraint could be modified as

$$C_t = (1-\psi_1)e^{z_t}K_t^{\alpha}\Big[\frac{1-\alpha}{\theta}\Big(1+\frac{s_t}{C_t}\Big)\Big]^{\frac{1-\alpha}{1+\chi}} - s_t$$

Notice that other than C_t, all the variables in the above equation are states and candidate polices (recall the price q_t is a function of exogenous shocks and K', B'). Thus, we can derive the optimal consumption by finding the roots of the above function of C_t.

A.2 Solving Long-Maturity Debt with Taste Shock

In this section we show how to implement taste shocks in the debt borrowing decision and default decision to induce convergence in value function iteration. I restrict debt policy B' and K' within a discrete set and associate each coordinate of B' and K' with an i.i.d. taste shock in Gumbel (Extreme Value Type I) distribution. The coordinates of debt and capital states are denoted as A and the according policy coordinates are A'. The government's optimization problem of repayment is rearranged as:

$$V^g(S, A, \langle\varepsilon_{A'}\rangle) = \mathbb{E}_{\varepsilon_{A'}}\Big[\max_{C,H,A'} \mathcal{W}(S', A') + \sigma_A \varepsilon_{A'}\Big] \tag{A.1}$$

where σ_A governs the relative importance of taste shock on debt and capital choice. σ_A should be big enough to ensure convergence. With $\sigma_A = 0$, $V^g(S, A, \langle\varepsilon_{A'}\rangle)$ returns to the non perturbed case, which suffers from convergence problem in value function

iteration solution method. $\mathcal{W}$ is the value of repayment for all possible choices of A':

$$\mathcal{W}(S, A, A') = u(C, H) + \beta \mathbb{E}_{S'|S} V(S', A') \tag{A.2}$$

Notice that the $\mathcal{W}$ associated with optimal debt and capital choice is denoted as $\mathcal{W}^*$:

$$\mathcal{W}^*(S, A) = \max_{A'} \mathcal{W}(S, A, A') \tag{A.3}$$

The ex ante choice probability of debt policy is given by

$$\mathbb{P}(A' = i|S, A) = \frac{\exp\Big[(\mathcal{W}(S, A, i) - \mathcal{W}^*(S, A))/\sigma_A\Big]}{\sum_{\tilde{i}} \exp\Big[(\mathcal{W}(S, A, \tilde{i}) - \mathcal{W}^*(S, A))/\sigma_A\Big]} \tag{A.4}$$

After introducing the taste shock on the default decision, the value of default becomes

$$V(S, A) = \mathbb{E}_{\varepsilon_{\mathcal{D}=1}, \varepsilon_{\mathcal{D}=0}} \left[\max_{\mathcal{D}=0,1} \Big\{ V^g(S, A) + \sigma_{\mathcal{D}} \varepsilon_{\mathcal{D}=0}, V^b(S, K) + \sigma_{\mathcal{D}} \varepsilon_{\mathcal{D}=1} \Big\} \right] \tag{A.5}$$

where $\sigma_{\mathcal{D}}$ governs the importance of taste shock on default decision. The probability of being in good financial state has following closed form expression:

$$\mathbb{P}(\mathcal{D} = 0|S, A) = \frac{\exp\Big[V^g(S, A)/\sigma_{\mathcal{D}}\Big]}{\exp\Big[V^b(S, K)/\sigma_{\mathcal{D}}\Big] + \exp\Big[V^g(S, A)/\sigma_{\mathcal{D}}\Big]} \tag{A.6}$$

Following the assumption of risk-neutral pricing, the price schedule of long-term debt becomes:

$$q(S, A') = \mathbb{E}_{S'|S} \left[\mathbb{P}(\mathcal{D} = 0|S', A') \frac{\lambda + (1 - \lambda)\Big(\eta + \sum_{A''} \mathbb{P}(A''|S', A') q(S', A'')\Big)}{1 + r^*} \right] \tag{A.7}$$

Now, $\mathbb{P}(\mathcal{D} = 1|S, A)$ and $\mathbb{P}(A' = i|S, A)$ moves continuously in a guess of price rule, facilitating convergence in price schedule. Without taste shock, there is possibility that in some states social planner is indifferent between two debt policies, therefore stationary solution cannot be obtained. I discrete the space of productivity shock

and government spending shock into 31 equally spaced grid points respectively. Debt and capital space are respectively discretized into 85 grid points. Therefore, there are 31×31 coordinates for exogenous states while 85×85 coordinates for endogenous states. Accordingly, I set σ_B to $3e^{-3}$ and $\sigma_{\mathcal{D}}$ to $5.0e^{-4}$. This choice of taste shock size ensures convergence of the long-term debt sovereign default model within 1000 iterations. The debt price as functions of capital and debt are depicted as follows

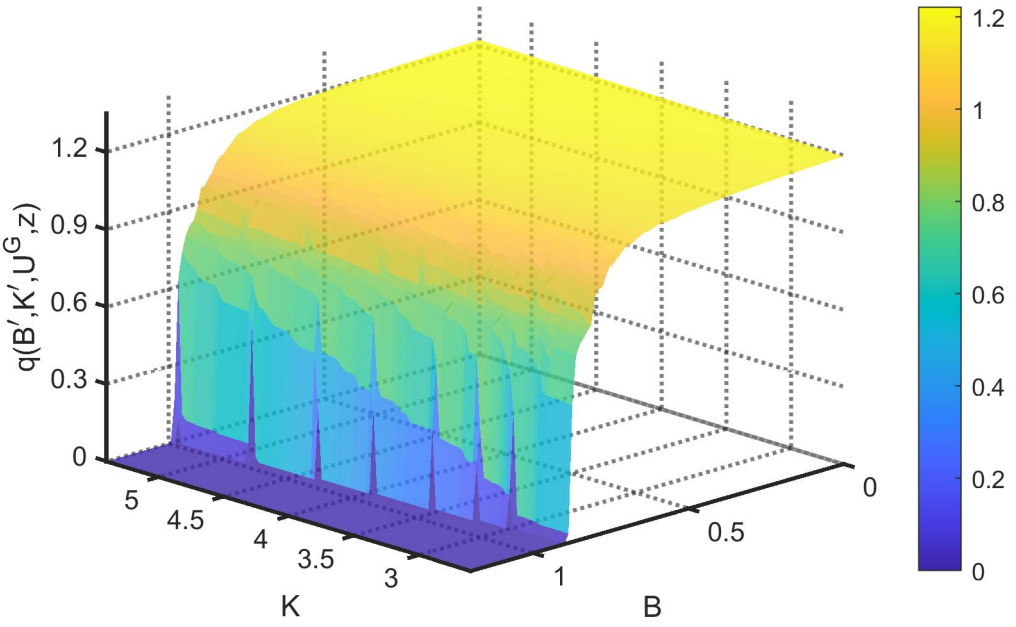

Figure A.1: Debt price as function of capital and debt state, with medium TFP, zero govt shock.

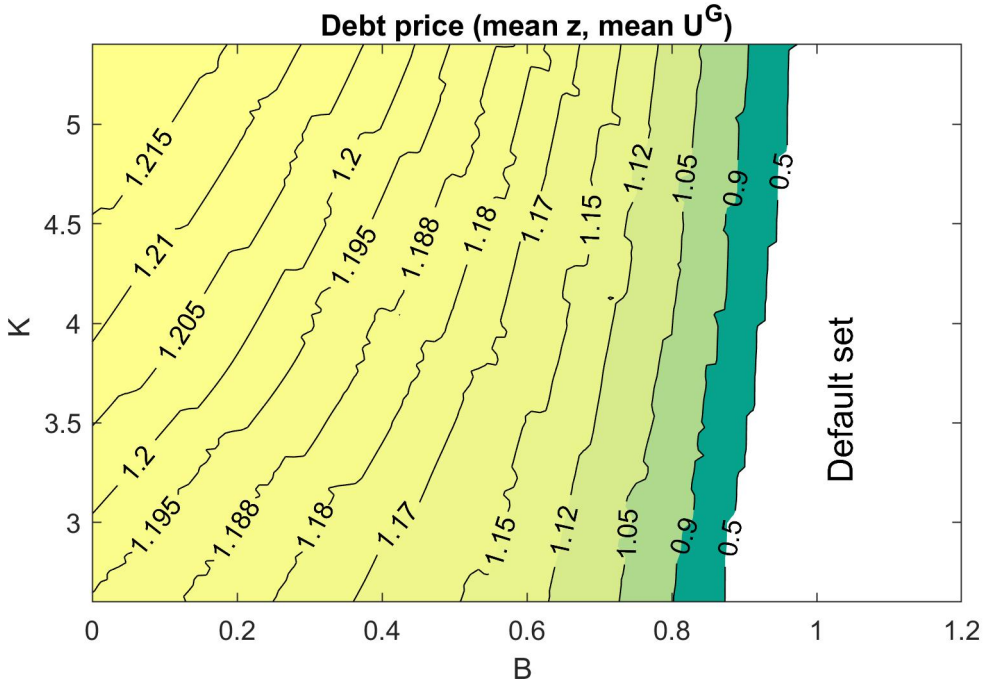

Figure A.2: Debt price contour lines on capital and debt states (medium TFP, zero govt shock).

Appendix B

Appendix to Chapter 2

B.1 Solving Long-Maturity Debt with Taste Shock

In this section I show the taste shock algorithm to solve the sovereign default model with long-maturity debts. Debt policy b' is restricted within a discrete set and each grid point of b' is associated with an i.i.d. taste shock in Gumbel (Extreme Value Type I) distribution. The government's optimization problem of repayment is rearranged as:

$$V^G(y, b, \langle \varepsilon_{b'} \rangle) = \mathbb{E}_{\varepsilon_{b'}} \Big[\max_{c \geq 0, b' \geq 0} \mathcal{W}(y', b') + \sigma_b \varepsilon_{b'} \Big] \tag{B.1}$$

where σ_b governs the relative importance of taste shock on debt issuance. With $\sigma_b = 0$, $V^G(y, b, \langle \varepsilon_{b'} \rangle)$ returns to the non perturbed case, which suffers from convergence problem in value function iteration solution method. In the implementation, I set σ_D to $5e^{-4}$ and $\sigma_{\mathcal{B}}$ to $2e^{-4}$ and this size of taste shock ensures the convergence of the long-term debt sovereign default model within 1000 iterations. $\mathcal{W}$ is the value of repayment for all possible choices of b':

$$\mathcal{W}(y, b, b') = u(c) + \beta \mathbb{E}_{y'|y} V(y', b') \tag{B.2}$$

Notice that the $\mathcal{W}$ associated with optimal debt and capital choice is denoted as $\mathcal{W}^*$:

$$\mathcal{W}^*(y,b) = \max_{b'} \mathcal{W}(y,b,b') \tag{B.3}$$

The ex ante choice probability of debt policy is given by

$$\mathbb{P}(b' = i|y,b) = \frac{\exp\Big[(\mathcal{W}(y,b,i) - \mathcal{W}^*(y,b))/\sigma_b\Big]}{\sum_{\tilde{i}} \exp\Big[(\mathcal{W}(y,b,\tilde{i}) - \mathcal{W}^*(y,b))/\sigma_b\Big]} \tag{B.4}$$

With taste shock, the value of being in bad financial status becomes

$$V(y,b) = \mathbb{E}_{\varepsilon_{\mathcal{D}=1},\varepsilon_{\mathcal{D}=0}}\left[\max_{\mathcal{D}=0,1}\Big\{V^G(y,b) + \sigma_{\mathcal{D}}\varepsilon_{\mathcal{D}=0}, V^B(y) + \sigma_{\mathcal{D}}\varepsilon_{\mathcal{D}=1}\Big\}\right] \tag{B.5}$$

where $\sigma_{\mathcal{D}}$ governs the importance of taste shock on default decision. The probability of being in good financial state has following closed form expression:

$$\mathbb{P}(\mathcal{D}=0|y,b) = \frac{\exp\Big(V^G(y,b)/\sigma_{\mathcal{D}}\Big)}{\exp\Big(V^B(y)/\sigma_{\mathcal{D}}\Big) + \exp\Big(V^G(y,b)/\sigma_{\mathcal{D}}\Big)} \tag{B.6}$$

and the price of long-term debt becomes:

$$q(y,b') = \mathbb{E}_{y'|y}\left[\mathbb{P}(\mathcal{D}=0|y',b')\frac{\lambda + (1-\lambda)\Big(\eta + \sum_{b''}\mathbb{P}(b''|y',b')q(y',b'')\Big)}{1+r^*}\right] \tag{B.7}$$

Now $\mathbb{P}(\mathcal{D}=1|y,b)$ and $\mathbb{P}(b'=i|y,b)$ moves continuously between debt grids and hence facilitates the convergence in price function. Without taste shock the social planner is likely to be indifferent between two debt policies and therefore no stationary solution could be obtained.

B.2 Debt Price Schedules

In this section I show sovereign debt price as a function of endowment y and debt issuance b', i.e. $q = q(y, b')$, for one-period debt (Figure B.1) and long-maturity debt (Figure B.2). We set $N_y = 25$ and $N_b = 200$ for the upper panels of two figures while $N_y = 25$ and $N_b = 3000$ for the lower panels. We can see that for both models, low endowments and high debt policies are related to lower debt prices (higher spreads). It is also clear that higher number of debt grid points (N_b) leads to better approximation for the DVFI solutions: the debt prices in the lower panels looks smoother than those in the upper panels.

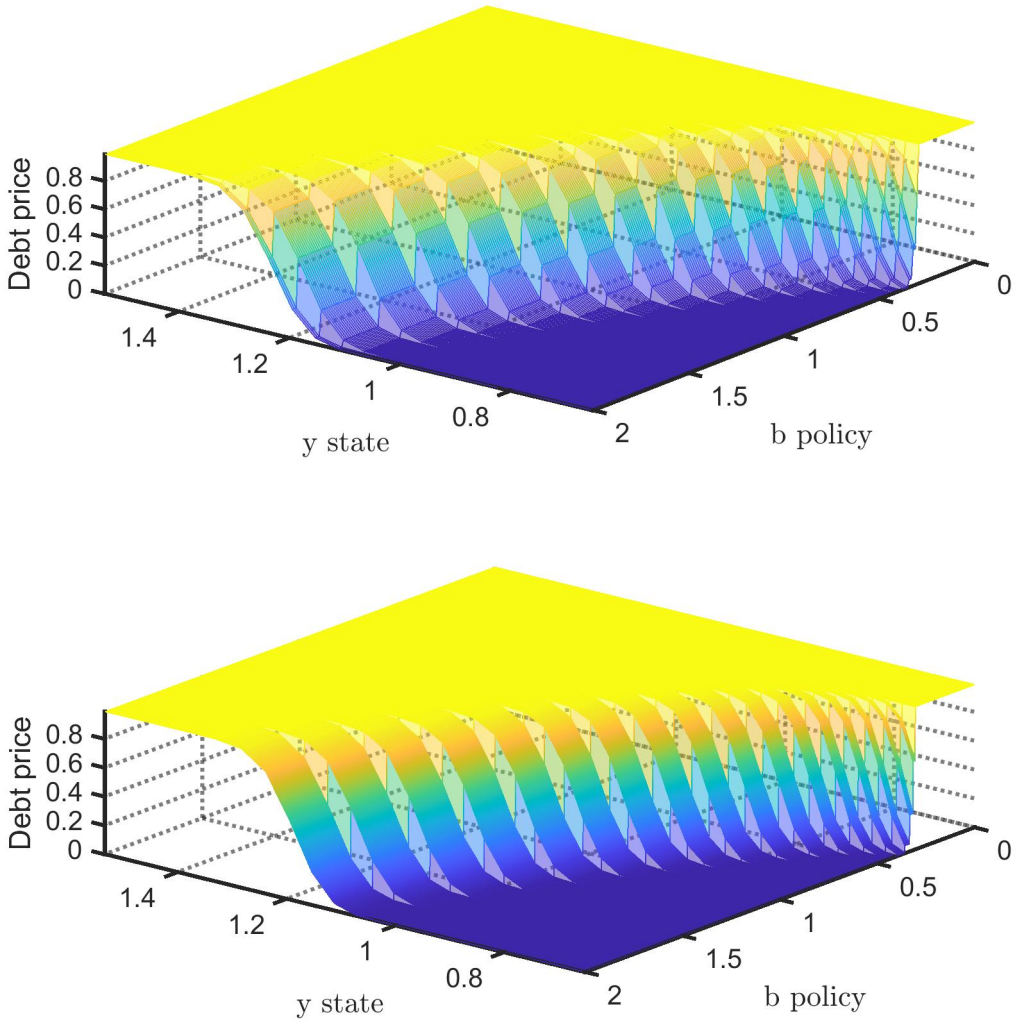

Figure B.1: One-period debt price as a function of endowment y and debt policy b'.

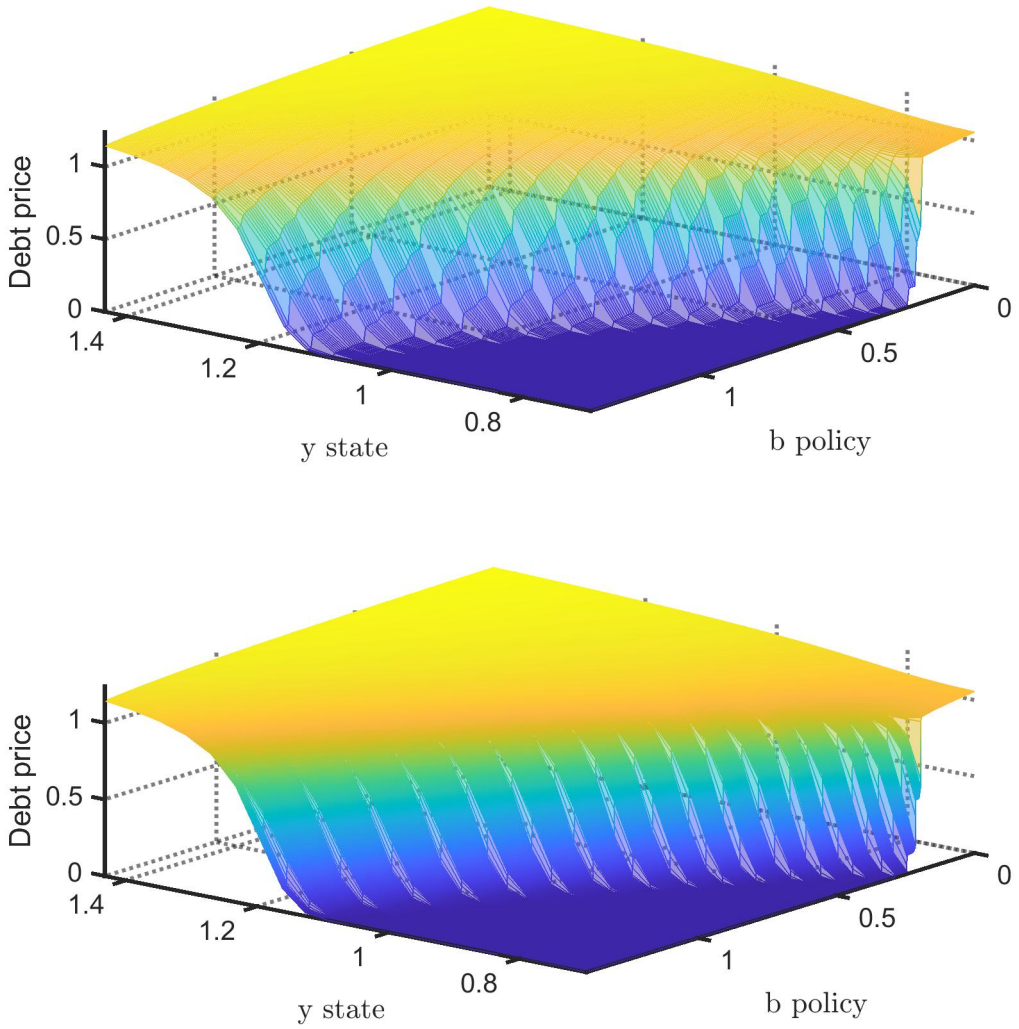

Figure B.2: Long-maturity debt price as a function of endowment y and debt policy b'.

Appendix C

Appendix to Chapter 3

C.1 First Order Conditions

In this section, I show the derivation of equilibrium consumption and labour. To solve household's problem, build the Lagrangian

$$\mathcal{L} = E_t \sum_{t=0}^{\infty} \beta^t \left\{ u(C_t, h_t) - \Lambda_t \Big[C_t - W_t h_t - \Pi_t - F_t \Big] \right\} \tag{C.1}$$

where Λ_t is the Lagrangian multiplier with trend. We can derive the First Order Conditions (F.O.C.) with respect to consumption and labour supply (working hours):

$$C_t : \qquad \left(C_t - \frac{1}{\omega} \Gamma_{t-1} h_t^{\omega} \right)^{-\sigma} = \Lambda_t \tag{C.2}$$

$$h_t : \qquad \left(C_t - \frac{1}{\omega} \Gamma_{t-1} h_t^{\omega} \right)^{-\sigma} \Gamma_{t-1} h_t^{\omega - 1} = \Lambda_t W_t \tag{C.3}$$

From output function (3.7) and profit function (3.6), firm's F.O.C. with respect to labour demand is:

$$h_t : \qquad (1 - \alpha) e^{z_t} \Gamma_t h_t^{-\alpha} = W_t \tag{C.4}$$

We induce stationary by normalizing all variables with trend by Γ_{t-1}, as in Boz et al. (2011). Specifically, let lowercase letter denote detrended variables, then $x_t \equiv \frac{X_t}{\Gamma_{t-1}}$ and $\lambda_t \equiv (\Gamma_{t-1})^{\sigma}\Lambda_t$, where $X = \{C, W, D, Y\}$.

First we detrend households' sequential budget constraint:

$$\frac{C_t}{\Gamma_{t-1}} = \frac{W_t h_t}{\Gamma_{t-1}} + \frac{(Y_t - W_t h_t)}{\Gamma_{t-1}} + \frac{F_t}{\Gamma_{t-1}}$$

$$\Rightarrow \quad c_t = y_t + f_t \tag{C.5}$$

We can combine the household's F.O.C. with respect to consumption and labour supply to derive the optimal labour as a function of wage. Because we use GHH preference, labour supply is irrelevant to consumption decisions:

$$\Gamma_{t-1} h_t^{\omega-1} = W_t$$

$$\Rightarrow \quad h_t = w_t^{\frac{1}{\omega-1}} \tag{C.6}$$

where w_t is detrended wage, $w_t = W_t/\Gamma_{t-1}$. From firm's F.O.C. with respect to labour demand, we derive wage as a function of labour:

$$\frac{W_t}{\Gamma_{t-1}} = (1-\alpha) e^{z_t} \frac{\Gamma_t}{\Gamma_{t-1}} h_t^{-\alpha}$$

$$\Rightarrow \quad w_t = (1-\alpha) e^{z_t} \gamma_t h_t^{-\alpha} \tag{C.7}$$

We obtain the equilibrium labour by combining labour supply and demand function to diminish wage:

$$h_t = \left((1-\alpha) e^{z_t} \gamma_t h_t^{-\alpha}\right)^{\frac{1}{\omega-1}}$$

$$\Rightarrow \quad h_t = \left((1-\alpha) e^{z_t} \gamma_t\right)^{\frac{1}{\omega+\alpha-1}} \tag{C.8}$$

then equilibrium output in good financial status can be written as function of productivity, beginning from detrended production function:

$$\frac{Y_t}{\Gamma_{t-1}} = e^{z_t} \frac{\Gamma_t}{\Gamma_{t-1}} h_t^{1-\alpha}$$

$$\Rightarrow \quad y_t = (1-\alpha)^{\frac{1-\alpha}{\omega+\alpha-1}} \Big(e^{z_t} \gamma_t \Big)^{\frac{\omega}{\omega+\alpha-1}} \tag{C.9}$$

For the government transfer, divide both sides by Γ_{t-1}:

$$\frac{F_t}{\Gamma_{t-1}} = \mathcal{I}_t \left(-\frac{D_t}{\Gamma_{t-1}} + q_t \frac{D_{t+1}}{\Gamma_t} \frac{\Gamma_t}{\Gamma_{t-1}} \right)$$

$$\Rightarrow \quad f_t = \mathcal{I}_t \Big(-d_t + \gamma_t q_t d_{t+1} \Big) \tag{C.10}$$

The detrended consumption rule is derived by replacing government transfer f_t in flow budget constraint of households (C.5). When the country is in good financial status ($\mathcal{I}_t = 1$):

$$c_t = y_t - d_t + \gamma_t q_t d_{t+1} \tag{C.11}$$

and consumption rule in bad financial status ($\mathcal{I}_t = 0$)

$$c_t^{aut} = y_t^{aut} = (1-\alpha)^{\frac{1-\alpha}{\omega+\alpha-1}} \Big(\gamma_t e^{z_t^{aut}} \Big)^{\frac{\omega}{\omega+\alpha-1}} \tag{C.12}$$

where y_t^{aut} is related to default loss, see relevant section for details. Equilibrium working hours in bad financial status is

$$h_t^{aut} = \Big((1-\alpha) \gamma_t e^{z_t^{aut}} \Big)^{\frac{1}{\omega+\alpha-1}} \tag{C.13}$$

while detrended wage in this state is

$$w_t^{aut} = (1-\alpha) e^{z_t^{aut}} \gamma_t (h_t^{aut})^{-\alpha} \tag{C.14}$$

C.2 Algorithm

At time t, the social planner treat current trend belief $\tilde{\gamma}$ as a constant parameter to obtain solutions. During the simulation, given a chain of estimated trend growth with length T, i.e. $\{\tilde{\gamma}_1, \tilde{\gamma}_2, ..., \tilde{\gamma}_T\}$, we may need to obtain T decision rules $\{g(\tilde{z}, d; \tilde{\gamma})\}_{t=0}^{T}$.

Unfortunately, following literature, reliable solutions for sovereign default model resort to value function iteration method, which could be very slow if the number of T is big enough to deliver reliable analysis.

To speed up, we discrete the space of trend growth belief into a small group of candidate grid points. Suppose all the visited trend belief during the simulation lie in interval $[a, b]$, we define a sequence of n candidate grids: $\tilde{\gamma}_i$s and list them in ascending order: $\{\tilde{\gamma}_1, \tilde{\gamma}_2, ..., \tilde{\gamma}_n\}$, where $\tilde{\gamma}_1 \geq a$ and $\tilde{\gamma}_n \leq b$. n could be much smaller than T. For each candidate grid point $\tilde{\gamma}_i$, the dynamic programming problem is solved to get decision rule $g_i(\cdot; \tilde{\gamma}_i)$ and transition rule $h_i(\cdot; \tilde{\gamma}_i)$ For the total of n grids, we solve the model by n times and obtain a sequence of decision rules $\{g_1, g_2, ..., g_n\}$ as well as transition rules $\{h_1, h_2, ..., h_n\}$. During the simulation, given a trend belief $\tilde{\gamma}_t$, we find the ith candidate grid that minimizes its distance to $\tilde{\gamma}_t$, i.e. $i = \arg\min(|\tilde{\gamma}_t - \tilde{\gamma}_i|)$. With index i, corresponding $g_i(\cdot; \tilde{\gamma}_i)$ and $h_i(\cdot; \tilde{\gamma}_i)$ are picked out to run the calculation. For next period, we find the new index i to locate new solutions. We continue the loop until the simulation of T periods is completed.

C.3 Relevant Figures for Long-Maturity Debt

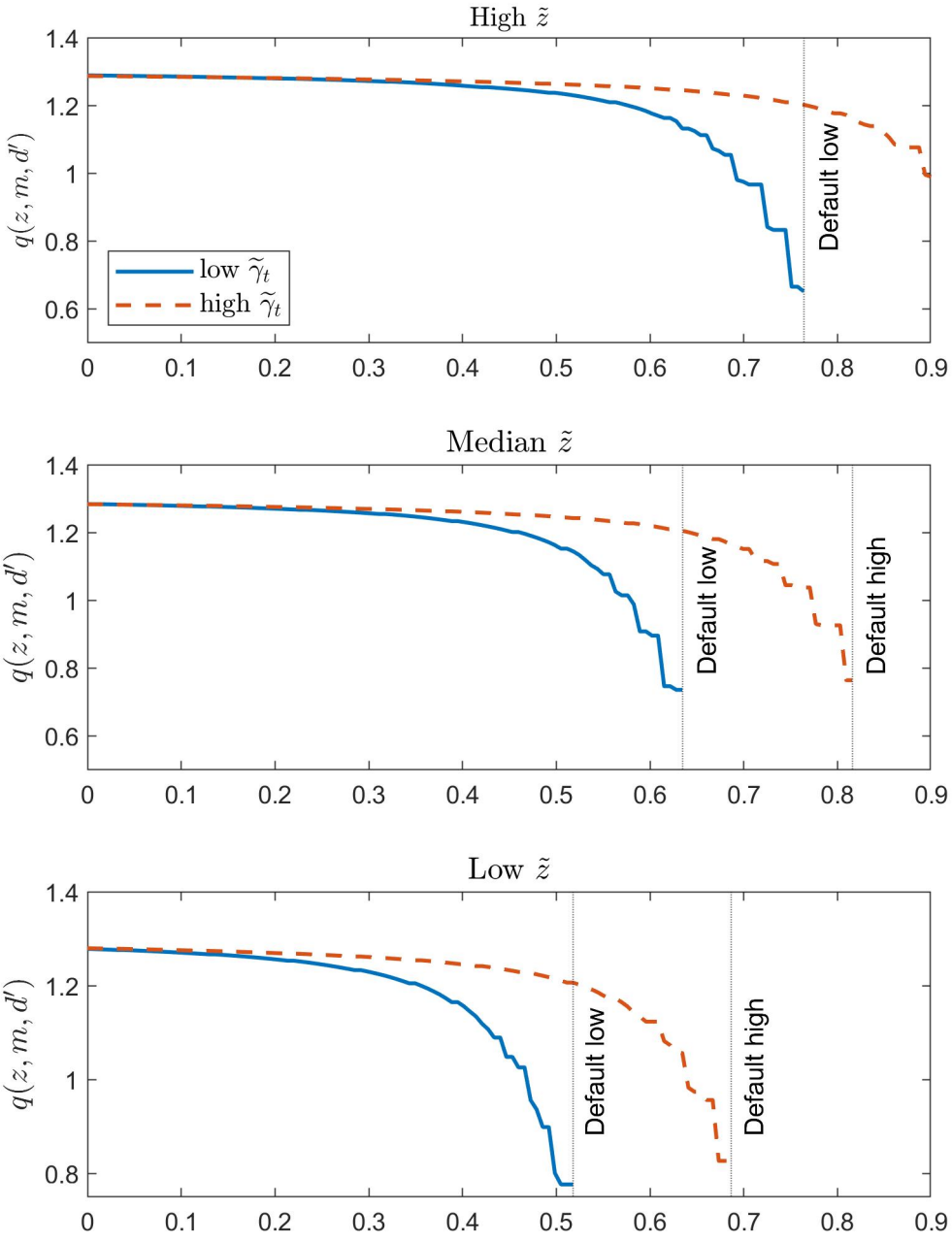

Figure C.1: Debt price schedules across different beliefs of transitory and trend growth beliefs in the sovereign default model with long-maturity debt. 0.9 is the upper limit for debt outstanding.

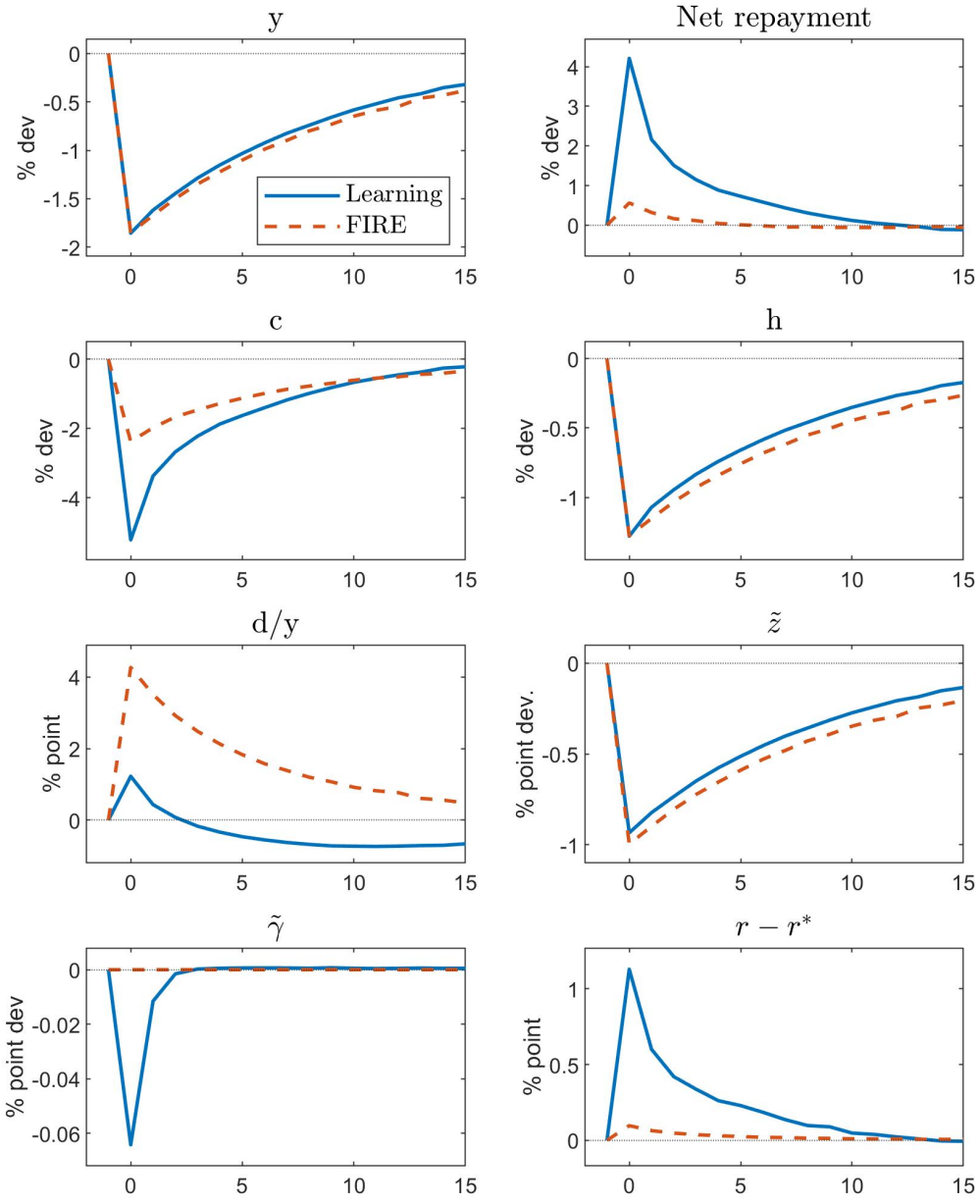

Figure C.2: Impulse response functions to 1% decline in the true transitory productivity. Debt-to-GDP ratio d/y and spreads $r - r^*$ are the percentage point deviations from respective steady states.

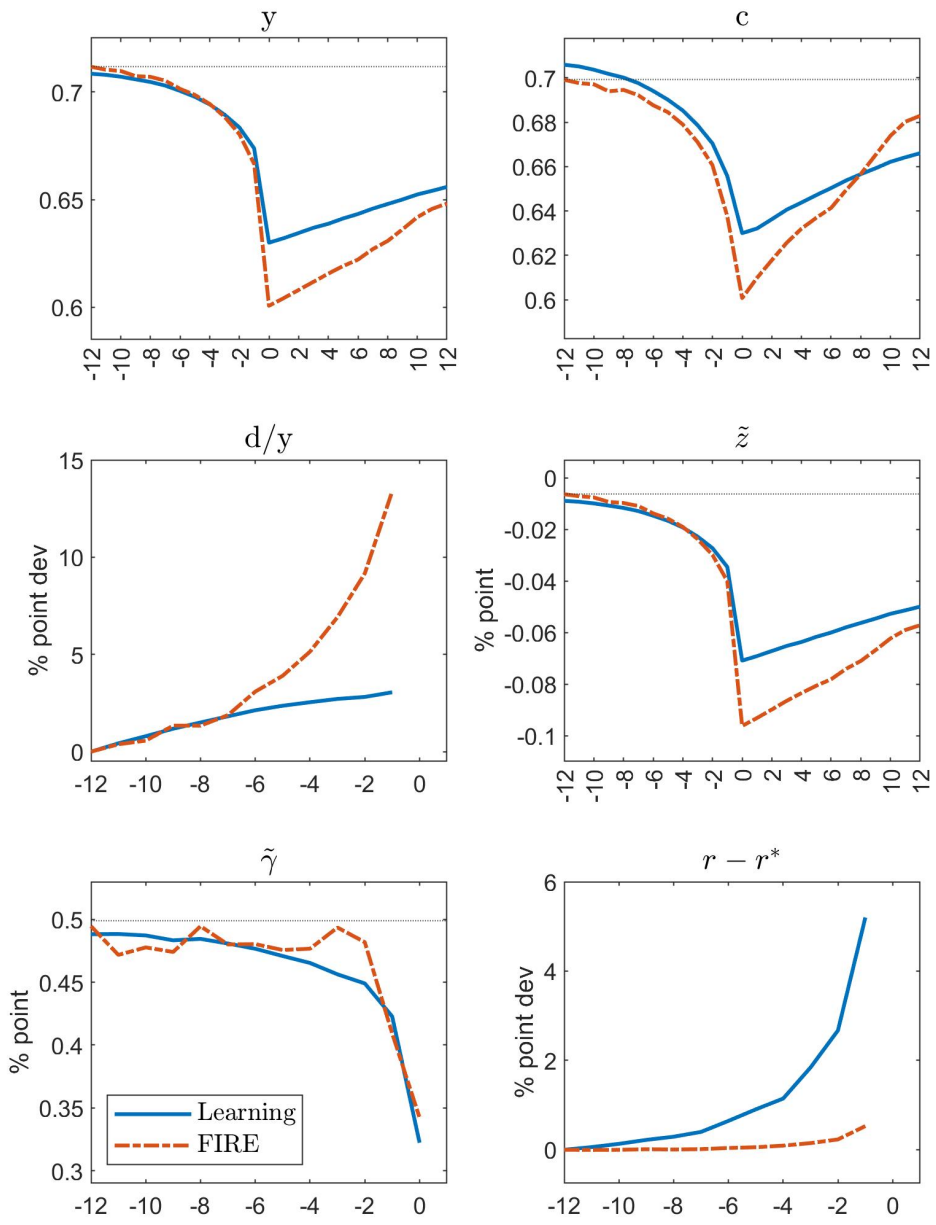

Figure C.3: Typical default episodes for long-maturity debt models. Debt-to-GDP ratio d/y and spreads $r - r^*$ are the percentage point deviations from respective steady states.